UC San Diego

Title

The role of acute stress response in translation regulation

Permalink

https://escholarship.org/uc/item/82x2z0bc

Author

Guzikowski, Anna Rose

Publication Date

2021

Peer reviewed|Thesis/dissertation

UNIVERSITY OF CALIFORNIA SAN DIEGO

The role of acute stress response in translation regulation

A dissertation submitted in partial satisfaction of the requirements for
the degree Doctor of Philosophy

in

Biology

by

Anna R. Guzikowski

Committee in Charge:

        Professor Brian Zid, Chair
        Professor Jens Lykke-Andersen, Co-chair
        Professor Amy Pasquinelli
        Professor James Wilhelm
        Professor Gene Yeo

2021

The dissertation of Anna R. Guzikowski is approved, and it is acceptable in quality and form for publication on microfilm and electronically.

University of California San Diego

2021

DEDICATION

This work is dedicated to my parents, Mary and Tony, and in loving memory of Dan, my brother.

TABLE OF CONTENTS

LIST OF FIGURES

LIST OF TABLES

ACKNOWLEDGMENTS

I would like to first thank Dr. Brian Zid for his constant guidance and seemingly limitless enthusiasm, availability, and optimism throughout this project. I had a limited idea of what I was getting myself into when I decided to join a new lab as a first-year graduate student. Six years later, I can confidently say I am grateful that I was willing to journey into uncharted territory. Brian is incredibly gifted at asking and answering questions and he has created an environment where lab members are supported when they pursue interests outside of their wheelhouses, take risks, and make mistakes. His ability to discuss biology in a way that is approachable and engaging was essential for our lab's ability to function with such a wide range of researchers approaching science with varied backgrounds and skillsets. Thank you for giving me the time and space to learn new skills and lead a fulfilling, balanced life. I can confidently say Brian's willingness to not only put up with but also support my pursuit of interests outside of the lab including outreach, teaching, and community leadership enriched my time at UCSD and made me a better scientist and communicator.

I would also like to thank all other members of my doctoral thesis committee including Drs. Jens Lykke-Andersen, Amy Pasquinelli, James Wilhelm, and Gene Yeo. Each offered feedback, suggestions, and advice in their own unique style and were critical to the completion of this dissertation. I am grateful for the ways they helped guide my research and for the wisdom they offered to me and to Brian when it came to more practical and logistical details that new PIs are not necessarily privy to, this was particularly true of Dr. Pasquinelli.

I would also like to thank all the members of the Zid lab, both two-legged and four-legged, whose advice, expertise, encouragement, and camaraderie were crucial to my progress.

Vince, thank you for always sharing your lunches, knowledge, sense of humor, and time with me. Tatsu, thank you for always answering my questions about yeast and offering experimental guidance. Ximena, thank you for patiently explaining physics to me and the rest of the biologists in our group. Ellie, thank you for always smiling when you greeted me at work each morning. I can't imagine spending so many years at the bench and making so many trips to the coffee cart without friends alongside. This is also true of the friends outside the lab I made in both the Division of Biological Sciences and the Department of Chemistry and Biochemistry. Thank you all. I am especially grateful to a group of ten incredible women scientists in my graduate program. We nicknamed ourselves 'Da Ladies' and more recently 'PhDaLadies' as we near or have already completed graduation. Each of you has inspired me and shaped my maturation into the scientist and person I am today. You all filled my time at UCSD with an overwhelming amount of love and laughter. I can't wait to see where life takes us next and look forward to having each of you along for the journey.

I would also like to thank the RNA labs inside Urey Hall including the Müller, Joseph, Toor, and McHugh labs for sharing your equipment, reagents, time, and expertise with me.

To the family I have gained in San Diego, thank you for your unconditional love. Herbert, Filbert, and Wally, you are a constant source of joy and companionship. I can confidently say that each one of you is a very good boy, even the mischievous Filbert. Thank you for being excited every time I returned home, regardless of whether my experiment worked that day. Josh, thank you for being my best friend, biggest advocate, and partner in adventures. I am lucky to have such a caring person by my side who also happens to understand what the journey through graduate school is like. I can't imagine how much trickier it would have been to make it to this point without your encouragement, generosity, and talents in the kitchen. I am

also grateful that the Arriola family has welcomed me and always made me feel included and loved.

Lastly, I would like to thank my family for their endless love, support, and encouragement. My mother and father have supported my academic interests and my love of the natural world throughout my life. They have always put my needs before theirs. My mom, who was working full time as a nurse for our county's health department, left the pursuit of her own PhD in public health when I was born. I am humbled that her sacrifice put me in a position to become the first woman in our family to earn a doctorate. Thank you both for always reminding me you are proud of me. Dad, thank you for nurturing and enriching my love of science throughout my life. I appreciate all you have done for me and would not have made it to the end of this journey without you.

I would also like to thank and acknowledge the people that contributed scientifically to this dissertation. Chapter 2 consists of a reprint of material from the article 'Stress-Induced mRNP Granules: Form and Function of P-bodies and Stress Granules' published in *Wiley Interdisciplinary Reviews RNA* (2019) by Anna R. Guzikowski, Yang S. Chen, and Brian M. Zid. This dissertation author and Y.S.C. are co-primary authors of this publication.

Chapter 3 consists of material from a manuscript submitted for publication entitled "Differential translation elongation directs protein synthesis in response to acute glucose deprivation in yeast" by Anna R. Guzikowski, Alex T. Harvey, Jingxiao Zhang, Shihui Zhu, Molly H. Cohn, Kyle Begovich, James E. Wilhelm, and Brian M. Zid. The dissertation author is the primary author of this work.

VITA

Education
University of California San Diego
    Ph.D. in Biology   2015 - 2021

Boston University
    B.A. in Biochemistry and Molecular Biology   2009 - 2013
    Minor in English Literature

Research Experience
University of California San Diego Division of Biological Sciences   2016 - 2021
Graduate Student Researcher in the laboratory of Dr. Brian M. Zid
Characterization of translation elongation during glucose starvation in *Saccharomyces cerevisiae*

Brigham Regenerative Medicine Center at Harvard Medical School   2013 - 2015
Research Assistant in the laboratory of Dr. Jessica L. Whited
Study of limb regeneration in axolotl salamanders

Boston University Department of Chemistry   2011 - 2013
Undergraduate Researcher in the laboratory of Dr. Sean J. Elliott
Characterization of the sulfite reductase SirA from *Mycobacterium tuberculosis*

Awards and Honors
Roger Tsien fellowship, UCSD	2017
Interfaces program in multi-scale biology funding award, UCSD	2016
Summer scholar research grant, BU	2012
College of Arts and Sciences honors program fulfillment, BU	2011
Dean's Scholarship, BU	2009 - 2013

Service
BioEASI Science Class instructor and organizer at county jails	2018 - 2021
UCSD Biology Graduate Student Council representative and founding member	2019 - 2021
UCSD Student Transportation and Advisory Committee graduate representative	2019 - 2021
UCSD Biology Undergraduate and Masters Mentorship Program mentor	2020 - 2021

UCSD Biology Admission Committee member   2020 - 2021
UCSD Graduate Student Association representative for Biology   2018 - 2020
San Diego RNA Club RNA Society RNA salon co-organizer   2018 - 2020
UCSD BioEASI principal member   2016 - 2019
UCSD Graduate RNA Club founder and co-organizer   2016 - 2019
UCSD Biology Instructional Assistant: 2017 - 2019
   Courses in Biochemical Techniques, Molecular Biology, and Human Nutrition
UCSD Biology Graduate Teaching Mentor: 2019 - 2020
   Course in Introduction to College Biology Education

ABSTRACT OF THE DISSERTATION

The role of acute stress response in translation regulation

by

Anna R. Guzikowski

Doctor of Philosophy in Biology

University of California San Diego, 2021

Professor Brian M. Zid, Chair

Professor Jens Lykke-Andersen, Co-Chair

The post-transcriptional regulatory mechanisms cells mount in response to environmental stresses are varied and complex. Of particular interest is how cells regulate protein synthesis in response to severe stress as proteins are the ultimate, functional product of the 'central dogma' and protein synthesis represents a large energy burden. Research into translation during stress has traditionally focused on discrete aspects such as limiting initiation or altering RNA localization. In this dissertation, I attempt to employ a holistic approach to studying protein synthesis by considering translation machinery in the context of the general cytoplasm and by acknowledging the important role that RNA has in the process. To accomplish this, we provide an in-depth discussion of the reorganization of RNA and protein that takes place in stress-induced granules in Chapter 2. Next, using acute glucose starvation in yeast, we interrogate engagement of ribosomes with mRNAs and characterize how differential elongation influences gene expression in Chapter 3. Chapter 4 then discusses the results from an *in vitro* translation system I developed. With it, we found hallmarks of translation regulation observed during acute glucose starvation were maintained in cell extracts. Finally, Chapter 5 discusses possible future directions that can continue this work and includes closing remarks.

Chapter 1:

Introduction

Careful and coordinated regulation of gene expression is essential for living organisms to appropriately undertake biological processes like metabolism and reproduction. Proteins, the ultimate product of gene expression, dictate cell function and, by extension, survival. Therefore, if one wishes to understand how an organism regulates gene expression and survives, one must first understand how proteins are made.

Synthesis of a protein is a complex process that can, when simplified, be broken down into three primary steps: initiation, elongation, and termination. Briefly, in eukaryotic organisms, initiation occurs after a scanning 40S ribosomal subunit encounters a start codon, traditionally coded by the nucleotide sequence AUG within an mRNA template, and assembles with a 60S subunit, many initiation factor proteins, and an initiator methionine tRNA (Dever et al., 2016; Kozak, 1999; Pestova et al., 2001). When successfully orchestrated, this process gives rise to an 80S ribosome that begins the elongation stage. During elongation, the ribosome undergoes a series of confirmational changes, interacts with elongation factors and aminoacyl-tRNAs, and synthesizes a nascent polypeptide as it moves along the mRNA template, decoding it codon by codon (Lareau et al., 2014; Schuller & Green, 2018). Finally, when a stop codon is reached, termination factors facilitate the release of the polypeptide (Hellen, 2018; Kisselev & Frolova, 1995). Then, the ribosome itself becomes eligible for disassembly and release whereby this translation process can start over again. It is through this process that gene expression is realized.

Understanding how ribosomes translate protein is the first part of understanding how gene expression takes place in such a way that cells accomplish the remarkable task of staying alive. The second part is understanding which genes are translated in a cell and, by extension, how the cell decides this. Decades of genetics research have enriched our understanding of the

coordinated programs of gene expression that facilitate important processes like division, development, and autophagy (Basson, 2012; Mizushima, 2018; Ong & Torres, 2019). Cues for such processes come from the environment generally and neighboring cells locally, as well as from internal signaling networks (Dasgupta & McCollum, 2019; Falcone & Mazzoni, 2016; Zarnack et al., 2020). Notably, the development and popularization of next-generation sequencing technology (NGS) at the start of the twenty-first century revolutionized the scale and resolution at which researchers can interrogate gene expression (Goodwin et al., 2016; van Dijk et al., 2014). Today, is it financially and technically feasible for a researcher interested in gene expression in their model organism of choice to examine it with unprecedented breadth and depth.

Considering we have both a comprehensive understanding of how proteins are made and unparalleled insight into gene expression on a genome-wide scale, it is natural to ask how protein synthesis is manifested across a variety of specific cell types and environmental conditions. Answering such questions can help biologists gain deeper insight into the fundamental ways gene expression is fine-tuned and, importantly, to understand when it goes awry. One might wonder what genes are expressed in a given situation, what amount of translation of those genes is appropriate, and what processes decide which genes are expressed when. I would argue that the latter of these questions is the most complicated and enigmatic. This dissertation aims to contribute to our understanding of the relationship between gene regulation, protein synthesis, and cell survival. To do so, I not only examine expression in a specific environmental setting, but I examine how gene expression is altered and regulated as the environment changes. In particular, this project explores responses to unfavorable, challenging changes in the environment.

It is typical to maintain model systems in a laboratory environment under optimized conditions. After all, if a researcher wants to study something living, they must keep it alive. However, it is also well-appreciated that organisms don't always find themselves in optimal conditions in nature. Decades of research have established experimental techniques that challenge organisms with stress in the lab (Advani & Ivanov, 2019; McKenzie et al., 1975). The word stress can have different connotations in different scientific disciplines but, in general, molecular biologists interested in gene regulation consider stress to be adverse environmental flux. Common examples include exposure to toxins, temperature fluctuations, nutrient deprivation, introduction of pathogens, UV exposure, osmotic changes, and oxidative stress. Critically, knowing how cells sense and respond to unfavorable external changes is relevant to understanding human conditions like disease and aging where internal states become misregulated and the cellular environment becomes unfavorable for routine growth and function (Fulda et al., 2010; Macario & Conway de Macario, 1997; Moseley, 2000; Poljšak & Milisav, 2012).

In this dissertation, I use the budding yeast *Saccharomyces cerevisiae* and acute glucose deprivation as a model organism and model stress, respectively, to study how protein synthesis changes in response to severe stress. First, Chapter 2 will set the stage by discussing a reorganization of RNAs and translational machinery that occurs within the cytoplasm in response to stress. I would argue that it is helpful to understand both how translation works and how the machinery that carries it out is spatially confined when trying to understand ways protein synthesis is regulated. Chapter 2 also contains a review of recent stress response literature that will cover how compartmentalization of the cytoplasm occurs broadly in response to stress by focusing on the formation, constituents, and dynamics of two stress-

induced granules: P-bodies and stress granules. Chapter 3 will explore how translation is regulated in response to glucose starvation with NGS and reporter assay approaches. Our findings indicate that ribosomes remain engaged with preexisting mRNAs and their distribution changes upon stress. This is notable given that stress response literature can often focus on reduced levels of ribosome-mRNA engagement that result from ribosome runoff and precede P-body and stress granule formation (Lee & Seydoux, 2019). Chapter 4 will then detail the results of a yeast *in vitro* translation assay that mimics the downregulation in protein synthesis caused by glucose starvation. Together, these chapters culminate in a thorough and wide-ranging examination of how gene expression is changed and regulated in response to stressful changes in the cellular environment.

References:

Advani, V. M., & Ivanov, P. (2019). Translational Control under Stress: Reshaping the Translatome. *BioEssays: News and Reviews in Molecular, Cellular and Developmental Biology*, *41*(5), e1900009. https://doi.org/10.1002/bies.201900009

Basson, M. A. (2012). Signaling in cell differentiation and morphogenesis. *Cold Spring Harbor Perspectives in Biology*, *4*(6), a008151. https://doi.org/10.1101/cshperspect.a008151

Dasgupta, I., & McCollum, D. (2019). Control of cellular responses to mechanical cues through YAP/TAZ regulation. *Journal of Biological Chemistry*, *294*(46), 17693–17706. https://doi.org/10.1074/jbc.REV119.007963

Dever, T. E., Kinzy, T. G., & Pavitt, G. D. (2016). Mechanism and Regulation of Protein Synthesis in Saccharomyces cerevisiae. *Genetics*, *203*(1), 65–107. https://doi.org/10.1534/genetics.115.186221

Falcone, C., & Mazzoni, C. (2016). External and internal triggers of cell death in yeast. *Cellular and Molecular Life Sciences, 73*(11–12), 2237–2250. https://doi.org/10.1007/s00018-016-2197-y

Fulda, S., Gorman, A. M., Hori, O., & Samali, A. (2010). Cellular stress responses: Cell survival and cell death. *International Journal of Cell Biology*, *2010*, 214074. https://doi.org/10.1155/2010/214074

Goodwin, S., McPherson, J. D., & McCombie, W. R. (2016). Coming of age: Ten years of next-generation sequencing technologies. *Nature Reviews. Genetics*, *17*(6), 333–351. https://doi.org/10.1038/nrg.2016.49

Hellen, C. U. T. (2018). Translation Termination and Ribosome Recycling in Eukaryotes. *Cold Spring Harbor Perspectives in Biology*, *10*(10), a032656. https://doi.org/10.1101/cshperspect.a032656

Kisselev, L. L., & Frolova L. Y. (1995). Termination of translation in eukaryotes. *Biochemistry and Cell Biology*, *73*(11–12), 1079–1086. https://doi.org/10.1139/o95-116

Kozak, M. (1999). Initiation of translation in prokaryotes and eukaryotes. *Gene*, *234*(2), 187–208. https://doi.org/10.1016/S0378-1119(99)00210-3

Lareau, L. F., Hite, D. H., Hogan, G. J., & Brown, P. O. (2014). Distinct stages of the translation elongation cycle revealed by sequencing ribosome-protected mRNA fragments. *ELife*, *3*, e01257. https://doi.org/10.7554/eLife.01257

Lee, C.-Y., & Seydoux, G. (2019). Dynamics of mRNA entry into stress granules. *Nature Cell Biology*, *21*(2), 116–117. https://doi.org/10.1038/s41556-019-0278-5

Macario, A. J. L., & Conway de Macario E. (1997). Mini-Review; Stress Genes: An Introductory Overview. *Stress*, *1*(3), 123–134. https://doi.org/10.3109/10253899709001102

McKenzie, S. L., Henikoff, S., & Meselson, M. (1975). Localization of RNA from heat-induced polysomes at puff sites in Drosophila melanogaster. *Proceedings of the National Academy of Sciences of the United States of America*, *72*(3), 1117–1121. https://doi.org/10.1073/pnas.72.3.1117

Mizushima, N. (2018). A brief history of autophagy from cell biology to physiology and disease. *Nature Cell Biology*, *20*(5), 521–527. https://doi.org/10.1038/s41556-018-0092-5

Moseley, P. (2000). Stress proteins and the immune response. *Immunopharmacology*, *48*(3), 299–302. https://doi.org/10.1016/s0162-3109(00)00227-7

Ong, J. Y., & Torres, J. Z. (2019). Dissecting the mechanisms of cell division. *Journal of Biological Chemistry*, *294*(30), 11382–11390. https://doi.org/10.1074/jbc.AW119.008149

Pestova, T. V., Kolupaeva, V. G., Lomakin, I. B., Pilipenko, E. V., Shatsky, I. N., Agol, V. I., & Hellen, C. U. (2001). Molecular mechanisms of translation initiation in eukaryotes. *Proceedings of the National Academy of Sciences of the United States of America*, *98*(13), 7029–7036. https://doi.org/10.1073/pnas.111145798

Poljšak, B., & Milisav, I. (2012). Clinical implications of cellular stress responses. *Bosnian Journal of Basic Medical Sciences*, *12*(2), 122–126. https://doi.org/10.17305/bjbms.2012.2510

Schuller, A. P., & Green, R. (2018). Roadblocks and resolutions in eukaryotic translation. *Nature Reviews. Molecular Cell Biology*, *19*(8), 526–541. https://doi.org/10.1038/s41580-018-0011-4

van Dijk, E. L., Auger, H., Jaszczyszyn, Y., & Thermes, C. (2014). Ten years of next-generation sequencing technology. *Trends in Genetics*, *30*(9), 418–426. https://doi.org/10.1016/j.tig.2014.07.001

Zarnack, K., Balasubramanian, S., Gantier, M. P., Kunetsky, V., Kracht, M., Schmitz, M. L., & Sträßer, K. (2020). Dynamic mRNP Remodeling in Response to Internal and External Stimuli. *Biomolecules*, *10*(9), E1310. https://doi.org/10.3390/biom10091310

Chapter 2:

Stress-Induced mRNP Granules: Form and Function of P-bodies and Stress Granules

2.1 Abstract

In response to stress cells must quickly reprogram gene expression to adapt and survive. This is achieved in part by altering levels of mRNAs and their translation into proteins. Recently, the formation of two stress-induced messenger ribonucleoprotein (mRNP) assemblies named stress granules and processing bodies has been postulated to directly impact gene expression during stress. These assemblies sequester and concentrate specific proteins and RNAs away from the larger cytoplasm during stress, thereby providing a layer of post-transcriptional gene regulation with the potential to directly impact mRNA levels, protein translation, and cell survival. The function of these granules has generally been ascribed either by the protein components concentrated into them or, more broadly, by global changes that occur during stress. Recent proteome-wide and transcriptome-wide studies have provided a more complete view of stress-induced mRNP granule composition in varied cell types and stress conditions. However, direct measurements of the phenotypic and functional consequences of stress granule and processing body formation are lacking. This leaves our understanding of their roles during stress incomplete. Continued study into the function of these granules will be an important part in elucidating how cells respond to and survive stressful environmental changes.

2.2 Introduction

Cells are frequently exposed to fluctuating, potentially adverse environmental conditions. To survive adverse changes they must rapidly alter gene expression in order to maintain internal homeostasis. The cellular reprogramming that occurs in response to a disruptive or inimical external fluctuation is broadly termed as stress response. Cellular stress response typically includes slowing or ceasing growth that is concomitant with repression of overall translation, though certain genes important for survival and repair are highly induced. Concurrently, while overall translation is repressed, many post-transcriptional regulatory proteins and mRNAs undergo a process called phase separation that results in the formation of concentrated, non-membranous cytoplasmic structures generally described as granules or foci. During stress, this phase separation process might segregate proteins and mRNAs in a way that is functionally important for the cell and that promotes survival. Therefore, these structures are a subject of emergent interest. Although much progress has been made recently to identify the proteins and mRNAs that reside in these granules and the physical characteristics that underlie their formation, there is little known about the phenotypic or functional consequences of their formation during stress and therefore how significantly they contribute to stress response.

There are many different types of cellular granules involved in a wide variety of biological processes such as nucleoli, paraspeckles, PML bodies, and Cajal bodies in the nucleus as well as the stress-induced processing bodies (PBs) and stress granules (SGs) in the cytoplasm. Here we highlight the cytoplasmic PBs and SGs, two well-studied mRNP granules that are present across eukaryotes during a variety of stressful conditions such as exposure to heat shock, oxidative stress, UV irradiation, osmotic stress, and nutrient starvation. The formation of these mRNP granules, which occurs on the scale of minutes after exposure to

stress stimuli, is mediated by a physical process called liquid-liquid phase separation (LLPS). There are common biophysical characteristics and some shared components between SGs and PBs as well as granule-specific features. It should be noted that, while the aptly named SGs are broadly induced during stress, PBs are a bit more organismal specific. *S. cerevisiae* induces visible PBs primarily during stress response while, in mammalian cells, small, microscopically visible PBs are constitutive but they become much larger and more abundant during stress. It should also be noted that the majority of research into these stress-induced granules is performed with yeast and mammalian cell culture systems. Ultimately, we posit SGs and PBs should be considered as distinct yet closely related mRNP granules; their properties and role in post-transcriptional gene expression during stress response is the focus of this review and we will address them individually, as SGs or PBs, and together more generally, as stress-induced mRNP granules, when appropriate.

Initial characterization of conditions that bring about stress-induced mRNP granules began in the late 1990s when researchers observed that impairment of translation initiation causes SG formation (Bashkirov et al., 1997; Kedersha et al., 1999). A decrease in initiation is one hallmark of stress response; the canonical mechanism of eIF2α-phosphorylation can drive robust granule formation in some stress conditions (Kedersha et al., 1999). Importantly, however, the formation of SGs is not dependent on eIF2α-phosphorylation as the addition of small molecules that block translation initiation through different mechanisms are sufficient to drive granule assembly (Mazroui et al., 2006; Mokas et al., 2009). Moreover, the genetic knockdown of specific translation initiation factor proteins (Mokas et al., 2009) or the overexpression of RNA-binding proteins that function to repress translation (De Leeuw et al.,

2007; Gilks, 2004; Kedersha et al., 2005; Mazroui et al., 2006; Wilczynska, 2005) also lead to mRNP granule formation.

The observation that impaired translation drives SG and PB formation spurred further inquiry into their induction and the degree of interrelation between the two granules during stress response. Evidence emerged that SGs and PBs, each lacking membranes, are able to interact, potentially docking and swapping components (Kedersha et al., 2005; Buchan et al., 2008; Wilbertz et al., 2018). Nonetheless, it is known that these granules retain unique protein content and presumably RNA content, though the dynamics and degree of retention of RNAs with an individual granule is more poorly understood than it is for proteins. Interestingly, one study found SG assembly was dependent on and promoted by the presence of pre-existing PBs in yeast cells, demonstrating the akin yet distinct nature of SGs and PBs (Buchan et al., 2008). On the other hand, a different study found that induction of PBs and SGs occurs via independent signaling pathways in yeast and reported no such dependency (Shah et al., 2013). These results highlight the complexity that underlies stress-induced mRNP granule formation. Ultimately, it is not only a loss of translation initiation but also complex networks of signaling pathways, granule-granule interactions, protein-RNA interactions, protein-protein interactions, and RNA-RNA interactions that shape and define both types of distinct but closely related stress-induced mRNP granules.

Understanding when SGs and PBs form is an important first step into recognizing what purpose they have in the broader changes elicited during stress. During the stress response a cell must confront a potential dearth of resources, including of resources necessary to synthesize new proteins, as it responds to the challenge of environmental stress. The direct connection between SG and PB induction coincident with the overall reduction of translation

during stress suggests mRNP granule formation may directly control the rapidly changing

proteome, yet the extent of this is not clear. The function and molecular relevance of SGs and

PBs has been attributed largely based on the protein components concentrated within them.

Specifically, the majority of mRNP granule proteins function in translation initiation,

translational repression, or mRNA degradation. Consequently, it is generally thought that SGs

and PBs function to segregate mRNAs from the larger cytoplasm to regulate their fate, either

by storage, decay, or eventual reintroduction to the translating pool. Below we discuss the

protein and RNA content of SGs and PBs before we switch to a discussion of what information

is known and lacking about their function during stress (Figure 2.1).
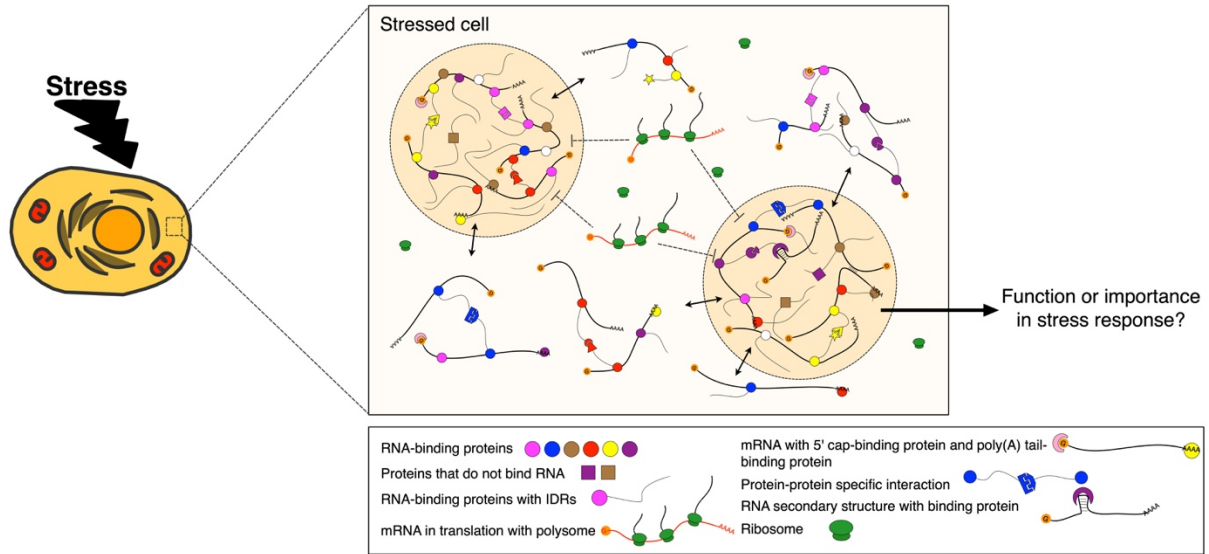
Figure 2.1. Diverse macromolecular interactions lead to the phase separation of protein and RNA during stress.
While the identities of many proteins and RNAs contained in these granules (tan spheres) have been elucidated recently, the function of this conserved compartmentalization of the cytoplasm during stress response is still an open question.

2.3 Stress-Induced mRNP Granules: Characteristics and Composition

The function of a stress-induced mRNP granule is presumably related to its molecular composition and so it is important to understand the identity of resident proteins and RNAs in both SGs and PBs. Insight into the ever-expanding catalog of SG and PB residents, discussed below, has enabled informed speculation about granule function; however, it is important to note that simply knowing what is inside these structures has, thus far, been insufficient to clearly elucidate their roles during stress response.

2.3.1 Protein composition of stress-induced mRNP granules

Over the past decade, more and more protein factors residing in PBs and SGs were detected and characterized biochemically and genetically (Buchan & Parker, 2009; Parker & Sheth, 2007). For example, dozens of PB protein components were identified originally in yeast, including Lsm1-7, Xrn1, and Pop2 (Decker et al., 2007). However, due to the challenge of capturing and isolating an intact, membrane-less granule structure in the cytoplasm, a comprehensive profile of the hundreds of resident proteins in mRNP granules under various conditions remained experimentally challenging and therefore elusive. More recently, by taking advantage of mass spectrometry-based high-throughput proteomics and proximity labeling techniques, several studies profiled the larger proteome of PBs and SGs in yeast and different mammalian cell types under various stresses and, for mammalian PBs, native conditions. More than one hundred protein factors were newly identified and extensive interactomes within mRNP granules were characterized (Alberti, 2018; Hubstenberger et al., 2017; Jain et al., 2016; Markmiller et al., 2018; Youn et al., 2018). Overall, mammalian mRNP granule proteomes are larger than yeast proteomes but they have substantial overlap with each other. Therefore, mammalian granules are more complex but stress-induced phase separation is an evolutionarily

conserved event. In both mammals and yeast, PBs and SGs only share 10% - 25% of their

protein components (5 are shared in yeast and 28 in mammalian cells), leaving the majority of

the proteome granule-specific (Table 2.1). Intriguingly, even though the majority of the

proteome is granule-specific, several protein families and classifications are highly enriched in

both types of mRNP granules across species. Most notably, there is very high enrichment in

RNA-binding proteins (RBPs), with over 50% of proteins present in human SGs and yeast or

human PBs having annotated RNA-binding functionality. There are also many proteins that

contain intrinsically disordered regions (IDRs), which will be discussed in more detail later.

Amid a general ability to bind RNA, many other sub-categorizations of stress-induced

mRNP granule proteins arise from a thorough analysis of their proteomes (Table 2.1). For

example, in PBs, the majority of protein components are involved in RNA decay and

translational repression in yeast and mammals. They include RNA decay factors (EIF4E-T,

LSM14A (Scd6 in yeast), LSM14B, and IGF2BP2), decapping complex components

(DCP1A/1B, DCP2, EDC4, DDX6 (Dhh1 in yeast), Edc3 and Pat1), factors in the miRNA

pathway (Ge-1, GW182, AGO1/2/3, TRNC6A, and ZCCHC3), deadenylation complex

components (CCR4-NOT, LSM1-7), ribonucleases (XRN1), nonsense-mediated decay (NMD)

factors (UPF1, SMG5/7), and, finally, translation repressors (EIF4E-T, CPEB1) (Andrei et al.,

2005; Luo et al., 2018; Serman et al., 2007; Sheth & Parker, 2003). Like PBs, SGs harbor

proteins that are related to RNA decay, such as ribonucleases (XRN1, G3BP, SND1) and

components in the miRNA pathway (ZFP36, TNRC6B, AGO2), although mRNAs in SGs are

not typically considered targets for decay (Lavut & Raveh, 2012). SGs also house translation

repressors (CIRP, DDX3 (Ded1 in yeast), FXR1/2, Staufen1). Unlike PBs, SGs contain many

components involved in translation including initiation factors (EIF2A/3/4A/4B/4G) and,

notably, 40S ribosomal subunits. Transcripts stalled at the initiation step of translation are thought to be enriched in SGs though, to our knowledge, this has not been directly validated. Furthermore, whether these translation factors are directly associated with mRNAs as complete pre-initiation complexes remains to be tested.

The classifications of proteins discussed above are notable in how broad they are. After all, factors involved in general cellular processes like decay and translation have to be able to recognize and regulate the diverse set of mRNAs that comprise a cell's transcriptome. This raises the question of how specificity arises in targeting the mRNAs that proteins interact with to cytoplasmic granules during stress. To find clues into potential mechanisms one can look to more specific functions in the categories of proteins that arise from classification of PB and SG proteomes. Interestingly, proteins that recognize both RNA secondary structures like G-quadruplexes (FXR1, FMR1) and the epitranscriptional RNA modification N^6-methyladenosine (m^6A) (YTHDF1/2/3) are enriched in SGs. Relatedly, YTHDF2, a m^6A reader, is a recently identified PB component (Luo et al., 2018; Wang et al., 2013). Therefore, RNA structures and modifications recognized by these proteins may provide means to determine specificity in targeting certain mRNAs to mRNP granules, though experimental validation of this potential mechanism remains to be realized.

In addition to enabling classification of the functions of proteins found in SGs and PBs, approaches that combine proximity labeling with mass spectrometry have provided insight into the degree of heterogeneity in the proteomes of stress-induced mRNP granules formed in different cell types and in response to different stresses. Certain proteins are thought to be present in all SGs, particularly those that have been shown to nucleate SG formation, but the protein composition of SGs does vary across different conditions. For example, comparison of

SGs formed during arsenite stress with those formed during heat shock showed that 23% of protein components are stress-type specific (Jain et al., 2016; Markmiller et al., 2018). Markmiller and colleagues also reported differences in SG composition in different cell types as well as different stress and disease conditions; SGs in amyotrophic lateral sclerosis (ALS) motor neurons contained particularly distinct proteins. They estimated that up to 20% of the SG proteome is stress and cell type specific. This context-dependence and diversity of SG composition suggests SGs arise and potentially function according to the specific cellular needs and demands brought about by a given stress condition. Similarly, studies of PB composition showed that PB protein content changes during stress compared to native conditions in mammalian systems (Ohn et al., 2008). PBs were found uniquely enriched with ubiquitination-related proteins under arsenite stress (Youn et al., 2018). Understanding how the protein composition of mRNP granules changes in specific conditions may reveal mechanisms of how these granules are fine-tuned to allow the cell to best survive specific stressors and regulate gene expression to meet stress-dependent challenges. This may ultimately help ascertain the function of stress-induced mRNP granules.

Table 2.1. Protein composition of stress granules and p-bodies.
(A) Properties of yeast and mammalian SG and PB proteomes. Upper: Summary of protein activities of SG and PB proteomes. Lower: Overlap of SG and PB proteome components identified in both granule types for yeast and mammalian systems. Yeast and human SG proteomes and yeast PB proteome are from (Jain et al., 2016). The human PB proteome is from (Hubstenberger et al., 2017). Prion-like domains were predicted by PrionScan (Angarica et al., 2014) and PLAAC (Lancaster et al., 2014). The RNA-binding proteomes are from (Beckmann et al., 2015). ATPase activity annotations are from SGD and NCBI. (B) Representative functional, gene ontology (GO) classification of PB and SG proteomes. Yeast homologs are shown in parentheses. Components that are essential for PB/SG assembly and maintenance are highlighted in bold. GO analysis was performed by GO consortium (Ashburner et al., 2000; Carbon et al., 2017). Citations showing the presence and functions of listed components and those used to generate GO data include Serman et al., 2007; Luo et al., 2018; Andrei et al., 2005; Sheth & Parker, 2003; Hubstenberger et al., 2017; Franks & Lykke-Andersen, 2008; Eulalio et al., 2007; Marnef et al., 2010; Decker et al., 2007; Gilks, 2004; Kedersha et al., 2016; Yang et al., 2014; Buchan & Parker, 2009; Tourriere et al., 2003; Jain et al., 2016; & Markmiller et al., 2018.

A

Features	Yeast SG (159)	Human SG (411)	Yeast PB (52)	Human PB (109)
RNA-binding proteins (RBPs)	39	224	36	70
Prion-like domains	23	32	21	24
RBP & prion-like domains	18	30	11	13
ATPase activity	10	37	5	19

SG and PB overlap	Yeast	Human
Number	5	28
Components	Dhh1, Sbp1, Eap1, Dcp1, Scd6	ACTBL2, AGO2, DCP1A, DDX21, DDX50, DDX6, DHX30, EDC4, ELAVL1, ELAVL2, FAM120A, HSPB1, IGF2BP1, IGF2BP2, IGF2BP3, KIF23, LSM14A, LSM14B, MCM7, MEX3A, MOV10, MSI1, NOP58, PUM1, S100A9, STAU2, UPF1, ZC3HAV1

B Processing Body (P-body/PB)

Translation repression	**CPEB1, EIF4E-T**
RNA decay and stabilization	**LSM14A**/B **(Scd6)**, **DDX6 (Dhh1)**, IGF2BP2
miRNA pathway	**Ge-1**, GW182, AGO1/2, MOV10, ZCCHC3, PUM1
Nonsense-mediated mRNA decay (NMD)	UPF1, SMG7
Decapping complex components	**DCP1A/1B/2, EDC3/4, PATL1**
Deadenylation complex components	**LSM1-7, CCR4-NOT**

Stress Granule (SG)

Translation repression	**TIA-1/TIAR (Pub1/Ngr1)**, **Caprin-1**, FMRP/FXR1, Ataxin-2
Translation initiation	EIF2A, EIF3, EIF4A/B, EIF4G (Tif4631/**Tif4632**)
RNA decay and stabilization	**TDP-43**, **PAB1**, ELAVL1, IGF2BP1, TTP
Ribonuclease activity	**G3BP**, SND1, XRN1, DDX1, CCR-NOT
miRNA pathway	TNRC6B, AGO2, EIF3A
ATPase activity	**DDX6 (Ded1), MCM, CCT, RUVBL1/2 (Rvb1/2)**

2.4 Protein-dependent Dynamics, Assembly, and Interactions in Stress-Induced mRNP Granules

2.4.1 Dynamics: liquid and solid states of stress-induced granules

One of the initial observations made about stress-induced mRNP granules was their dynamic nature, reflected in both their rapid formation during stress and dissolution upon recovery. Recently, the biophysical basis of this has been ascribed to LLPS. The biophysical properties inherent to LLPS also lead to dynamic granule states during the duration of stress response as both proteins and mRNAs can rapidly exchange with the non-phase separated cytoplasm while stress-induced granules are present. Much of the insight into stress-induced granule dynamics has come from fluorescence recovery after photobleaching (FRAP) studies. FRAP of mRNP granule proteins showed that these granules can hold liquid-like and therefore dynamic structures, with components moving in and out after photobleaching (Brangwynne et al., 2009; Kroschwald et al., 2015). However, it is important to note that not all stress-induced mRNP granules have been found to be liquid-like.

The type and duration of stress stimuli seems to influence the material state of the granules it induces and can shift them to a more solid-like state in certain contexts. For instance, yeast stress granules induced by heat shock were found to be less dynamic and more solid-like generally (Kroschwald et al., 2015). This is in contrast to mammalian stress granules induced by sodium arsenite, which were very dynamic and liquid-like (Kroschwald et al., 2015). The extent of species-specific or stress-specific influences in determining the material state of SGs is indeed a complicated matter. One cannot simply assume that, in general, yeast SGs are more solid-like and mammalian SGs are more liquid-like. More recently, the same research group has shown that yeast SGs induced by lowered pH are dynamic and behave in a

more liquid-like manner akin to mammalian arsenite-induced SGs (Kroschwald et al., 2018). At the same time, ALS-linked mutations that increase protein misfolding drove the material state of heat shock-induced mammalian SGs from fluid to more solid-like (Mateju et al., 2017). This indicates that differences in material state are more strongly influenced by the specific stress stimuli used to induce them rather than species-specific differences (Kroschwald et al., 2018). Moreover, other studies have found that SGs can have differing material states within an individual granule. Specifically, mammalian SGs in lysates were found to be smaller than those in cells, suggesting that individual granules have a distinct, less liquid-like core inside a more soluble, outer shell structure (Jain et al., 2016). Protein components in the shell are more dynamic and fast moving, while components in the core dwell within the structure longer. Taken together, these results indicate that the material states of stress-induced mRNP granules cannot be assumed without direct study and that continued, careful parsing of their dynamics in different contexts will be important to fully understand the nuances of phase separation in biological systems.

2.4.2 Assembly: the necessity of certain proteins in stress-induced mRNP granule formation

As previously discussed, proteomic studies revealed hundreds of proteins that reside in PBs and SGs. Though hundreds of proteins reside in these granules, only a fraction of them are considered important for granule assembly or maintenance during stress. Some proteins have been reported to be critical for granule assembly and maintenance as their disruption abolished or decreased the size and number of granules while overexpression had the opposite effect. For instance, in PBs, some translation repressors (CPEB, EIF4E-T), RBPs related to RNA decay and stabilization (LSM14A (Scd6 in yeast), DDX6 (Dhh1 in yeast)), and components in

decapping and deadenylation complexes (DCP1/2, EDC3/4, PATL1, LSM1-7, CCR-NOT) were shown to be essential (Ayache et al., 2015; Eulalio et al., 2007; Franks & Lykke-Andersen, 2008; Luo et al., 2018; Sheth & Parker, 2003). In SGs, translation repressors (Caprin-1, TIA-1/TIAR (Pub1/Ngr1 in yeast)), RBPs related to RNA decay and stabilization (G3BP, DDX6 (Ded1 in yeast), TDP-43, PAB1), and enzymes with ATPase activity (RUVBL1/2 (Rvb1/2), MCM, CCT) were all shown to be essential (Buchan & Parker, 2009; Gilks, 2004; Jain et al., 2016; Kedersha et al., 2016; Tourriere et al., 2003). The latter class stands out in particular as it indicates that granule assembly likely depends on ATP. In fact, the ATPase complexes CCT, RVB, and MCM were shown to regulate distinct steps of SG assembly and disassembly, indicating that the properties and functions of SGs are modulated and maintained by active ATPases in an energy-consuming manner (Jain et al., 2016). Similarly, DEAD-box proteins with ATPase activity were also found to be important for maintaining and regulating PB dynamics and turn-over of mRNAs and protein components (Kim & Myong, 2016; Mugler et al., 2016).

Laboratory techniques like genetic screens and knockdown approaches are particularly useful for identifying which proteins mediate granule assembly but are not without caveats. For instance, a screen of yeast SG-defective mutants identified many factors related to translation such as eIF4G2 (Tif4632) and Arc1 (Yang et al., 2014). However, the results of this screen are complicated because the necessity of a given factor for SG nucleation can change in different stress conditions and cell types. For example, G3BP is not required for SG assembly in some osmotic or heat shock stresses but is thought essential for assembly under arsenite-induced oxidative stress (Kedersha et al., 2016). To further add to this complexity, the necessity of these components can be redundant. For example, double-deletion of Edc3 and Lsm4 abolished PB

formation in yeast but this was rescued by overexpressing Dhh1 (Rao & Parker, 2017). This complexity calls to mind the complexity that underlies stress-dependent differences in mRNP material state discussed above. Understanding what proteins are necessary for stress-induced mRNP granule formation must be done with proper care; consideration of cell-type and stressor used must be accounted for when one determines what proteins are essential for both SG and PB assembly. Tracking differences in the necessity and redundancy of proteins that mediate stress-induced mRNP granule assembly across stress conditions will likely offer clues into the different functions that these granules have in responding to distinct environmental cues.

2.4.3 Interaction networks between proteins influence stress-induced mRNP granules

Complex networks of interactions mediate mRNP granule assembly, maintenance, and disassembly. Understanding the interactions between macromolecular components may give insight into why some proteins are more important than others in granule assembly and maintenance. Resident protein components can be classified as scaffolds or clients (Ditlev et al., 2018). Scaffolds are proteins required for mRNP granule assembly as described above, while clients are concentrated in the granule via interactions with scaffold components. The distinction between scaffolds and clients can be blurred and condition-dependent in varied biological contexts. Scaffolds are considered to be more concentrated than clients in the granule and are supposed to have higher degrees of interactions. We analyzed the interactions of SG and PB protein components (Figure 2.2); the hubs in these interaction networks have higher likelihoods to function as scaffolds that are essential for granule assembly (Hubstenberger et al., 2017; Jain et al., 2016; Youn et al., 2018). It is important to note that many interactions identified during stress were preexistent in non-stressed conditions, although no SGs and only small numbers of PBs were formed. One possible explanation is that interactions during normal

growth state are sub-stoichiometric, while interactors become more concentrated in granules during stress. Additionally, the preexisting interactions may drive the pre-assembly of sub-microscopic granules in normal conditions that cannot be observed with conventional microscopy techniques. These possibilities remain to be tested (Youn et al., 2018). Regardless, there is little doubt that understanding protein-protein interaction networks will shed light on the formation of stress-induced mRNP granules and offer potential insight into their function during stress.

The interactions in mRNP granules can be classified as specific interactions when proteins or mRNAs have limited binding partners or as promiscuous, non-specific interactions when they do not. Specific interactions in granules are usually mediated by well-folded domains or short linear motifs (SLiMs) of IDRs that specifically interact with well-folded domains of other RBPs (Fromm et al., 2014). For example, Edc3 dimerization via a YjeF-N domain is important for PB formation in yeast (Decker et al., 2007). G3BP dimerization and interactions with Caprin-1 are important for mammalian SG formation (Kedersha et al., 2016). Also, post-translational modifications (PTMs) can regulate granule formation by altering specific interactions. For example, methylation of the RGG domains of FUS or EWS recruits Tudor domain-containing proteins (Goulet et al., 2008). NEDDylation of SRSF3 in SGs is required for interaction with TIA-1 (Jayabalan et al., 2016). Banani et al. showed one possibility of how specific interactions drive scaffolds to recruit specific clients and promote LLPS through use of a SUMO/SIM system. Despite these specific interactions, formation of complex, *in vivo* granules also requires promiscuous interactions mediated by longer IDRs (Figure 2.3). Since IDRs do not hold well-folded structure they can interact with other proteins non-specifically. It has been shown that *in vitro* LLPS driven by specific protein-RNA

interactions is enhanced by addition of promiscuously interacting IDRs. In yeast, PB formation

is promoted by IDRs in cooperation with specific interactions (Protter et al., 2018). It is

generally thought that neither specific nor non-specific interactions are individually sufficient

to drive stress-induced granule formation, as promiscuous IDRs are not sufficient to form

granules *in vivo* if specific interactions are not also present in certain contexts. For example,

high expression levels of fusion proteins hnRNPA1-Cry2 or DDX4-Cry2 cannot phase separate

in cells, unless the Cry2 protein is triggered to assemble via light-activated, specific

interactions (Shin et al., 2017). Notably, as previously described, RBPs are vastly enriched in

both SGs and PBs, suggesting that interactions between RBPs and mRNA transcripts might

also play an important role granule assembly that goes beyond protein-protein interactions (Jain

et al., 2016). In fact, in addition to multivalent proteins, some longer RNAs can actually serve

as scaffolds and thus promote LLPS (Schütz et al., 2017). Overall, synergistic and tuned

networks of interactions mediate the formation and maintenance of stress-induced mRNP

granules. The identity of these protein components and their interactions potentially drive the

specificity of what mRNA transcripts are enriched and excluded from these granules and

parsing them might further inform our understanding of how SGs and PBs influence gene

expression during cellular stress response.
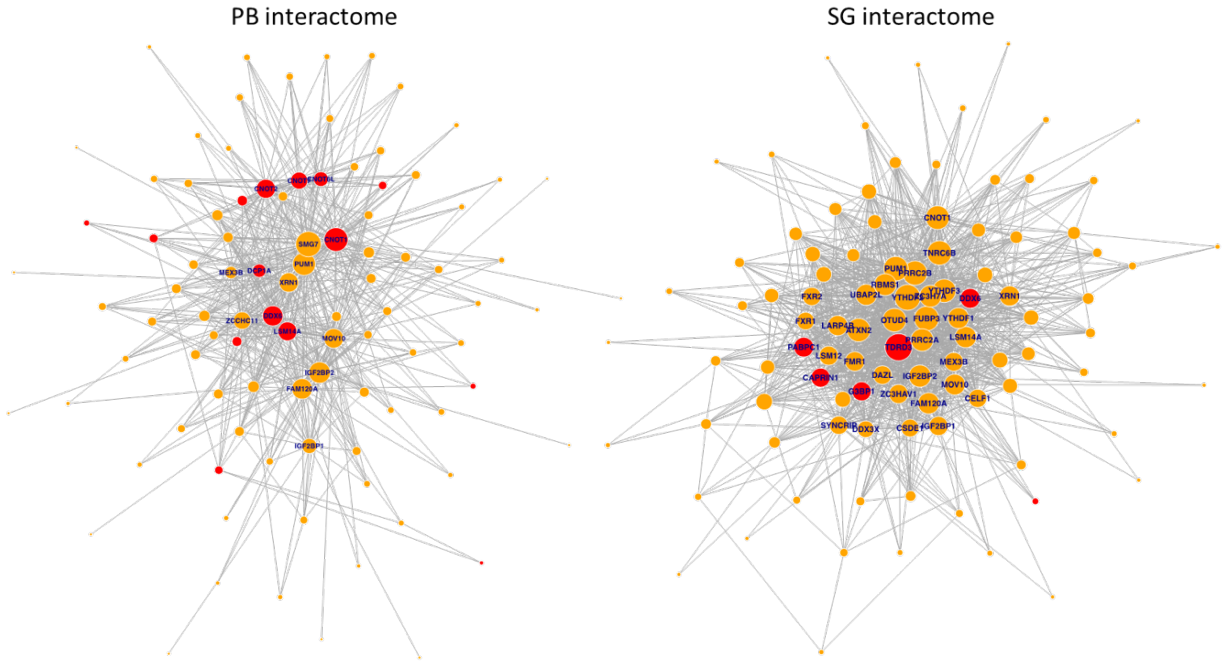
Figure 2.2. Interactions between mammalian PB and SG protein components.
Gene names of proteins with more than 15 interacting protein components in PBs are shown (left network) while those with more than 30 interacting protein components in SGs are shown (right network). Proteins that were identified as essential components for PB or SG assembly are highlighted in red; these tend to have increased numbers of interacting partners. Mammalian interactome datasets of PB and SG components are from Young et al., 2016. The mammalian SG proteome is from Jain et al., 2016 and the PB proteome is from Hubstenberger et al., 2017.
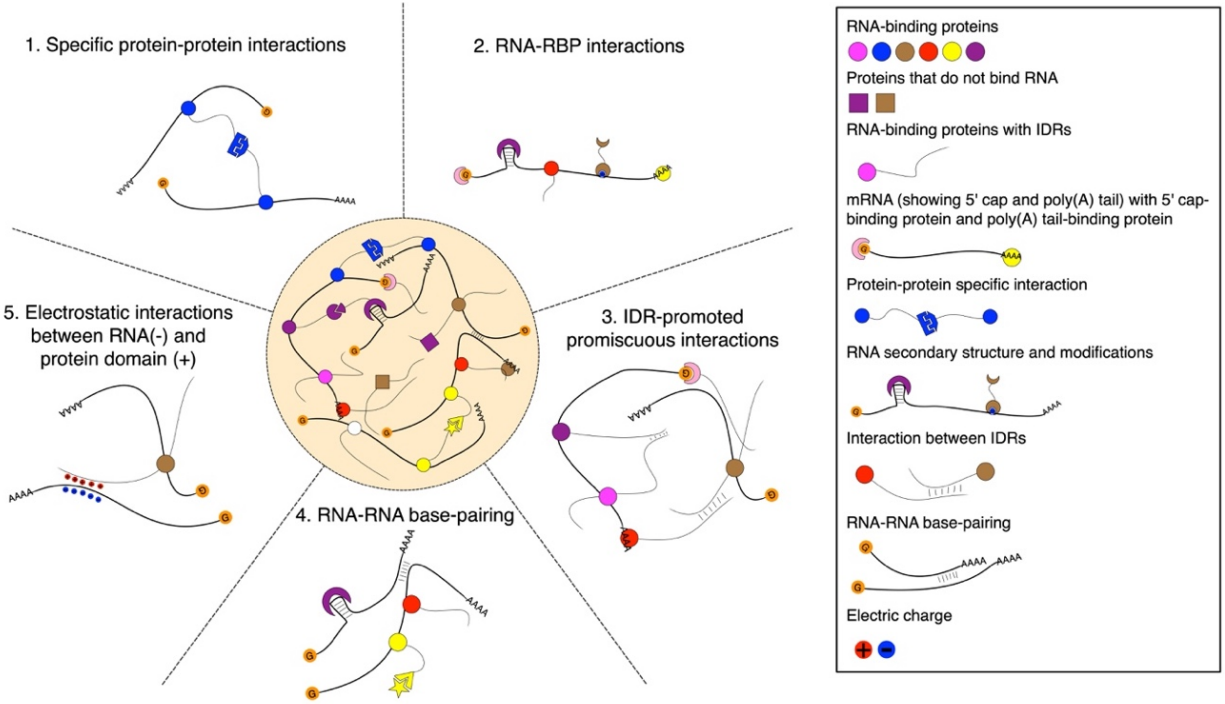
Figure 2.3. Diverse sets of interactions drive mRNP granule assembly and LLPS.
Five classes of interactions that contribute to SG and PB formation are modeled. Different protein-protein, protein-RNA, and protein-protein interactions contribute to phase separation and drive the formation of stress-induced mRNP granules.

2.5 RNA Properties and Composition in Stress-Induced mRNP Granules

Although a thorough and accurate understanding of the proteins found in SGs and PBs across organisms, cell types, and stressors is necessary to gain deep insight into granule function, one must take an equally deep look at RNA content, particularly at mRNA, to fully realize granule influence on gene expression during stress. The identity and fate of mRNAs in SGs and PBs has remained more elusive than those of proteins for many reasons. First, RNA is more transient and unstable in the cell relative to protein. This makes isolation and subsequent characterization of RNA from a liquid-like, membrane-less granule contained within the larger cytoplasm a challenge. There are also larger varieties of RNAs relative to proteins in SGs and PBs; recent studies identify hundreds of proteins but thousands of RNA species, indicating the necessity of genome-wide approaches for systematic identification (Hubstenberger et al., 2017; Khong et al., 2017). Furthermore, initial studies that provided insight into granule formation and utility during stress paid limited attention to the contribution of individual RNA components in stress-induced granules relative to protein components. Researchers proposed roles based on the functions and identities of proteins, rather than RNAs, identified within them and it was not until recently that studies began to provide genome-wide analyses of enriched RNAs. The protein components of granules enable one to make informed speculations about how these structures influence the fate of mRNAs. However, it is important to directly study the fate of mRNAs that are recruited to RNP granules in order to fully appreciate their function. Fortunately, advances in mRNP granule purification, RNA-sequencing, and single-molecule resolution mRNA imaging have provided valuable insight into the RNAs of SGs and PBs and have advanced and refined our understanding of their regulation. We discuss below a current view of RNA properties relevant to phase separation, RNA components in both SGs and PBs,

and how this understanding further informs our perception of the role RNP granules might have in gene expression during stress.

2.5.1 General, biophysical properties of RNAs can influence mRNP granule dynamics

When considering mRNP granule-mediated translation regulation from an RNA-centric perspective, it is prudent to consider how general biophysical properties of RNAs influence phase separation. Unsurprisingly, mRNP granule stability is dependent on RNA concentration and identity, in addition to the presence of previously discussed mRNP-nucleating proteins. For instance, PBs can be dissolved by RNase treatment (Teixeir et al., 2005). Positively charged IDRs on proteins interact with negatively charged mRNAs via electrostatic interactions that influence LLPS propensity (Aumiller & Keating, 2015; Schütz et al., 2017). In addition to charge, RNA secondary structure can influence the properties of phase-separated granules and in fact can control whether LLPS occurs at all. For example, an *in vitro* reconstitution system shows that recruitment of CLC3 RNA as well as other RNAs into droplets of Whi3, a disordered RBP found in PBs and SGs, is dependent upon CLC3 RNA secondary structure (Langdon et al., 2018). A similar system demonstrated that some RNAs prevent Whi3 droplets from aggregating and help maintain their liquid-like state (Zhang et al., 2015). Conversely, disease-associated RNAs with repeat expansions can serve as templates for multivalent base pairing that drives granule self-assembly and shifts the equilibrium towards phase separation *in vitro* and in human cells (Jain & Vale, 2017). Ultimately, an appreciation of how RNA's physical properties affect its capacity to act as a protein scaffold and influence granule formation will be important considerations during analysis of sequence and structural elements both shared and lacking in mRNAs present in SGs and PBs. One must understand and

appreciate both RNA-RNA and RNA-protein interactions to determine to what extent a given RNA species may be found in a granule.

2.5.2 RNA-polysome interactions influence mRNP dynamics

The degree of interaction between ribosomes and mRNAs is of particular importance when considering the relationship between stress-induced mRNP granule formation, protein translation, and changing gene expression during stress. The repression of translation during stress response yields an abundance of nontranslating mRNAs disengaged from polysomes in the cytoplasm within minutes (Kershaw & Ashe, 2017). As previously stated, stress also induces SG and PB formation on the same time scale. Both types of stress-induced mRNP granules accumulate nontranslating mRNAs (Buchan et al., 2008). These observations suggest that there is a direct balance or stoichiometry between levels of polysome engagement, free mRNAs, and stress-induced mRNP granule abundance (Figure 2.4). This balance, in turn, might help control or limit protein production during a period when overall translation is greatly reduced. Levels of polysome engagement and RNA abundance have been shown to directly influence granule assembly in an RNA-dependent manner. For example, cycloheximide (CHX), an inhibitor of ribosomal translocation that traps mRNAs in polysomes, can repress formation of both PBs and SGs and even dissolve preformed granules (Teixeira et al., 2005). Conversely, addition of puromycin, a drug that dissociates ribosomes from mRNAs actually triggers SG formation (Buchan et al., 2008; Kedersha et al., 2000). This implies that one must consider the translational status of mRNAs as well as the more general biophysical properties of RNAs discussed above to understand RNA's roles in granule assembly, maintenance, and disassembly as well as broader mRNP function during stress.

Finally, to fully parse the biological function of SGs and PBs in the context of stress response, one needs to understand not only general changes in polysome engagement but also what transcripts are localized where in the cytoplasm, how transient this localization is, and what distinguishes mRNAs selected for translation into protein during and after stress. It has been suggested the mRNAs can move in and out of mRNP granules due to their liquid-like state. In fact, some mRNAs have been proposed not only to move in and out of a PB or SG but to actually shuttle between granules and polysomes on the timescale of minutes, linking mRNPs to highly controlled regulation of translation during stress even more directly (Brengues et al., 2005; Mollet et al., 2008). These observations, in turn, lead to many questions: what are the proportions and identities of cytoplasmic mRNAs and their bound proteins recruited into granules when translation is downregulated, how dynamically does the mRNA pool actually move into and out of these granules during and after stress in living cells, what proteins accompany such movements, how specific or promiscuous is mRNA recruitment to granules, and how are stress-induced, pro-survival genes excluded from these granules during times of stress to ensure their robust translation. It was not until very recently that we had a genome-wide snapshot of the mRNAs included and excluded from SGs and PBs (Hubstenberger et al., 2017; Namkoong et al., 2018; Wang et al., 2018). The datasets generated by these studies, discussed in more detail below, provide a newfound opportunity to begin to answer to some of the questions outlined above and provide clues or directions for research that can begin to address the others.
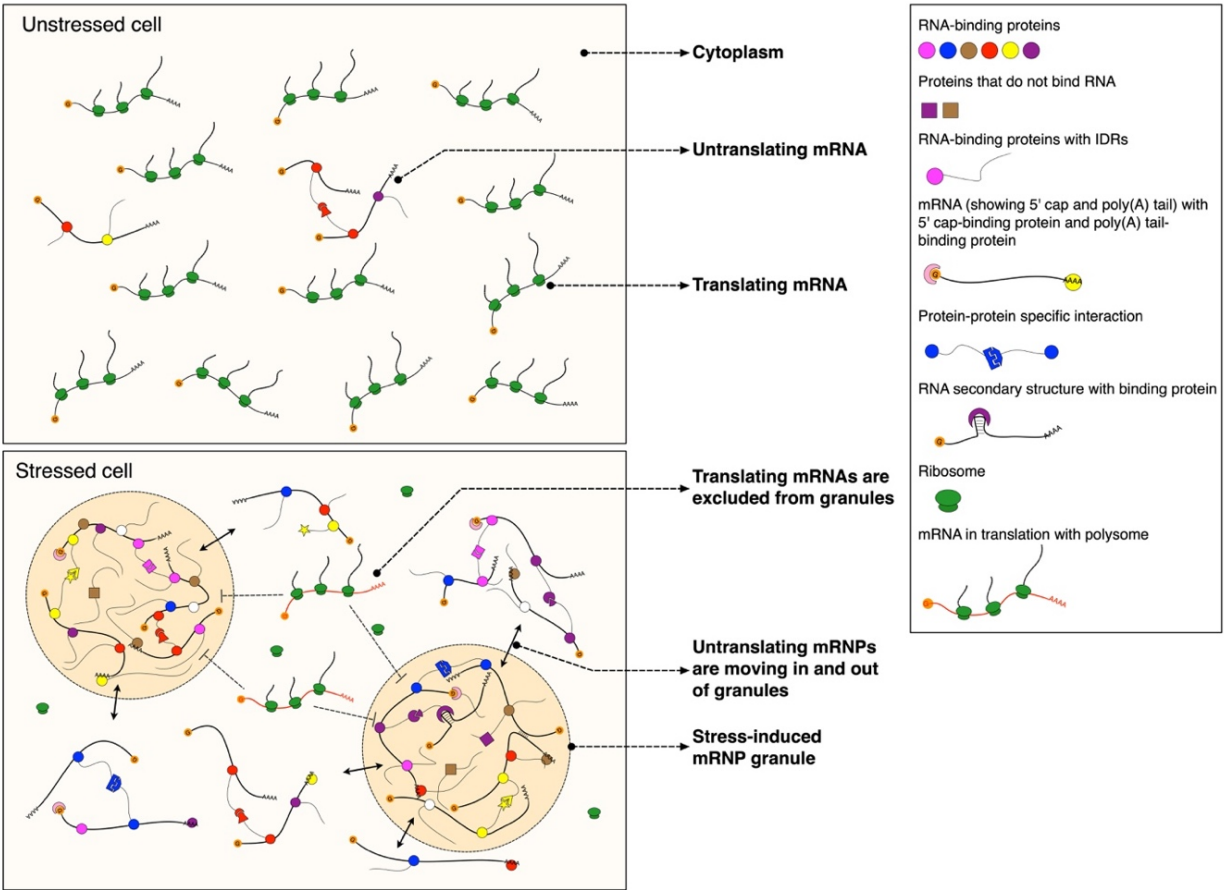
Figure 2.4. Model for composition dynamics and potential function of stress-induced mRNP granules.
Lines with double arrows show that mRNAs associated with RBPs move in and out of stress-induced mRNP granules. Dashed lines with inhibitory arrows show that mRNAs engaged in translation are excluded from stress-induced mRNP granules.

2.5.3 Characteristics of mRNAs targeted to mRNPs during stress

A surge of recent studies has provided the broadest look into the RNP granule transcriptome to date for both yeast and mammalian models (Hubstenberger et al., 2017; Namkoong et al., 2018; Wang et al., 2018). These studies used varied methods to purify intact RNP granules and report that approximately 10-20% of bulk RNAs in the cytoplasm localize to them; the vast majority (~80%) are mRNAs though ncRNAs are also recruited. A portion of these studies discovered a relationship between certain 3' UTR features and favorable granule recruitment. For instance, swapping the endogenous 3'UTRs of specific PB-localized transcripts with non-eukaryotic 3' UTRs was sufficient to halt PB localization of those mRNAs in stressed yeast (Wang et al., 2018). Additionally, a motif search revealed 3' AU-rich elements (AREs) are most strongly correlated with SG-targeting of mRNAs upon analysis of motifs in the SG-enriched transcriptome isolated during mammalian ER stress (Namkoong et al., 2018). This suggests the possibility that interactions between certain 3' UTRs and ARE-binding, SG-localized proteins such as TIAR and TIA-1 might contribute to directing and sequestering mRNAs to mRNP granules. More generally, it is likely that 3' UTR sequences and other untranslated features influence localization of some mRNAs into SGs and PBs.

Although the presence of ARE motifs and the 3'UTR dependence of some granule-localized RNAs is intriguing, it is not sufficient to explain the complex regulatory interactions that target the huge range of mRNAs that localize to granules during stress. Nonetheless, deeper dives into other motifs or sequence features common to stress-induced mRNP granule-localized RNAs have provided very limited insight into what other characteristics intrinsic to mRNAs might drive them to PBs and SGs. Systematic analysis of binding motifs is complicated by the huge variety of RBPs found in these granules, which in turn, have an even

larger range of client mRNAs. Furthermore, not all RBPs that localize to PBs or SGs have strong binding motifs. In fact, for many prominent mRNP granule-localized RNA-binding proteins, researchers have failed to identify consensus binding motifs (Ishigaki et al., 2012; Mitchell et al., 2013; Rogelj et al., 2012). For instance, for the PB proteins Pat1, Dhh1, and Lsm1, CLIP-Seq data failed to identify any strong consensus sequence (Mitchell et al., 2013). More generally, the degree of promiscuity and randomness versus tightly regulated specificity of mRNA recruitment into mRNP granules during stress remains unclear. Therefore, there might not be all that many RNA sequence features that cause recruitment to SGs and PBs through recognition by specific RBPs. It is possible that the concentrated environment of a phase-separated granule promotes more nonspecific protein-RNA interactions and so identifying consensus sequences in RNA targets will continue to be elusive. Furthermore, it has been shown that RNA-RNA interactions also contribute to granule formation (Van Treeck & Parker, 2018). Therefore, taken together, not only do some specific RNA-protein interactions contribute to the identity and proportion of mRNAs that are recruited into a PB or SG during a specific stress but so do RNA-RNA interactions and nonspecific RNA-protein interactions. Importantly, the relative extent of each contribution is an open question.

Although the search for sequence commonalities has returned limited results there is another characteristic of mRNAs more strongly correlated with SG and PB enrichment: length. Khong et al. performed RNA-sequencing of purified SG cores from U2OS cells and found that SG-enriched mRNAs are, on average, thousands of base pairs longer than those depleted from SGs. Similarly, bulk purification of all RNP granules (PBs and SGs) from stressed NIH3T3 cells revealed that granule-enriched mRNAs are thousands of base pairs longer than mRNAs not targeted to granules (Namkoong et al., 2018). If the length of a transcript is indeed the most

correlative indicator of RNP granule localization during stress this also sheds relatively little light on how sequences within mRNAs target them to granules, thus leaving the specificity in targeting an open question. It might even indicate that longer mRNAs are recruited into SGs and PBs more often simply because a longer mRNA necessarily has a longer primary sequence and this provides more chances for potential nonspecific, promiscuous interactions with RBPs or other RNAs.

The lion's share of analysis on transcriptome-wide sequencing data from stress-induced mRNP-isolated RNAs has focused on parsing characteristics and identities of genes that reside within SGs and PBs. However, to fully understand how stress impacts translation, one must consider the other side of the data: what mRNAs are not found in SGs and PBs and what mechanisms prevent certain RNAs from recruitment into them? It is known that some transcripts such as those encoding certain heat-shock proteins (HSPs) remain diffusely localized and well translated in the cytoplasm during stress. These are predominantly stress associated mRNAs such as Hsp30, Hsp26, Hsp12, Hsp70, and Hsp90 (Kedersha & Anderson, 2002; Lavut & Raveh, 2012; Stöhr et al., 2006; Zid & O'Shea, 2014). Our previous data implied that during glucose starvation in yeast, it is not the mRNA sequence that determines exclusion of Hsp mRNAs from mRNP granules. Instead, information in the promoter sequence drives cytoplasmic mRNA localization (Zid & O'Shea, 2014). The details of mechanisms that enable this exclusion remain elusive and could likely be informed by a thorough parsing of the SG and PB-excluded transcriptome. In general, we expect that researchers will need to think outside the box and look beyond primary sequences of mRNAs that are recruited to SGs and PBs to solve the puzzle of what directs their recruitment to mRNP granules during stress. Fortunately, some preliminary clues to this puzzle might have already been discovered. For

example, it is known that ribosomal proteins, which interact with mRNAs during non-stress

conditions, are depleted from PBs while protein-coding mRNAs are enriched. At the same

time, noncoding RNAs are depleted from PBs (Hubstenberger et al., 2017). This hints that

previous translation and engagement with ribosomes might be a factor in driving mRNA

localization to PBs through an unknown mechanism. When it comes to SGs, very recent work

has highlighted how the compaction status of a transcript influences its propensity for

recruitment. Two separate groups used single-molecule FISH to observe the distance between

the 3' and 5' ends of mRNAs; both found that compaction increased for mRNAs recruited into

granules, indicating that the spatial organization of a transcript influences its localization

(Adivarahan et al., 2018; Kong & Parker, 2018). Lastly, a correlation exists between a

transcript's mRNP enrichment and its translational efficiency (TE), as determined by ribosome

profiling. Ribosome profiling is an RNA-sequencing based technique that provides a

nucleotide-resolution 'snapshot' of translation by generating a library of RNA fragments

engaged with ribosomes. Traditionally, the occupancy of ribosomes across a gene is quantified

and compared to whole transcriptome measurements to generate a measurement of TE (Ingolia

et al., 2009). It was found that TE measurements are lower for mRNAs enriched in SGs and

PBs relative to depleted mRNAs (Hubstenberger et al., 2017; Khong et al., 2017). This

information begets speculation that characteristics that determine the translatability of a mRNA

might impact its propensity for ribosome engagement and mRNP localization in an interrelated

way, hinting that well-translated mRNAs have characteristics that confer granule exclusion.

What exactly these characteristics are remains to be seen.

2.6 Stress-Induced mRNP Granules: Function

The stress-inducible formation of SGs and PBs is conserved from yeast to mammals in response to a broad array of stresses. It has also been found that mutants that cannot appropriately form these mRNP granules are more sensitive to stress (Eisinger-Mathason et al., 2008; Kwon et al., 2007; Lavut & Raveh, 2012; Riback et al., 2017; Yang et al., 2014). These data imply that mRNP granules play an important role during stress, yet identifying the actual molecular function of the membrane-less compartments in the cell has proven challenging. One reason for this is that stress in itself has such dramatic effects on gene expression. It can be hard to decouple the formation of mRNP granules from the broad changes induced by stress. While stress-induced mRNP granules were originally posited to have functions related to the function of the proteins concentrated within them, it is unclear if the physical properties of the cytoplasm that govern protein-RNA interactions can be directly compared to those inside phase separated mRNP granules (Helder et al., 2016). Therefore, many established hypotheses on mRNP granule function are currently being reassessed through *in vitro* models of phase separation that can be tested outside of the context of stress response as well as through modern technological advances that allow higher resolution in imaging and sequencing. Below we discuss current attitudes about SG and PB function, unresolved questions related to function, and potential experimental approaches that might help elucidate them.

2.6.1 Stress granule function

As described above, many translation initiation components and translational repressors are concentrated in SGs. While certain mRNAs are enriched in SGs, the impact this sequestration has on gene expression is unclear. Only ~10-20% of bulk mRNA species reside in SGs yet there is a global shutdown of translation during stress. Some speculate that SGs assist

with this aspect of stress response but it is unclear how SGs can act as broad and global

translational repressors during stress if up to ~80-90% of mRNAs remain excluded and

distributed through the cytoplasm. Secondly, inhibiting visible SG formation was shown to

have no effect on global translation during stress (Buchan et al., 2008; Kedersha et al., 2016) or

on mRNA half-life (Bley et al., 2015; Buchan et al., 2008). While some specific mRNAs have

been found to be altered translationally when specific SG proteins are mutated and SG

formation is perturbed (Damgaard & Lykke-Andersen, 2011; Gilks, 2004; Mazroui et al., 2007;

Moeller et al., 2004; Tsai et al., 2008), it is unclear whether these effects are mediated by

aberrant SG localization itself or if they simply reflect changes made by the absence of the wild

type protein.

An alternative function for SGs may be in helping cells recover upon cessation of the

stress response. As much of the translation initiation machinery is present in SGs, it may be that

mRNAs enriched in SGs are translationally repressed during stress but some portion of this

population is translationally primed for protein synthesis upon stress relief. The knowledge of

which mRNAs are enriched in SGs combined with the advent of ribosome profiling provides

opportunity for an exciting direction: measurement of the effects that SG dissolution has on

mRNA-specific ribosome loading as well as comparison of the timing of ribosome loading onto

SG-enriched versus SG-depleted mRNAs after stress ends. Such an experiment would provide

insight into the possibility that SGs form to enable rapid engagement of translation machinery

with sequestered mRNAs and provide insight into the purpose of SG formation more generally.

A very exciting application of this approach would be to isolate SGs and perform profiling

specifically on the 40S subunit, as described in Archer et al., 2016. The abundance and

identities of transcripts found by this approach would shed light on the presumed but unverified

notion that SGs house mRNAs that are engaged with pre-initiation complexes and are primed

for reintroduction into the translating pool upon cessation of stress and resumption of growth.

2.6.2 P-body function

PBs were historically proposed to be sites of mRNA degradation due to the abundance

of decapping factors and exonucleases found within them. Furthermore, yeast strains that had

mutations in mRNA degradation machinery showed large increases in the number and size of

visible PBs (Sheth & Parker, 2003). Finally, an unstable mRNA that had a polyG sequence

inserted to block the exonuclease Xrn1 from fully degrading it accumulated in PBs (Sheth &

Parker, 2003). From these results it was concluded that PBs are likely concentrated hubs of

mRNA degradation. While these results did point to mRNA decay intermediates, which

presumably have very low translatability, accumulating in PBs they did not show whether the

actual processing of these mRNAs was taking place inside or outside of the membrane-less

compartments. A number of papers have presented contradictory evidence to the notion that

PBs serve as hubs of decay and the field is now considering the possibility of a more storage-

based role for PBs during stress, leaving active mRNA decay as a process that takes place in

the larger cytoplasm. Researchers have found that visible PB formation is not directly

necessary for RNA decay; these granules can be disrupted without inhibiting global RNA

decay pathways (Ayache et al., 2015; Eulalio et al., 2007). There has also been a lack of

degradation intermediates present in recently sequenced, PB-enriched mRNAs (Hubstenberger

et al., 2017). This same study reports that depletion of the PB protein DDX6 causes PB

dissolution but does not increase levels of PB-enriched mRNAs. Further studies have used

fluorescent microscopy to follow the decay of single mRNAs that are labeled at their 5' and 3'

ends with different fluorescently tagged coat proteins. Over time there was no accumulation of

degradation products in PBs (Horvathova et al., 2017). It was also found that there is a general

decline in mRNA degradation during stress that is independent of where the reporter mRNA

was localized, either in PBs or outside of PBs. This general stabilization of mRNAs during

stress has also been previously seen in both yeast and mammalian cells (Gowrishankar et al.,

2006; Hilgers et al., 2006). Further microscopy-based studies found that inhibition of reporter

mRNA degradation continues for about two hours after stress removal and that the kinetics of

degradation appear to be independent of whether an mRNA was localized to a PB or not

(Wilbertz et al., 2018). Finally, using purified decapping proteins along with accessory proteins

and RNA, studies were able to drive *in vitro* LLPS, potentially reconstituting PBs (Schütz et

al., 2017). It was found that RNA contained within these *in vitro* reconstituted PBs was

protected from endonucleolytic cleavage and that enzymatic activity of the decapping enzyme

was greatly decreased (Schütz et al., 2017). Combined, this evidence strongly points towards a

storage role for PBs that house a subset of translationally repressed mRNAs during stress and,

more generally, demonstrates that caution should be applied when speculating about the

function of stress-induced granules.

2.6.3 mRNP granules: alternative functions

While much of the research on mRNP granules has rightly focused on the function of

the proteins and mRNAs within the granules, an alternative possibility is that the phase

separation of translation initiation factors and mRNA degradation machinery into SGs and PBs,

respectively, is to reduce the working concentration of these proteins in the aqueous regions of

the cytoplasm. This possibility would help to remedy the contradiction that, though only a

small portion of mRNAs in the cell are present in SGs or PBs, the majority of mRNAs present

during early stages of stress are from non-stress induced mRNAs. We have observed that after

15 minutes of glucose starvation in yeast, about 90% of the mRNAs present within the cell are from non-stress induced mRNAs (B.M.Z, unpublished data). One factor that must be taken into account when considering this alternative possibility is the intracellular volume that SGs and PBs occupy. Generally, mRNP granules constitute only a minor portion of cellular volume, approximately 1% or less (Banani S. et al 2017). And while proteins are very highly concentrated within granules (for example in mammalian SGs, G3BP1 protein is 13-fold more concentrated in the SG shell than the cytoplasm and about 30-fold more concentrated in the core than it is in the shell; Jain S et al., 2016), it is unclear if this would cause significant enough depletion to have a functional impact. Very recently, quantitative measurements have been performed on yeast PB proteins to compare their concentration inside and outside of PBs (Xing et al., 2018). For Dcp2 protein, the catalytic subunit of the decapping enzyme complex, more than 30% becomes sequestered in PBs. Other accessory decapping proteins such as Edc3 and Pat1 have greater than 20% of their protein content sequestered into P-bodies. The supports the notion that the function of PBs would be to reduce mRNA decapping activity in the bulk cytoplasm, rather than to concentrate it in a granule, which is consistent with the previously mentioned observations that there is a general decline in mRNA degradation during stress regardless of whether a transcript is sequestered into PBs or not.

A different possibility is that visible phase separation during stress is just an indicator or consequence of broader remodeling happening globally to smaller mRNP complexes that exist throughout the cell. Proteins interact with a transcript throughout its life, creating sub-microscopic mRNP complexes that can be translationally active or inactive. At any given point in time, a relatively small number of total cellular protein and RNA is contained in a granule. However, we know that both proteins and mRNAs are dynamically exchanging between mRNP

granules and the cytoplasm. Could mRNP complexes that are competent to enter or have previously exited an mRNP granule be in a 'modified' state, even outside of the granule? To date, we don't know if there are changes to the molecular composition of interacting RNAs and proteins as they leave the membrane-less compartment; current techniques only capture granules at a given point in time and don't reveal if and how many molecules in the general cytoplasm were prior mRNP residents. This alternative proposal is not without some grounding in previous research. For example, during non-stress conditions, the SG component protein Pab1 is predominantly in a soluble, i.e. non-pelletable, state when cell extracts are treated with RNase I (Riback et al., 2017). Yet, during a mild heat stress, about half of the Pab1 molecules transition to insoluble, pelletable quinary assemblies, though no visible SGs form. At higher temperatures when visible SGs do form, over 90% of Pab1 transitions to a pelletable state even though a much smaller portion of total Pab1 resides within phase separated mRNP granules. Therefore, it could be that some mRNAs not directly contained within mRNP granules still interact with their protein partners in "altered", mRNP-dependent states relevant for survival during stress. For example, post-translational modifications of proteins have been implicated in granule formation. If these proteins are rapidly exchanging with the environment, presumably many proteins not found in the granule at any specific time will still be modified upon leaving the granule. What percent of proteins are modified? How would these modifications affect protein function when they exist as part of mRNP complexes that are sub-microscopic and are no longer contained within the granule? Further investigations into the changes mRNP complexes undergo both within and outside mRNP granules during stress will need to be undertaken to address this possibility. One exciting, relevant direction would be to perform a timecourse experiment that employs a proximity labeling and proteomics approach to see if

certain PTMs are upregulated on PB or SG-enriched proteins in both granule and cytoplasmic fractions. If a certain protein is modified in the granule and then released back into the cytoplasm, thereby changing its function, you would expect this to be reflected over the timecourse.

Finally, the role of stress-induced mRNP granules could be entirely passive. As previously described, one proposed function of mRNP granules it to store RNAs throughout the duration of stress to allow optimal growth upon recovery as this provides avoidance of extraneous transcription and nuclear export. A recently considered possible, complementary function of mRNP granules is that instead of only serving as RNA storage depots they may also serve as protein storage depots for growth proteins that are not needed during stressful conditions but that the cell may not want to immediately degrade. After all, stress is transitory and dynamic in nature. As evidence consider the yeast pyruvate kinase protein Cdc19, a key regulator of glycolytic metabolism and cell growth. This protein has been found to form reversible aggregates that co-localize with stress granules during stress. This aggregation was found to be a protective mechanism from stress-induced degradation as, upon stress relief, it proves to be reversible and allows quick re-entry into the cell cycle because these proteins do not have to be re-expressed (Saad et al., 2017). It is possible, therefore, that stress-induced granule formation evolved as a means to coordinate cellular machinery in a way that enables its rapid and efficient deployment in the cell once conditions are more favorable for growth and energy-consumption.

2.7 Conclusion

There has been a recent surge in research focusing on phase separation in biological processes. The formation of stress-induced mRNP granules is a broadly conserved example of this phase separation, but for all of this intense study the importance of this phase separation remains unclear. Overall, there has been much progress in understanding the formation and composition of stress-induced mRNP granules. Yet, somewhat surprisingly, this knowledge has only led to marginal increases in our understanding of the function of these membrane-less compartments within the cell. Moving forward, there are a number of distinct directions that may prove fruitful in elucidating the function of stress-induced mRNP granules. *In vitro* reconstitution has been an important tool for understanding many biochemical and biophysical processes. Several recent advances that helped elucidate mechanisms of biological LLPS have come from reconstitution of these systems *in vitro* (Banani et al., 2016; Han et al., 2012; Jain & Vale, 2017; Li et al., 2012; Molliex et al., 2015). While progress has been made in making reductionist systems *in vitro*, some of the properties of mRNP granules may arise because of their complexity. Thus, reduction of granules to limited protein or mRNA components may mask some emergent properties and it would be worth studying if and how an increase in protein and RNA types alters *in vitro* phase separation to more closely mimic granules in cells. *In vitro* studies of stress induced mRNP granules will also need to be cognizant of role that ATP plays in the dynamics of mRNP granules (Jain et al., 2016) and ATP's ability to directly solubilize molecules in aqueous solutions as a biological hydrotrope (Patel et al., 2017). Lastly, a worthwhile avenue would be combined use of techniques like single molecule FISH and SHAPE probing of RNA secondary structure before and after *in vitro* phase separation to

address the relationship between RNA compaction and granule entry to determine the extent to which RNAs undergo compaction before, during, or after entry into granules.

Another exciting direction important to understanding how the assembly of these granules directly affects function is the ability to perturb phase separation in a more controlled, stress-independent manner *in vivo*. While overexpression of certain proteins is sufficient to drive phase separation without stress, an exciting new direction is using the Arabidopsis thaliana cryptochrome 2 photolyase homology region to drive light-inducible phase separation (Shin et al., 2017; Taylor et al., 2018). This potentially allows experiments to dynamically drive phase separation in cells and thus provide understanding of what effect LLPS has on the physiology of the cell in a way that is decoupled from stress or obscured by consequences of overexpression. Intriguingly, recent experiments have shown that light-induced phase separation of the SG protein G3BP1 is sufficient to recruit many other core SG components and polyadenylated RNA (Taylor et al., 2018). Lastly, more work must be done that employs methods to directly measure the impact of mRNP granules on gene expression. Recent work using microscopy based *in vivo* reporters of translation and mRNA decay have given interesting insights into what these mRNP granules may and may not be doing (Horvathova et al., 2017; Moon et al., 2018; Pitchiaya et al., 2018; Wilbertz et al., 2018). Further single molecule measurements are needed, particularly in live cells, to increase the diversity of mRNA species analyzed and to directly follow mRNAs that were previously localized to mRNP granules after stress is abated to resolve their fate. Such single molecule approaches could be complemented by a genome-wide approach described in two exciting, recently posted preprints that utilize a novel technique that applies APEX-based proximity labeling to RNA called APEX-seq (Fazal et al., 2018; Padròn et al., 2018). The latter preprint analyzed stress-

specific impacts on mRNA localization and offers powerful insight into the relationship

between protein localization and RNA localization during stress. Combinations of these *in vitro*

and *in vivo* approaches will likely help shed light on the elusive function of PBs and SGs and

ultimately inform our understanding of cellular function during stress, potentially offering

insight into disease states linked to aberrant stress response and granule assembly.

Acknowledgements

References

Adivarahan, S., Livingston, N., Nicholson, B., Rahman, S., Wu, B., Rissland, O. S., & Zenklusen, D. (2018). Spatial organization of single mRNPs at different stages of the gene expression pathway. *Molecular Cell, 72*(4), 727– 738. https://doi.org/10.1016/j.molcel.2018.10.010

Alberti, S. (2018). Guilty by Association: Mapping Out the Molecular Sociology of Droplet Compartments. *Molecular Cell*, *69*(3), 349–351. https://doi.org/10.1016/j.molcel.2018.01.020

Andrei, M. A., Ingelfinger, D., Heintzmann, R., Achsel, T., Rivera-Pomar, R., & Lührmann, R. (2005). A role for eIF4E and eIF4E-transporter in targeting mRNPs to mammalian processing bodies. *RNA*, *11*(5), 717–727. https://doi.org/10.1261/rna.2340405

Angarica, E. V., Ventura, S., & Sancho, J. (2013). Discovering putative prion sequences in complete proteomes using probabilistic representations of Q/N-rich domains. *BMC Genomics*, *14*(1), 1–17. https://doi.org/10.1186/1471-2164-14-316

Archer, S.K., Shirokikh, N. E., Beilharz, T. H., & Preiss, T. (2016). Dynamics of ribosome scanning and recycling revealed by translation complex profiling. *Nature, 535,* 570–574. https://doi.org/10.1038/nature18647

Ashburner, M., Ball, C. A., Blake, J. A., Botstein, D., Butler, H., Cherry, J. M., Davis, A. P., Dolinski, K., Dwight, S. S., Eppig, J. T., Harris, M. A., Hill, D. P., Issel-Tarver, L., Kasarskis, A., Lewis, S., Matese, J. C., Richardson, J. E., Ringwald, M., Rubin, G. M., & Sherlock, G. (2000). Gene Ontology: tool for the unification of biology. *Nature Genetics*, *25*(1), 25–29. https://doi.org/10.1038/75556

Aumiller, W. M., & Keating, C. D. (2015). Phosphorylation-mediated RNA/peptide complex coacervation as a model for intracellular liquid organelles. *Nature Chemistry*, *8*(2), 129– 137. https://doi.org/10.1038/nchem.2414

Ayache, J., Bénard, M., Ernoult-Lange, M., Minshall, N., Standart, N., Kress, M., & Weil, D. (2015). P-body assembly requires DDX6 repression complexes rather than decay or Ataxin2/2L complexes. *Molecular Biology of the Cell*, *26*(14), 2579–2595. https://doi.org/10.1091/mbc.e15-03-0136

Banani, S. F., Lee, H. O., Hyman, A. A., & Rosen, M. K. (2017). Biomolecular condensates: organizers of cellular biochemistry. *Nature Reviews. Molecular Cell Biology*, *18*(5), 285– 298. https://doi.org/10.1038/nrm.2017.7

Banani, S. F., Rice, A. M., Peeples, W. B., Lin, Y., Jain, S., Parker, R., & Rosen, M. K. (2016). Compositional Control of Phase-Separated Cellular Bodies. *Cell*, *166*(3), 651–663. https://doi.org/10.1016/j.cell.2016.06.010

Bashkirov, V. I., Scherthan, H., Solinger, J. A., Buerstedde, J. M., & Heyer, W. D. (1997). A mouse cytoplasmic exoribonuclease (mXRN1p) with preference for G4 tetraplex substrates. *Journal of Cell Biology, 136*(4): 761–773. https://doi.org/10.1083/jcb.136.4.761

B Beckmann, B. M., Horos, R., Fischer, B., Castello, A., Eichelbaum, K., Alleaume, A. M., Schwarzl, T., Curk, T., Foehr, S., Huber, W., Krijgsveld, J., & Hentze, M. W. (2015). The RNA-binding proteomes from yeast to man harbour conserved enigmRBPs. *Nature Communications, 6*(1), 10127. https://doi.org/10.1038/ncomms10127

Bley, N., Lederer, M., Pfalz, B., Reinke, C., Fuchs, T., Glaß, M., Möller, B., & Hüttelmaier, S. (2015). Stress granules are dispensable for mRNA stabilization during cellular stress. *Nucleic Acids Research, 43*(4), e26–e26. https://doi.org/10.1093/nar/gku1275

Brangwynne, C. P., Eckmann, C. R., Courson, D. S., Rybarska, A., Hoege, C., Gharakhani, J., Jülicher, F., & Hyman, A. A. (2009). Germline P granules are liquid droplets that localize by controlled dissolution/condensation. *Science, 324*(5935), 1729–1732. https://doi.org/10.1126/science.1172046

Brengues, M., Teixeira, D., & Parker, R. (2005). Movement of eukaryotic mRNAs between polysomes and cytoplasmic processing bodies. *Science, 310*(5747), 486–8075. https://doi.org/10.1126/science.1115791

Buchan, J. R., Muhlrad, D., & Parker, R. (2008). P bodies promote stress granule assembly in Saccharomyces cerevisiae. *Journal of Cell Biology, 183*(3), 441–455. https://doi.org/10.1083/jcb.200807043

Buchan, J. R., & Parker, R. (2009). Eukaryotic Stress Granules: The Ins and Outs of Translation. *Molecular Cell, 36*(6), 932–941. https://doi.org/10.1016/j.molcel.2009.11.020

Carbon, S., Dietze, H., Lewis, S. E., Mungall, C. J., Munoz-Torres, M. C., Basu, S., … Westerfield, M. (2017). Expansion of the gene ontology knowledgebase and resources: The gene ontology consortium. *Nucleic Acids Research, 45*(D1), D331–D338. https://doi.org/10.1093/nar/gkw1108

Damgaard, C. K., & Lykke-Andersen, J. (2011). Translational coregulation of 5'TOP mRNAs by TIA-1 and TIAR. *Genes and Development, 25*(19), 2057–2068. https://doi.org/10.1101/gad.17355911

Dang, Y., Kedersha, N., Low, W. K., Romo, D., Gorospe, M., Kaufman, R., Anderson, P., & Liu, J. O. (2006). Eukaryotic initiation factor 2alpha-independent pathway of stress granule induction by the natural product pateamine A. *Journal of Biological Chemistry, 281*(43), 32870–32878. https://doi.org/10.1074/jbc.M606149200

De Leeuw, F., Zhang, T., Wauquier, C., Huez, G., Kruys, V., & Gueydan, C. (2007). The cold-inducible RNA-binding protein migrates from the nucleus to cytoplasmic stress granules

by a methylation-dependent mechanism and acts as a translational repressor. *Experimental Cell Research*, *313*(20), 4130–4144. https://doi.org/10.1016/j.yexcr.2007.09.017

Decker, C. J., Teixeira, D., & Parker, R. (2007). Edc3p and a glutamine/asparagine-rich domain of Lsm4p function in processing body assembly in Saccharomyces cerevisiae. *Journal of Cell Biology*, *179*(3), 437–449. https://doi.org/10.1083/jcb.200704147

Ditlev, J. A., Case, L. B., & Rosen, M. K. (2018). Who's In and Who's Out-Compositional Control of Biomolecular Condensates. *Journal of Molecular Biology*, *430*(23), 4666–4684. https://doi.org/10.1016/j.jmb.2018.08.003

Eisinger-Mathason, T. S., Andrade, J., Groehler, A. L., Clark, D. E., Muratore-Schroeder, T. L., Pasic, L., Smith, J. A., Shabanowitz, J., Hunt, D. F., Macara, I. G., & Lannigan, D. A. (2008). Codependent functions of RSK2 and the apoptosis-promoting factor TIA-1 in stress granule assembly and cell survival. *Molecular Cell, 31*(5), 722–736. https://doi.org/10.1016/j.molcel.2008.06.025

Eulalio, A., Behm-Ansmant, I., Schweizer, D., & Izaurralde, E. (2007). P-body formation is a consequence, not the cause, of RNA-mediated gene silencing. *Molecular and Cellular Biology*, *27*(11), 3970–3981. https://doi.org/10.1128/MCB.00128-07

Fazal F.M., Han S., Kaewsapsak P., Parker K.R., Xu J., Boettiger A.N., Chang H.Y., & Ting A.Y. (2018) Atlas of Subcellular RNA Localization Revealed by APEX-seq. *BioRxiv*. https://doi.org/10.1101/454470

Franks, T. M., & Lykke-Andersen, J. (2008). The control of mRNA decapping and P-body formation. *Molecular Cell*, *32*(5), 605–615. https://doi.org/10.1016/j.molcel.2008.11.001

Fromm, S. A., Kamenz, J., Noldeke, E. R., Neu, A., Zocher, G., & Sprangers, R. (2014). In vitro reconstitution of a cellular phase-transition process that involves the mRNA decapping machinery. *Angewandte Chemie (International ed. in English)*, *53*(28), 7354–7359. https://doi.org/10.1002/anie.201402885

Gilks, N. (2004). Stress Granule Assembly Is Mediated by Prion-like Aggregation of TIA-1. *Molecular Biology of the Cell*, *15*(12), 5383–5398. https://doi.org/10.1091/mbc.E04-08-0715

Goulet, I., Boisvenue, S., Mokas, S., Mazroui, R., & Cote, J. (2008). TDRD3, a novel Tudor domain-containing protein, localizes to cytoplasmic stress granules. *Human Molecular Genetics*, *17*(19), 3055–3074. https://doi.org/10.1093/hmg/ddn203

Gowrishankar, G., Winzen, R., Dittrich-Breiholz, O., Redich, N., Kracht, M., & Holtmann, H. (2006). Inhibition of mRNA deadenylation and degradation by different types of cell stress. *Biological Chemistry*, *387*(3), 323–327. https://doi.org/10.1515/BC.2006.043

Han, T. W., Kato, M., Xie, S., Wu, L. C., Mirzaei, H., Pei, J., Chen, M., Xie, Y., Allen, J.,

Xiao, G., & McKnight, S. L. (2012). Cell-free formation of RNA granules: bound RNAs identify features and components of cellular assemblies. *Cell, 149*(4), 768–779. https://doi.org/10.1016/j.cell.2012.04.016

Helder, S., Blythe, A. J., Bond, C. S., & Mackay, J. P. (2016). Determinants of affinity and specificity in RNA-binding proteins. *Current Opinion in Structural Biology*, *38*, 83–91. https://doi.org/10.1016/j.sbi.2016.05.005

Hilgers, V., Teixeira, D., & Parker, R. (2006). Translation-independent inhibition of mRNA deadenylation during stress in Saccharomyces cerevisiae. *RNA*, *12*(10), 1835–1845. https://doi.org/10.1261/rna.241006

Horvathova, I., Voigt, F., Kotrys, A. V., Zhan, Y., Artus-Revel, C. G., Eglinger, J., Stadler, M. B., Giorgetti, L., & Chao, J. A. (2017). The Dynamics of mRNA Turnover Revealed by Single-Molecule Imaging in Single Cells. *Molecular Cell, 68*(3), 615–625.e9. https://doi.org/10.1016/j.molcel.2017.09.030

Hubstenberger, A., Courel, M., Bénard, M., Souquere, S., Ernoult-Lange, M., Chouaib, R., Yi, Z., Morlot, J. B., Munier, A., Fradet, M., Daunesse, M., Bertrand, E., Pierron, G., Mozziconacci, J., Kress, M., & Weil, D. (2017). P-Body Purification Reveals the Condensation of Repressed mRNA Regulons. *Molecular Cell*, *68*(1), 144–157 e5. https://doi.org/10.1016/j.molcel.2017.09.003

Ishigaki, S., Masuda, A., Fujioka, Y., Iguchi, Y., Katsuno, M., Shibata, A., Urano, F., Sobue, G., & Ohno, K. (2012). Position-dependent FUS-RNA interactions regulate alternative splicing events and transcriptions. *Scientific Reports, 2*, 529. https://doi.org/10.1038/srep00529

Jain, A., & Vale, R. D. (2017). RNA phase transitions in repeat expansion disorders. *Nature*, *546*(7657), 243–247. https://doi.org/10.1038/nature22386

Jain, S., Wheeler, J. R., Walters, R. W., Agrawal, A., Barsic, A., & Parker, R. (2016). ATPase-Modulated Stress Granules Contain a Diverse Proteome and Substructure. *Cell*, *164*(3), 487–498. https://doi.org/10.1016/j.cell.2015.12.038

Jayabalan, A. K., Sanchez, A., Park, R. Y., Yoon, S. P., Kang, G. Y., Baek, J. H., Anderson, P., Kee, Y., & Ohn, T. (2016). NEDDylation promotes stress granule assembly. *Nature Communications, 7*, 12125. https://doi.org/10.1038/ncomms12125

Kedersha, N., & Anderson, P. (2002). Stress granules: sites of mRNA triage that regulate mRNA stability and translatability. *Biochemical Society Transactions*, *30*(Pt 6), 963–969. https://doi.org/10.1042/bst0300963

Kedersha, N., Cho, M. R., Li, W., Yacono, P. W., Chen, S., Gilks, N., Golan, D. E., & Anderson, P. (2000). Dynamic Shuttling of Tia-1 Accompanies the Recruitment of mRNA to Mammalian Stress Granules. *Journal of Cell Biology*, *151*(6), 1257–1268.

https://doi.org/10.1083/jcb.151.6.1257

Kedersha, N. L., Gupta, M., Li, W., Miller, I., & Anderson, P. (1999). RNA-binding proteins TIA-1 and TIAR link the phosphorylation of eIF-2α to the assembly of mammalian stress granules. *Journal of Cell Biology*, *147*(7), 1431–1442. https://doi.org/10.1083/jcb.147.7.1431

Kedersha, N., Panas, M. D., Achorn, C. A., Lyons, S., Tisdale, S., Hickman, T., Thomas, M., Lieberman, J., McInerney, G. M., Ivanov, P., & Anderson, P. (2016). G3BP-Caprin1-USP10 complexes mediate stress granule condensation and associate with 40S subunits. *Journal of Cell Biology*, *212*(7), 845–860. https://doi.org/10.1083/jcb.201508028

Kedersha, N., Stoecklin, G., Ayodele, M., Yacono, P., Lykke-Andersen, J., Fritzler, M. J., Scheuner, D., Kaufman, R. J., Golan, D. E., & Anderson, P. (2005). Stress granules and processing bodies are dynamically linked sites of mRNP remodeling. *Journal of Cell Biology*, *169*(6), 871–884. https://doi.org/10.1083/jcb.200502088.

Kershaw, C. J., & Ashe, M. P. (2017). Untangling P-Bodies: Dissecting the Complex Web of Interactions that Enable Tiered Control of Gene Expression. *Molecular Cell*, *68*(1), 3–4. https://doi.org/10.1016/j.molcel.2017.09.032

Khong, A., Matheny, T., Jain, S., Mitchell, S. F., Wheeler, J. R., & Parker, R. (2017). The Stress Granule Transcriptome Reveals Principles of mRNA Accumulation in Stress Granules. *Molecular Cell*, *68*(4), 808–820.e5. https://doi.org/10.1016/j.molcel.2017.10.015

Kim, Y., & Myong, S. (2016). RNA Remodeling Activity of DEAD Box Proteins Tuned by Protein Concentration, RNA Length, and ATP. *Molecular Cell*, *63*(5), 865–876. https://doi.org/10.1016/j.molcel.2016.07.010

Kroschwald, S., Maharana, S., Mateju, D., Malinovska, L., Nüske, E., Poser, I., Richter, D., & Alberti, S. (2015). Promiscuous interactions and protein disaggregases determine the material state of stress-inducible RNP granules. *ELife*, *4*, e06807. https://doi.org/10.7554/eLife.06807

Kwon, S., Zhang, Y., & Matthias, P. (2007). The deacetylase HDAC6 is a novel critical component of stress granules involved in the stress response. *Genes and Development*, *21*(24), 3381–3394. https://doi.org/10.1101/gad.461107

Lancaster, A. K., Nutter-Upham, A., Lindquist, S., & King, O. D. (2014). PLAAC: A web and command-line application to identify proteins with prion-like amino acid composition. *Bioinformatics*, *30*(17), 2501–2502. https://doi.org/10.1093/bioinformatics/btu310

Langdon, E. M., Qiu, Y., Ghanbari Niaki, A., McLaughlin, G. A., Weidmann, C. A., Gerbich, T. M., Smith, J. A., Crutchley, J. M., Termini, C. M., Weeks, K. M., Myong, S., & Gladfelter, A. S. (2018). mRNA structure determines specificity of a polyQ-driven phase

separation. *Science, 360*(6391), 922–927. https://doi.org/10.1126/science.aar7432

Lavut, A., & Raveh, D. (2012). Sequestration of highly expressed mrnas in cytoplasmic granules, p-bodies, and stress granules enhances cell viability. *PLoS Genetics*, *8*(2), e1002527. https://doi.org/10.1371/journal.pgen.1002527

Li, P., Banjade, S., Cheng, H. C., Kim, S., Chen, B., Guo, L., Llaguno, M., Hollingsworth, J. V., King, D. S., Banani, S. F., Russo, P. S., Jiang, Q. X., Nixon, B. T., & Rosen, M. K. (2012). Phase transitions in the assembly of multivalent signalling proteins. *Nature, 483*(7389), 336–340. https://doi.org/10.1038/nature10879

Li, X. H., Chavali, P. L., Pancsa, R., Chavali, S., & Babu, M. M. (2018). Function and Regulation of Phase-Separated Biological Condensates. *Biochemistry*, *57*(17), 2452–2461. https://doi.org/10.1021/acs.biochem.7b01228

Luo, Y., Na, Z., & Slavoff, S. A. (2018). P-Bodies: Composition, Properties, and Functions. *Biochemistry*, *57*(17), 2424–2431. https://doi.org/10.1021/acs.biochem.7b01162

Markmiller, S., Soltanieh, S., Server, K. L., Mak, R., Jin, W., Fang, M. Y., Luo, E. C., Krach, F., Yang, D., Sen, A., Fulzele, A., Wozniak, J. M., Gonzalez, D. J., Kankel, M. W., Gao, F. B., Bennett, E. J., Lécuyer, E., & Yeo, G. W. (2018). Context-Dependent and Disease-Specific Diversity in Protein Interactions within Stress Granules. *Cell*, *172*(3), 590–604.e13. https://doi.org/10.1016/j.cell.2017.12.032

Marnef, A., Maldonado, M., Bugaut, A., Balasubramanian, S., Kress, M., Weil, D., & Standart, N. (2010). Distinct functions of maternal and somatic Pat1 protein paralogs. *RNA*, *16*(11), 2094–2107. https://doi.org/10.1261/rna.2295410

Mateju D., Franzmann T. M., Patel A., Kopach A., Boczek E. E., Maharana S., …Alberti, S. (2017). An aberrant phase transition of stress granules triggered by misfolded protein and prevented by chaperone function. *The EMBO Journal, 36*(12), 1669–1687. http://doi.org/10.15252/embj.201695957

Mazroui, R., Di Marco, S., Kaufman, R. J., & Gallouzi, I.-E. (2007). Inhibition of the Ubiquitin-Proteasome System Induces Stress Granule Formation. *Molecular Biology of the Cell*, *18*(7), 2603–2618. https://doi.org/10.1091/mbc.E06

Mazroui, R., Sukarieh, R., Bordeleau, M. E., Kaufman, R. J., Northcote, P., Tanaka, J., Gallouzi, I., & Pelletier, J. (2006). Inhibition of ribosome recruitment induces stress granule formation independently of eukaryotic initiation factor 2alpha phosphorylation. *Molecular Biology of the Cell, 17*(10), 4212–4219. https://doi.org/10.1091/mbc.e06-04-0318

Mitchell, S. F., Jain, S., She, M., & Parker, R. (2013). Global analysis of yeast mRNPs. *Nature Structural and Molecular Biology*, *20*(1), 127–133. https://doi.org/10.1038/nsmb.2468

Moeller, B. J., Cao, Y., Li, C. Y., & Dewhirst, M. W. (2004). Radiation activates HIF-1 to regulate vascular radiosensitivity in tumors: Role of reoxygenation, free radicals, and stress granules. *Cancer Cell*, *5*(5), 429–441. https://doi.org/10.1016/S1535-6108(04)00115-1

Mokas, S., Mills, J. R., Garreau, C., Fournier, M. J., Robert, F., Arya, P., Kaufman, R. J., Pelletier, J., & Mazroui, R. (2009). Uncoupling stress granule assembly and translation initiation inhibition. *Molecular Biology of the Cell, 20*(11), 2673–2683. https://doi.org/10.1091/mbc.e08-10-1061

Mollet, S., Cougot, N., Wilczynska, A., Dautry, F., Kress, M., Bertrand, E., & Weil, D. (2008). Translationally Repressed mRNA Transiently Cycles through Stress Granules during Stress. *Molecular Biology of the Cell*, *19*(10), 4469–4479. https://doi.org/10.1091/mbc.E08-05-0499

Molliex, A., Temirov, J., Lee, J., Coughlin, M., Kanagaraj, A. P., Kim, H. J., Mittag, T., & Taylor, J. P. (2015). Phase separation by low complexity domains promotes stress granule assembly and drives pathological fibrillization. *Cell*, *163*(1), 123–133. https://doi.org/10.1016/j.cell.2015.09.015

Moon, S. L., Morisaki, T., Khong, A., Lyon, K., Parker, R., & Stasevich, T. J. (2018). Imaging of single mRNA translation repression reveals diverse interactions with mRNP granules. *BioRxiv*. https://doi.org/10.1101/332692

Mugler, C. F., Hondele, M., Heinrich, S., Sachdev, R., Vallotton, P., Koek, A. Y., Chan, L. Y., & Weis, K. (2016). ATPase activity of the DEAD-box protein Dhh1 controls processing body formation. *ELife, 5*, e18746. https://doi.org/10.7554/eLife.18746

Namkoong, S., Ho, A., Woo, Y. M., Kwak, H., & Lee, J. H. (2018). Systematic Characterization of Stress-Induced RNA Granulation. *Molecular Cell, 70*(1), 175–187.e8. https://doi.org/10.1016/j.molcel.2018.02.025

Ohn, T., Kedersha, N., Hickman, T., Tisdale, S., & Anderson, P. (2008). A functional RNAi screen links O-GlcNAc modification of ribosomal proteins to stress granule and processing body assembly. *Nature Cell Biology*, *10*(10), 1224–1231. https://doi.org/10.1038/ncb1783

Padròn A., Iwasaki S., & Ingolia N.T. (2018). Proximity RNA labeling by APEX-Seq Reveals the Organization of Translation Initiation Complexes and Repressive RNA Granules. *BioRxiv*. https://doi.org/10.1101/454066

Parker, R., & Sheth, U. (2007). P bodies and the control of mRNA translation and degradation. *Molecular Cell*, *25*(5), 635–646. https://doi.org/10.1016/j.molcel.2007.02.011

Patel, A., Malinovska, L., Saha, S., Wang, J., Alberti, S., Krishnan, Y., & Hyman, A. A. (2017). ATP as a biological hydrotrope. *Science, 356*(6339), 753–756.

https://doi.org/10.1126/science.aaf6846

Pitchiaya, S., Mourao, M., Jalihal, A. P., Xiao, L., Jiang, X., Chinnaiyan, A. M., Schnell, S., & Walter, N. G. (2018). Dynamic recruitment of single RNAs to processing bodies depends on RNA functionality. *BioRxiv*. https://doi.org/10.1101/375295

Protter, D. S. W., Rao, B. S., Van Treeck, B., Lin, Y., Mizoue, L., Rosen, M. K., & Parker, R. (2018). Intrinsically Disordered Regions Can Contribute Promiscuous Interactions to RNP Granule Assembly. *Cell Reports*, *22*(6), 1401–1412. https://doi.org/10.1016/j.celrep.2018.01.036

Rao, B. S., & Parker, R. (2017). Numerous interactions act redundantly to assemble a tunable size of P bodies in Saccharomyces cerevisiae. *Proceedings of the National Academy of Sciences of the United States of America, 114*(45), E9569–E9578. https://doi.org/10.1073/pnas.1712396114

Riback, J. A., Katanski, C. D., Kear-Scott, J. L., Pilipenko, E. V, Rojek, A. E., Sosnick, T. R., & Drummond, D. A. (2017). Stress-Triggered Phase Separation Is an Adaptive, Evolutionarily Tuned Response. *Cell*, *168*(6), 1028–1040 e19. https://doi.org/10.1016/j.cell.2017.02.027

Rogelj, B., Easton, L. E., Bogu, G. K., Stanton, L. W., Rot, G., Curk, T., Zupan, B., Sugimoto, Y., Modic, M., Haberman, N., Tollervey, J., Fujii, R., Takumi, T., Shaw, C. E., & Ule, J. (2012). Widespread binding of FUS along nascent RNA regulates alternative splicing in the brain. *Scientific Reports, 2*, 603. https://doi.org/10.1038/srep00603

Saad, S., Cereghetti, G., Feng, Y., Picotti, P., Peter, M., & Dechant, R. (2017). Reversible protein aggregation is a protective mechanism to ensure cell cycle restart after stress. *Nature Cell Biology*, *19*(10), 1202–1213. https://doi.org/10.1038/ncb3600

Schütz, S., Nöldeke, E. R., & Sprangers, R. (2017). A synergistic network of interactions promotes the formation of in vitro processing bodies and protects mRNA against decapping. *Nucleic Acids Research*, *45*(11), 6911–6922. https://doi.org/10.1093/nar/gkx353

Serman, A., Le Roy, F., Aigueperse, C., Kress, M., Dautry, F., & Weil, D. (2007). GW body disassembly triggered by siRNAs independently of their silencing activity. *Nucleic Acids Research*, *35*(14), 4715–4727. https://doi.org/10.1093/nar/gkm491

Shah, K. H., Zhang, B., Ramachandram, V., & Herman, P. K. (2013). Processing body and stress granule assembly occur by independent and differentially regulated pathways in Saccharomyces cerevisiae. *Genetics,* 193(1):109-23. https://doi: 10.1534/genetics.112.146993

Sheth, U., & Parker, R. (2003). Decapping and decay of messenger RNA occur in cytoplasmic processing bodies. *Science*, *300*(5620), 805–8075.

Shin, Y., Berry, J., Pannucci, N., Haataja, M. P., Toettcher, J. E., & Brangwynne, C. P. (2017). Spatiotemporal Control of Intracellular Phase Transitions Using Light-Activated optoDroplets. *Cell*, *168*(1–2), 159–171 e14. https://doi.org/10.1016/j.cell.2016.11.054

Stöhr, N., Lederer, M., Reinke, C., Meyer, S., Hatzfeld, M., Singer, R. H., & Hüttelmaier, S. (2006). ZBP1 regulates mRNA stability during cellular stress. *Journal of Cell Biology*, *175*(4), 527–534. https://doi.org/10.1083/jcb.200608071

Taylor, J. P., Zhang, P., Fan, B., Yang, P., Temirov, J., Messing, J., & Kim, H. J. (2018). OptoGranules reveal the evolution of stress granules to ALS-FTD pathology. *BioRxiv*. https://doi.org/10.1101/348870

Teixeira, D., Sheth, U., Valencia-Sanchez, M. A., Brengues, M., & Parker, R. (2005). Processing bodies require RNA for assembly and contain nontranslating mRNAs. *RNA*, *11*(4), 371–382. https://doi.org/10.1261/rna.7258505

Tourriere, H., Chebli, K., Zekri, L., Courselaud, B., Blanchard, J. M., Bertrand, E., & Tazi, J. (2003). The RasGAP-associated endoribonuclease G3BP assembles stress granules. *Journal of Cell Biology*, *160*(6), 823–831. https://doi.org/10.1083/jcb.200212128

Tsai, N. P., Ho, P. C., & Wei, L. N. (2008). Regulation of stress granule dynamics by Grb7 and FAK signalling pathway. *EMBO Journal*, *27*(5), 715–726. https://doi.org/10.1038/emboj.2008.19

Van Treeck, B., & Parker, R. (2018). Emerging Roles for Intermolecular RNA-RNA Interactions in RNP Assemblies. *Cell*, *174*(4), 791–802. https://doi.org/10.1016/j.cell.2018.07.023

Wang, C., Schmich, F., Srivatsa, S., Weidner, J., Beerenwinkel, N., & Spang, A. (2018). Context-dependent deposition and regulation of mRNAs in P-bodies. *Elife*, *7*. https://doi.org/10.7554/eLife.29815

Wang, X., Lu, Z., Gomez, A., Hon, G. C., Yue, Y., Han, D., Fu, Y., Parisien, M., Dai, Q., Jia, G., Ren, B., Pan, T., & He, C. (2013). N6-methyladenosine-dependent regulation of messenger RNA stability. *Nature*, *505*(7481), 117–120. https://doi.org/10.1038/nature12730

Wilbertz, J. H., Voigt, F., Horvathova, I., Roth, G., Zhan, Y., & Chao, J. A. (2018). Single-molecule imaging of mRNA localization and regulation during the integrated stress response. *BioRxiv*. https://doi.org/10.1101/332502

Wilczynska, A. (2005). The translational regulator CPEB1 provides a link between dcp1 bodies and stress granules. *Journal of Cell Science*, *118*(Pt 5), 981–992. https://doi.org/10.1242/jcs.01692

Yang, X., Shen, Y., Garre, E., Hao, X., Krumlinde, D., Cvijović, M., Arens, C., Nyström, T., Liu, B., & Sunnerhagen, P. (2014). Stress granule-defective mutants deregulate stress responsive transcripts. *PLoS Genetics, 10*(11), e1004763. https://doi.org/10.1371/journal.pgen.1004763

Youn, J. Y., Dunham, W. H., Hong, S. J., Knight, J., Bashkurov, M., Chen, G. I., Bagci, H., Rathod, B., MacLeod, G., Eng, S., Angers, S., Morris, Q., Fabian, M., Côté, J. F., & Gingras, A. C. (2018). High-Density Proximity Mapping Reveals the Subcellular Organization of mRNA-Associated Granules and Bodies. *Molecular Cell, 69*(3), 517–532.e11. https://doi.org/10.1016/j.molcel.2017.12.020

Zhang, H., Elbaum-Garfinkle, S., Langdon, E. M., Taylor, N., Occhipinti, P., Bridges, A. A., Brangwynne, C. P., & Gladfelter, A. S. (2015). RNA Controls PolyQ Protein Phase Transitions. *Molecular Cell, 60*(2), 220–230. https://doi.org/10.1016/j.molcel.2015.09.017

Zid, B. M., & O'Shea, E. K. (2014). Promoter sequences direct cytoplasmic localization and translation of mRNAs during starvation in yeast. *Nature*, *514*(7520), 117–121. https://doi.org/10.1038/nature13578

Chapter 3:

Differential translation elongation directs protein synthesis in response to acute glucose deprivation in yeast

3.1 Abstract

Protein synthesis is energetically expensive and its rate is influenced by factors including cell type and environment. Suppression of translation is a canonical response observed during stressful changes to the cellular environment. In particular, inhibition of the initiation step of translation has been highlighted as the key control step in stress-induced translational suppression as mechanisms that quickly suppress initiation are well-conserved across organisms and stressors. However, cells have also evolved complex regulatory means to control translation beyond initiation. Here, we examine the role of the elongation step of translation in yeast subjected to acute glucose deprivation. Use of ribosome profiling and *in vivo* reporter assays demonstrated elongation rates slow progressively following glucose removal. We observed ribosome distribution broadly shifts towards the downstream ends of transcripts after both acute and gradual glucose deprivation but not in response to other stressors. Additionally, on assessed mRNAs, a correlation exists between ribosome density and protein production pre-stress but is lost after. Together, these results indicate that stress-induced elongation regulation causes ribosomes to slow and build up on a considerable proportion of the transcriptome in response to glucose withdrawal. Finally, we report ribosomes that build up along transcripts are competent to resume elongation and complete protein synthesis upon readdition of glucose to starved cells. This suggests yeast have evolved mechanisms to slow translation elongation in response to glucose starvation which do not preclude continuation of protein production from those ribosomes, thereby averting a need for new initiation events to take place to synthesize new proteins.

3.2 Introduction

Unicellular organisms such as the budding yeast *Saccharomyces cerevisiae* divide rapidly when environmental conditions are favorable, including under standard laboratory conditions where yeast is cultured in glucose-rich liquid media. When glucose levels are high, robust expression of an abundance of glycolytic mRNAs is well-coordinated (Gonçalves & Planta, 1998; Morales-Polanco et al., 2021; Schaaff et al., 1989). This allows yeast to take advantage of favorable conditions, ferment, and divide exponentially. Rapid growth requires a massive investment of cellular energy into new protein synthesis (Kafri et al., 2016); however, organisms including yeast must rapidly respond to adverse changes in their environment and adapt gene expression programs to survive stress (Advani & Ivanov, 2019). An important component of response to acute, sudden stress is regulation and reduction of protein synthesis from pre-existing cytoplasmic mRNAs (Liu & Qian, 2014). Logically, reduced translation tends to follow rapid stress induction as the existing transcriptome is no longer programmed for survival under current, newly onerous conditions. In addition, reducing translation from mRNAs encoding proteins that facilitate growth is prudent at the onset of severe stress as it circumvents the time required for nuclear changes in transcription to impact gene expression. Lowering translation also reduces energy consumption and is therefore considered a general hallmark of post-transcriptional gene regulation as rapidly growing cells respond to acute stress.

Decades of research have parsed mechanisms that limit protein synthesis in response to acute stresses (Sheikh & Fornace, 1999). A great deal has focused on initiation as it is proposed to be rate limiting during high growth (Costello et al., 2017; Janapala et al., 2019; Liu & Qian, 2014). Less attention has focused on the other steps of translation, although it is becoming

increasingly appreciated that cells have evolved regulatory steps to control translation in response to stress apart from initiation. For example, eEF2, the protein that catalyzes GTP-dependent ribosome translocation during the elongation step of protein synthesis, has been shown to be phosphorylated in response to acute hyperosmotic and oxidative stresses in yeasts (Sanchez et al., 2019; Teige et al., 2001; Wu et al., 2019). Phosphorylation reduces eEF2 activity, thereby generally attenuating elongation and global protein production (Kenney et al., 2014; Tavares et al., 2014). Mammalian systems also rely on eEF2 phosphorylation via eEF2 kinase to adapt to nutrient deprivation and ribosomal stress (Gismondi et al., 2014; Kang & Lee, 2001; Leprivier et al., 2013). In response to heat shock, researchers have shown that mammalian and yeast cells globally accumulate ribosomes close to their start codons, approximately 60-100 nucleotides downstream of the AUG, which indicates those ribosomes successfully initiated and were slowed early in elongation (Mühlhofer et al., 2019; Shalgi et al., 2013). Here, we employ the stress of acute glucose deprivation in exponentially dividing, log phase yeast to characterize how elongation is regulated temporally in response to glucose withdrawal and subsequent recovery.

Sudden glucose deprivation is a particularly arduous stress for log phase yeast to face because glucose is their preferred carbon source and a key substrate in fermentative growth (Ashe et al., 2000; Kim et al., 2013). Relatedly, understanding how simpler eukaryotic organisms have evolved to confront glucose starvation is relevant to understanding complex human diseases such as diabetes and cancer (Diaz-Ruiz et al., 2011; Jochem et al., 2019; Pineau & Ferreira, 2010). While it has been reported that, after 10 minutes of glucose starvation, there is extensive cessation of S^{35} methionine incorporation, researchers have also observed that housekeeping mRNAs remain engaged in polysomes at both a relative and an

absolute level (Arribere et al., 2011; Zid & O'Shea, 2014). For example, ribosomes remain

bound to the coding sequence (CDS) of the essential glycolytic gene *PGK1* after 10 and 15

minutes of glucose starvation (Brengues et al., 2005; Zid & O'Shea, 2014). As glucose

starvation leads to an extensive reduction in initiation (Ashe et al., 2000; Janapala et al., 2019),

this result indicates that elongation may not take place at pre-stress levels. Given the basal yeast

elongation rate is reported to range between 3-10 amino acids per second (Karpinets et al.,

2006; Riba et al., 2019), we would expect to see ribosomes run off the 1,251bp *PGK1* CDS

after approximately three minutes if elongation rate was unchanged and initiation is indeed

largely halted. This result is seemingly at odds with a narrative prevalent in some stress

response literature which underscores ribosomes run off mRNAs following severe stress.

Runoff is highlighted as a crucial early step in a process that sequesters abundant, pro-growth,

and preexisting mRNAs into phase separated granules (Khong & Parker, 2018; Lee &

Seydoux, 2019; Moon et al., 2019). Importantly, ribosome runoff does occur as evidenced by a

large collapse in the polysome repeatedly shown to take place on the timescale of minutes in

glucose-starved yeast (Arribere et al., 2011; Ashe et al., 2000; Brengues et al., 2005; Holmes et

al., 2004). *PGK1*'s high occupancy, simultaneous with polysome collapse, indicates runoff is

heterogeneous in response to glucose starvation. Therefore, differential elongation may play a

key role in regulating the translation process and explain, in part, why some ribosomes run off

transcripts and some remain bound.

In this article, we sought to better understand how yeast regulate protein synthesis and

alter ribosome-mRNA interactions in the initial minutes following glucose starvation by

focusing not only on general levels of engagement but where ribosomes bind along mRNAs.

We found that glucose starvation causes ribosomes to accumulate downstream on the 3' ends of

many mRNAs. This coincides with a progressively slower rate of elongation, a result we validated with *in vivo* approaches. Moreover, this accumulation is not observed in response to other stresses. We also explored protein synthesis in log phase and glucose starvation conditions to further support our measurements of slowed elongation during glucose starvation and observed that the extent of ribosome engagement on a transcript is not sufficient to predict differences in protein synthesis between pre- and post-stress conditions. Finally, we propose ribosomes that build up on the CDSs of genes can resume translation elongation upon glucose readdition. Furthermore, successful protein synthesis can be observed from these ribosomes independent of newly initiated ones.

3.3 Results

3.3.1 Glucose starvation causes a shift in ribosome allocation along preexisting transcripts

Ribosome profiling is a sequencing technique that isolates fragments of individual mRNAs bound by ribosomes which are then turned into sequencing libraries. It is common for researchers to prepare ribosome profiling and traditional RNA-seq libraries from the same sample to calculate ribosome occupancy (RO) on a gene-by-gene basis and compare changes between sample conditions. Such changes are traditionally ascribed as alterations in translational efficiency (TE) for a given gene (Gerashchenko et al., 2012; Ingolia et al., 2009; Li et al., 2017; Pop et al., 2014; Sen et al., 2015; Wang et al., 2019). However, analysis of the distribution and movements of ribosomes along transcripts at nucleotide resolution can provide deeper insight into translational regulation than simply considering proportionate changes in occupancy. Using ribosome profiling, we first examined the distribution of ribosome profiling reads, known as ribosome-protected fragments (RPFs), along mRNAs that have important roles in glycolysis and growth of a similar or longer length to the 1,251bp *PGK1* transcript in log phase and after 15 minutes of glucose starvation (Figure 3.1A). Ribosomes remain bound to the entire length of these mRNAs after starvation which suggests that elongation is regulated in a way such that ribosome runoff from them is not ubiquitous. If runoff were ubiquitous as a result of unaltered transit rates, we would expect preexisting transcripts of this length to be largely devoid of ribosomes after 15 minutes given that new initiation and aggregate protein synthesis are markedly reduced on a genome-wide (Ashe et al., 2000; Janapala et al., 2019).

We were also struck by the shift in the pattern of the distribution of RPF reads along these CDSs from the upstream 5' end in log phase towards the downstream 3' end during stress. Plotting the distribution of read density along thousands of yeast transcripts revealed a

general shift away from the start codon when compared to log phase, indicative of strong repression in translation initiation (Figure 3.1B; top and middle panels). Importantly, a small subset of stress-induced genes known to be upregulated transcriptionally and translationally mirror the distribution pattern observed during log phase whereby more read density occurs near the start codon (Figure 3.1B; bottom panel). These stress-responsive genes, mostly heat shock proteins, display a decreasing or negative ramp of distribution reported to be characteristic of well-translated genes (Shah et al., 2013). These stress-induced genes evade the general halt in initiation that occurs during glucose starvation and demonstrate our cells were undergoing a stress response. This more general increase in downstream read distribution supports the conjecture that ribosome runoff is heterogeneous, given that a polysome collapse also occurs in glucose starvation conditions relative to log phase.

We next assessed whether this small group of stress-responsive genes have a greater RO after 15 minutes of glucose starvation compared to the rest of the transcriptome as they are uniquely upregulated in response to stress. Furthermore, we would expect comparatively lower occupancy on genes that are well-translated in log phase if they underwent massive runoff during stress. Surprisingly, while transcriptional induction of stress-responsive mRNAs is very high compared to the entire genome, the magnitude of their RO at 15 minutes starvation did not vary from other genes, including the 150 genes that were most highly engaged with ribosomes as assessed by normalized RPF read count during log phase (Figure 3.1C). We were also curious to know the global representation of preexisting and stress-induced transcripts in our samples. The percentage of reads from stress-induced genes in both ribosome profiling and RNA-seq libraries from log phase and 15 minutes of glucose starvation were calculated (Figure 3.1D). Stress-induced transcripts made up a relatively small proportion of total library counts
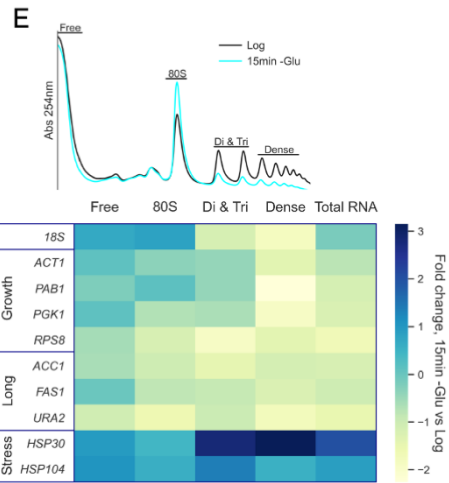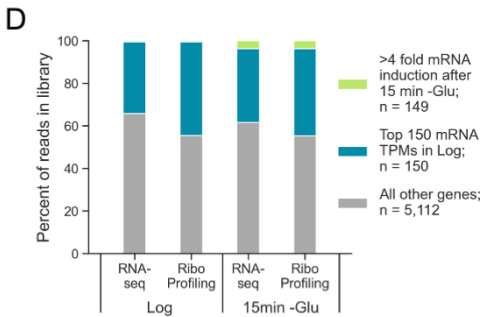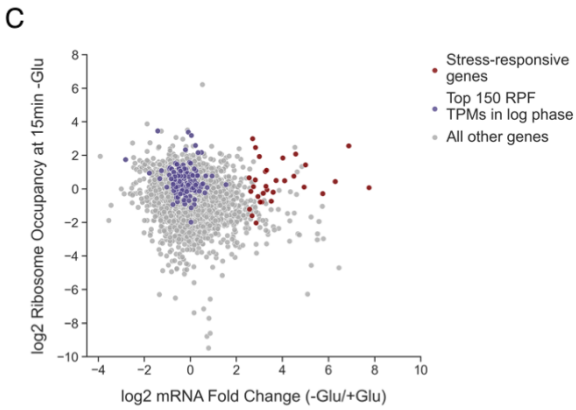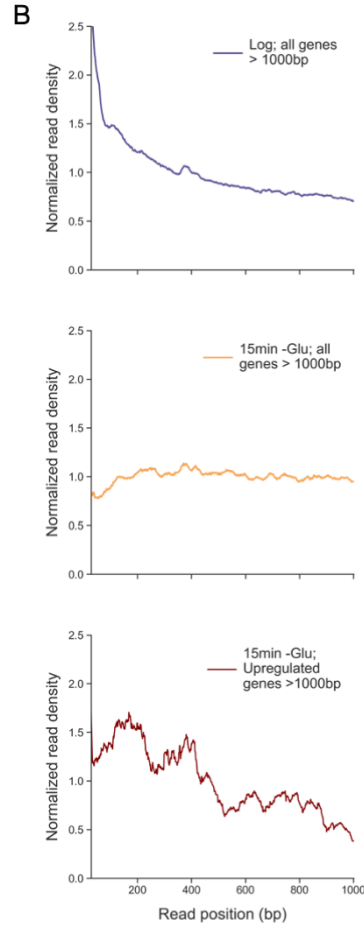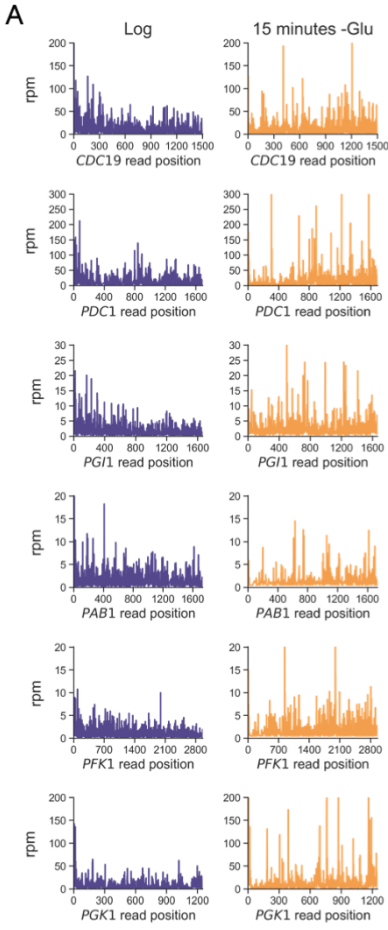
after 15 minutes of starvation. Moreover, the 150 most abundant mRNAs during log phase remain very abundant in both RPF reads and mRNA reads after 15 minutes of stress compared to stress-induced genes and the rest of transcriptome, further highlighting their sustained engagement with ribosomes.

As ribosome profiling and RNA-seq quantify relative changes in abundance of RPFs and mRNAs between samples of interest, polysome profiling was used to assess absolute changes in ribosome engagement to support our observation that considerable ribosome engagement with abundant pre-stress mRNAs continues during stress. Polysome profiling was performed on log phase and glucose starved samples, followed by RNA quantification of select genes with normalization to an exogenous spike-in RNA using qRT-PCR. Fractions were pooled and five total groups were analyzed: a total RNA pool, a free RNA pool, a monosome pool, and two polysome fractions made of a combined disome plus trisome pool and, finally, a dense polysome pool (Figure 3.1F). The polysomes from glucose starved cultures yielded concentrations for several pro-growth, abundant log phase mRNAs that were roughly 2-fold lower than polysomes from glucose replete, log phase cultures. We also assessed the movement of 18S rRNA, stress-induced heat shock genes, and genes that are extremely long, each greater than 6,000bp, considering that the median yeast gene length is 1,280bp. This more targeted approach corroborated our global ribosome profiling data by further showing there is an incomplete ribosome runoff during glucose starvation. It is evident that some transcripts do undergo runoff and leave the polysome. In addition, the polysome collapses though neither process is universal or complete. If ribosome runoff was a straightforward, universal explanation for how translation is regulated in response to glucose starvation, we would expect the magnitude of the shift of abundant growth genes out of heavier polysomes to be much

greater. We would also expect the shift of these growth genes to be several fold higher than the shift observed for extremely long genes, which we wouldn't expect to be able to undergo as much runoff during 15 minutes of starvation, given their length and expected ribosome transit rates. Our data also agrees with previous polysome profiling experiments that showed the continued presence of *PGK1* mRNAs in polysomes during acute glucose starvation (Arribere et al., 2011; Brengues et al., 2005). Together, our ribosome profiling and polysome profiling experiments highlight that sustained engagement broadly continues between preexisting mRNAs and ribosomes in response to acute glucose starvation.

Figure 3.1: Glucose starvation alters ribosome engagement with mRNAs.
(A) RPF reads per million (rpm) by nucleotide position for the indicated genes during log phase (purple; left) and after 15 minutes of glucose starvation (orange; right). (B) Normalized read density plots for indicated gene categories in log phase (purple; top) and after 15 minutes of glucose starvation (orange; middle and bottom; red, respectively). To generate read density plots the aggregate number of reads per single nucleotide position across all genes >1000bp with > 25 reads per gene per library were included and normalized to enable inter-library comparison. (C) Plot of log2 ribosome occupancy (RO) calculated as per gene RPF reads divided by mRNA reads for the same gene in glucose starvation conditions against log2 mRNA induction after 15 minutes of glucose starvation. Abundant log phase genes (purple) were categorized as the 150 transcripts with the highest mean TPM scores in two replicate ribosome profiling libraries. TPM = transcripts per million. For both B and C, genes with mRNA log2 fold change > 2.5 and RO log2 fold change > 0.09 were classified as upregulated in response to glucose starvation. (D) Percentage of all reads in the indicated sequencing libraries by category. 149 genes had >4-fold increase in mRNA reads after 15 minutes of glucose starvation compared to log phase (green). Abundant log phase mRNAs (blue) were categorized as the 150 mRNAs with the highest mean TPM scores in two replicate RNA-seq libraries. There is substantial overlap between the top 150 RFP TPM genes in C and the top 150 mRNA TPM genes in D with 123 total shared. (E) Traces of polysome fractionation gradients showing what fractions were combined (top). Pooled fractions underwent RNA extraction and RT-qPCR for the indicated genes to quantify the changes in transcript abundance in each fraction after 15 minutes of glucose starvation and log phase (bottom). An exogenous, spike-in RNA was used for standardization to quantify abundance in each pool and the fold change in RNA abundance as assessed by ΔΔCt analysis.

A

Log   15 minutes -Glu

CDC19 read position

PDC1 read position

PGI1 read position

PAB1 read position

PFK1 read position

PGK1 read position

B

Log; all genes > 1000bp

15min -Glu; all genes > 1000bp

15min -Glu; Upregulated genes >1000bp

Read position (bp)

C

Stress-responsive genes
Top 150 RPF TPMs in log phase
All other genes

log2 Ribosome Occupancy at 15min -Glu

log2 mRNA Fold Change (-Glu/+Glu)

D

Percent of reads in library

>4 fold mRNA induction after 15 min -Glu; n = 149
Top 150 mRNA TPMs in Log; n = 150
All other genes; n = 5,112

RNA-seq   Ribo Profiling   RNA-seq   Ribo Profiling
Log   15min -Glu

E

Free   80S   Di & Tri   Dense   Total RNA

18S
Growth   ACT1
PAB1
PGK1
RPS8
Long   ACC1
FAS1
URA2
Stress   HSP30
HSP104

Fold change, 15min -Glu vs Log

3.3.2. Ribosome polarity analyses reveal stress-induced ribosome distribution changes are stress-specific and an increase in downstream ribosome accumulation is unique to glucose-limited conditions

Next, we sought to gain insight into ribosome distribution along transcripts genome-wide in a way that would allow us to quantitatively characterize the buildup of ribosomes along mRNAs. To accomplish this, ribosome polarity scores for individual genes were calculated before and after glucose starvation (Kasari et al., 2019; Schuller et al., 2017) (Figure 3.2A). Plotting polarity score distribution densities revealed a shift from negative to positive where more ribosomes occupy the 3' halves of CDSs relative to the 5' halves after 15 minutes of glucose starvation (Figure 3.2B). This suggests elongating ribosomes could be slowing over time and consequently remaining bound to mRNAs during glucose starvation in the downstream regions of their CDSs. Notably, our initial ribosome profiling library was prepared with cycloheximide (CHX) pretreatment. Pretreatment is a technique that many labs have moved away from as it is reported to complicate the interpretation of ribosome distributions at the start codon and TE measurements on yeast transcripts including ribosomal biogenesis mRNAs (Gerashchenko & Gladyshev, 2014; Santos et al., 2019). To address this and to expand our analysis with an approach that would enable us to interrogate the dynamics of ribosome movement, we prepared replicate libraries without CHX pretreatment at log phase, 1 minute, 5 minutes, 10 minutes, fifteen minutes, twenty minutes, and thirty minutes time points.

A polarity analysis of this time course showed that polarity shifts positive within one minute of glucose starvation, but the magnitude of this shift does not continue to increase over time proportional to the amount of time elapsed (Figure 3.3). This result added nuance to our hypothesis that ribosome elongation slows during glucose starvation by suggesting that it does so increasingly with time. Ribosomes appear to move quickly at the onset of starvation, rapidly

shifting polarity to be positive, but don't continue doing so uniformly as stress induction

increases from one to several minutes. This, in turn, suggests that the regulation of elongation is

altered over time. This would enable runoff in the initial seconds following stress, particularly

on short genes which inherently have less sequence space for ribosomes to move along before

translation terminates. Our findings also shed light on how, simultaneously, longer transcripts

such as those in Figure 3.1 remain bound downstream by ribosomes after 15 minutes of
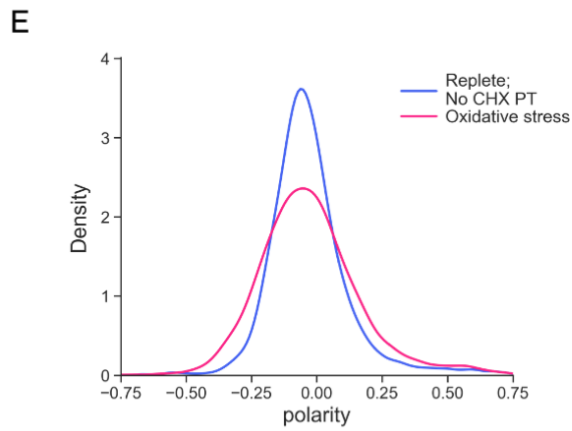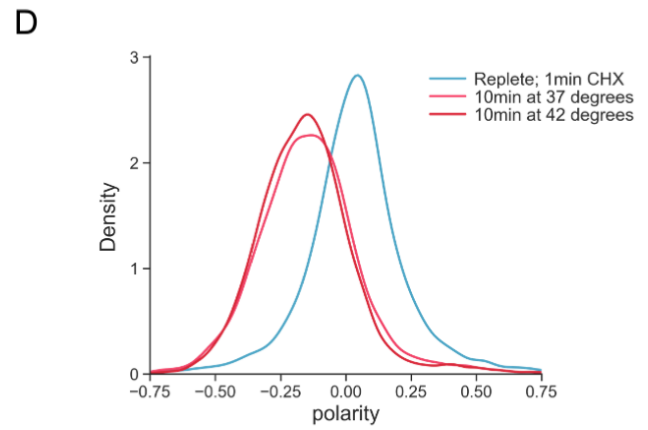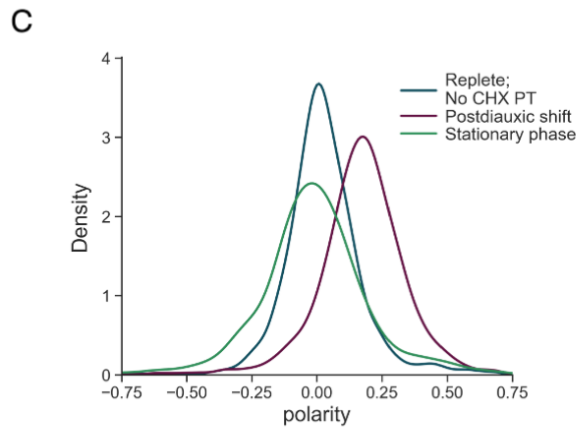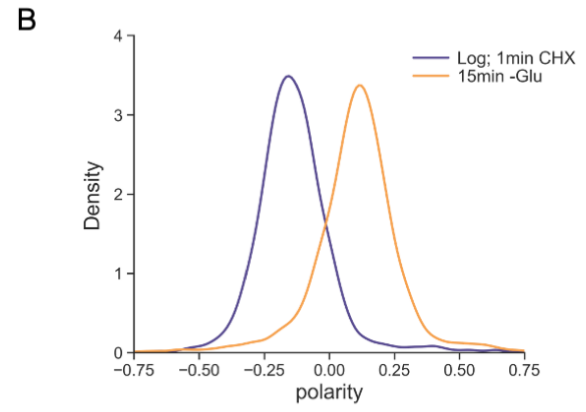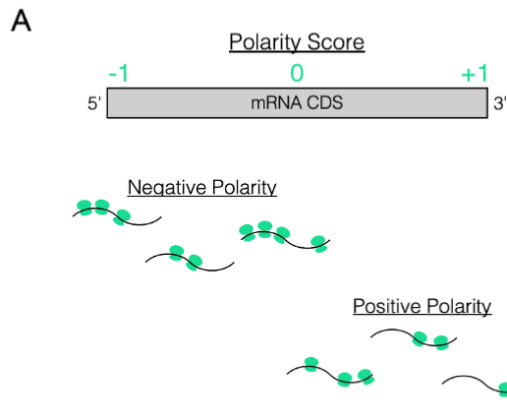
starvation.

   To further parse and confirm ribosome transit slows progressively, the distribution of

reads in the time course were plotted and we compared the magnitude in shift of read density

between different starvation timepoints (Figure 3.4). Notably, we observed a striking difference

in ribosome engagement around the start codon between libraries prepared either with or

without CHX pretreatment in log phase. We also used the temporal nature of our time course to

quantitatively measure how ribosome transit rates change between different time points (Figure

3.5). Finally, we calculated how polarity score on a per gene basis changes over time during

starvation as a function of gene length (Figure 3.6). Collectively these analyses indicate that, as

glucose starvation progresses, the average time needed for ribosomes to move along CDSs

increases. Both the magnitude of the drop in read density that occurs near the AUG and the

magnitude of how polarity scores change between samples are not proportional to time elapsed

between sample collection. These additional analyses lend support to our initial observation

that ribosomes build up along ORFs due to a decrease in transit during glucose starvation.

Taken together, these results point toward a regulated system whereby ribosome movement

slows temporally and, globally, ribosomes move more slowly as the duration of starvation

increases. Additionally, the consequences of foregoing pretreatment while harvesting and flash-

freezing yeast samples for ribosome profiling library preparation are reflected near the start codon in read distribution plots.

Next, we were curious if this buildup of ribosomes downstream on mRNAs, which we hypothesize reflects progressively decreasing ribosome transit, was a general response to stress. We prepared ribosome profiling libraries and plotted polarity in response to multi-day growth in cells as they transitioned from log phase to postdiauxic shift to stationary phase (Figure 3.2C). Additionally, we performed a polarity score analysis on published profiling libraries of oxidative stress, heat shock, and amino acid starvation samples prepared with a variety of library preparation protocols and pretreatment approaches (Figures 3.2D – F) (Mühlhofer et al., 2019; Santos et al., 2019; Wu et al., 2019). Strikingly, we found that the distribution of polarity scores did not change for amino acid starvation and oxidative stresses while heat shock showed a negative shift in polarity, corroborating the reports that ribosomes build up close to the start codon during this stress (Mühlhofer et al., 2019; Shalgi et al., 2013). The only positive change in polarity we observed in addition to acute glucose starvation was from day-old yeast cultures grown to postdiauxic shift conditions. Moreover, polarity shifted back to a distribution near 0 in our sample prepared after 5 days of growth when cells were in stationary phase. This indicates that, for the stresses analyzed, ribosomes build up on the 3' half of transcripts uniquely in conditions in which glucose is newly limited, either via acute removal from the media or upon a switch to ethanol utilization that results from consumption of glucose in the media over time causing the diauxic shift.

Figure 3.2: Polarity score analysis of yeast stress response ribosome profiling libraries.
(A) Schematic and cartoons showing how polarity scores are determined on a per gene basis. RPF reads reads on the 5' half of a transcript contribute to negative polarity such while reads on the 3' half of a transcript contribute to positive polarity. (B) Densities of polarity score distributions from log phase and 15 minutes post-acute glucose starvation. (C) Densities of polarity score distributions from yeast culture in log phase (replete), after 1 day of growth (postdiauxic shift), and after 5 days of growth (stationary phase). (D) Densities of polarity score distributions from pre- and post-acute oxidative stress. (E) Densities of polarity score distributions from log phase cells before heat stress (replete) and upon the indicated heat stress exposure. F: Densities of polarity score distributions from pre- and post-acute amino acid starvation. For B-F per-gene polarity scores were calculated and included in further analysis from all yeast genes that had > 25 reads per library. Plots were generated from the distribution of these scores. The inclusion or exclusion of a cycloheximide (CHX) pretreatment (PT) step prior to library preparation is specified for each library in the log phase, glucose replete entry in each legend. Although not at identical densities, all replete samples were in log phase as assessed by OD_{600} measurements in the range of 0.4-1.0.
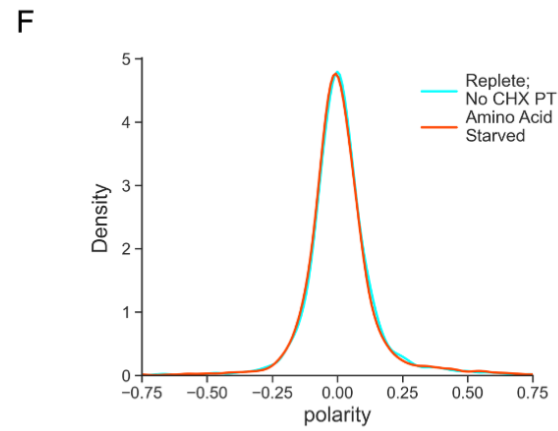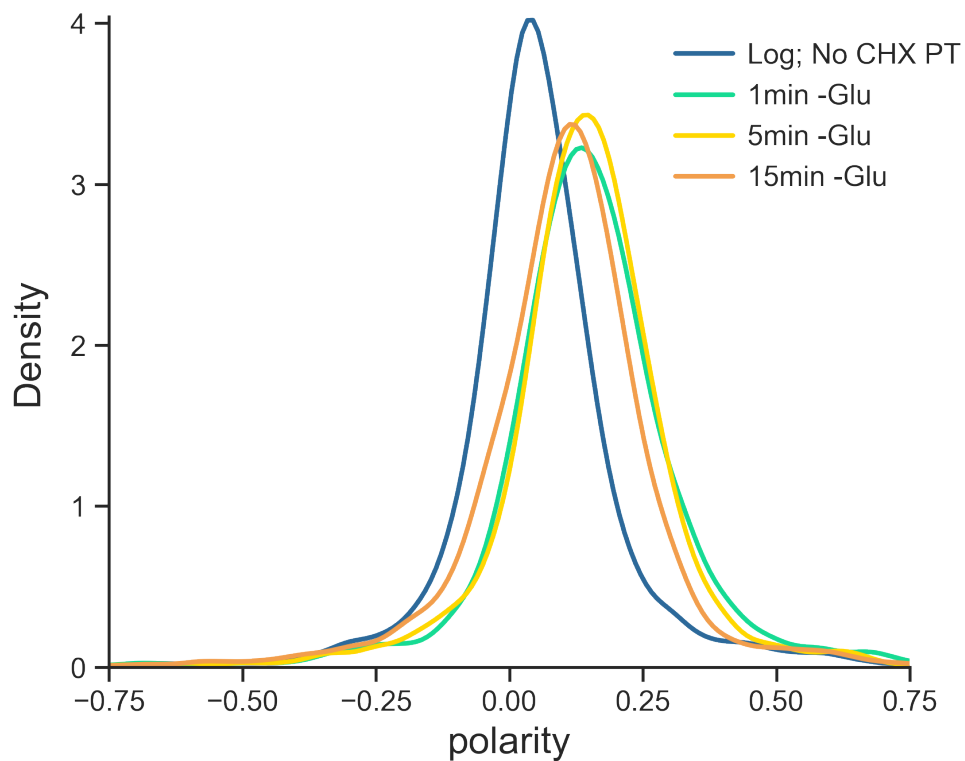
Figure 3.3: Polarity score analysis over a time course of acute glucose starvation.
Densities of polarity score distributions from the indicated log phase and glucose starvation time course samples. Polarity scores were calculated and included in the distributions for all genes that had > 25 reads per library. Libraries were prepared without CHX pretreatment.
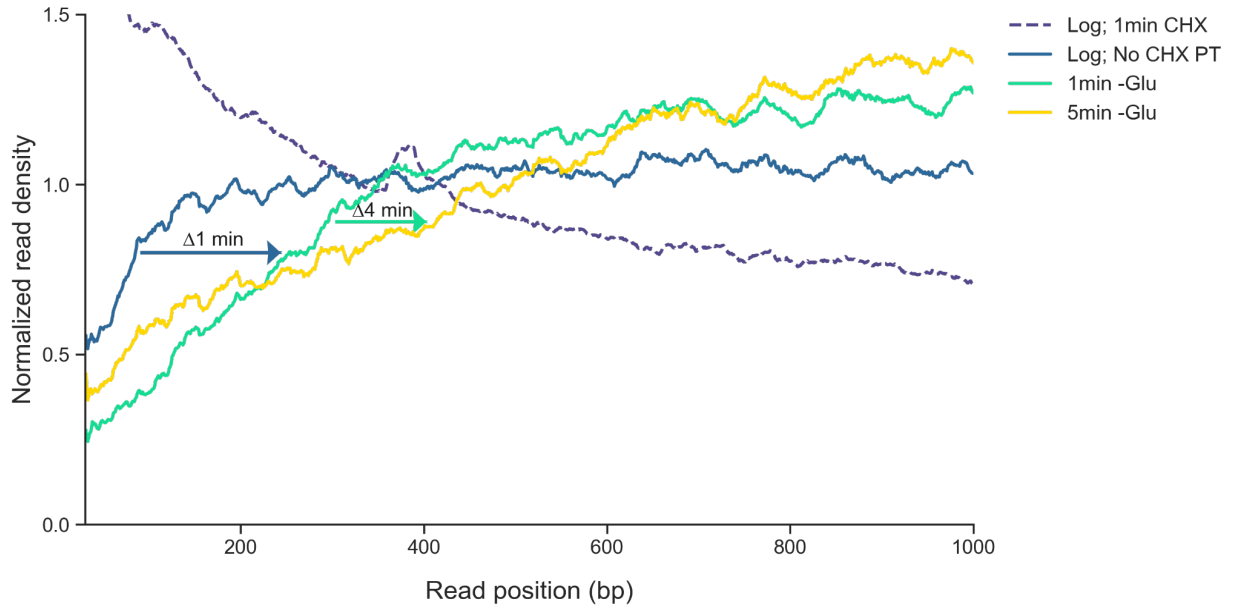
Figure 3.4: Read density near the AUG is impacted by CHX-pretreatment and its decrease slows progressively over a time course of acute glucose starvation.
Normalized read density plots generated from the aggregate number of reads per nucelotide position across all genes >1000bp with > 25 reads per gene per library. Arrows indicate the amount of time elapsed between sample collection. For the Log; No CHX PT sample to 1min -Glu sample there is a Δ1min while the 1min -Glu to 5min -Glu samples have Δ4min. Arrows were drawn at the read-density position on the y-axis that is halfway between the minimum and maximum read density score from the Log; No CHX PT and 1min -Glu samples, respectively. Arrows are intended to be visual aids to show how the vacancy of ribosome read density is greater between the Log: No CHX PT to 1min -Glu sample while less time elapsed between collection (1minute versus 4 minutes).
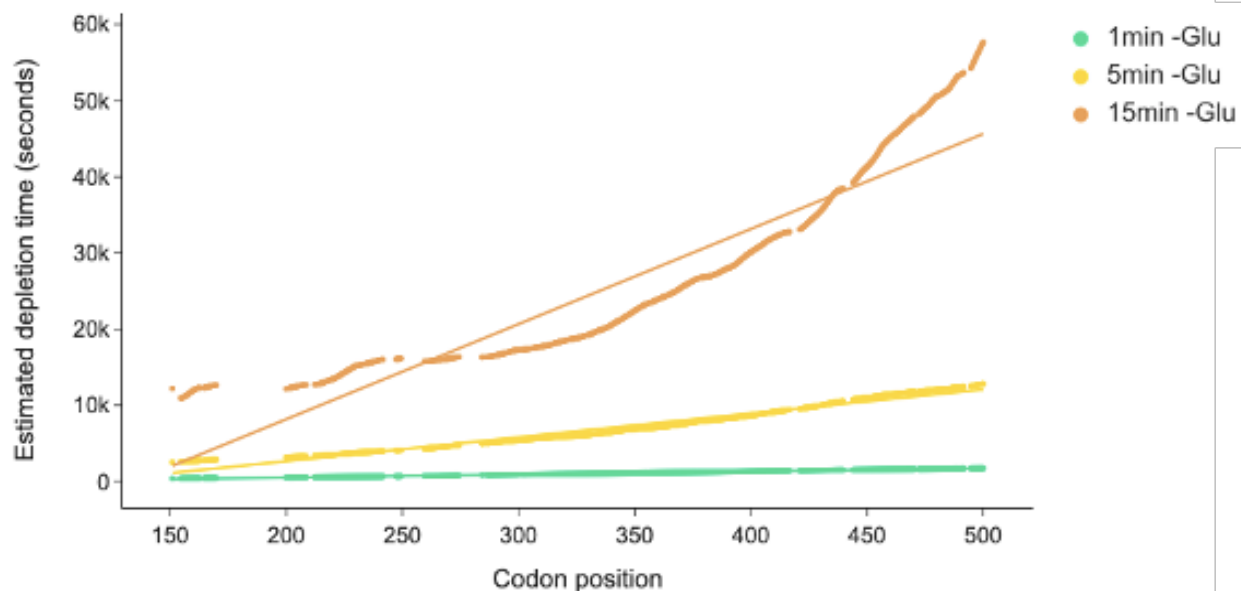
Figure 3.5: Ribosome depletion time calculations show a progressive slowing of ribosome transit in response to acute glucose starvation.

Ribosome profiling reads were used to estimate the depletion time required for ribosomes to move along genes as a function of codon position based on the relative movement of read density between samples collected at different time points. Methods to calculate depletion time were adopted from Sharma et al., 2019. For each time point, the relative ribosome density at each codon position is calculated by comparing ribosome density at glucose starvation to log phase conditions. This value is then used to estimate the time needed for ribosome depletion. The straight lines show the fitted data using a linear model. The coefficients of determination (R^2) of the fitted lines for 1 minutes, 5 minutes, and 15 minutes are 0.996, 0.970, and 0.862, respectively.
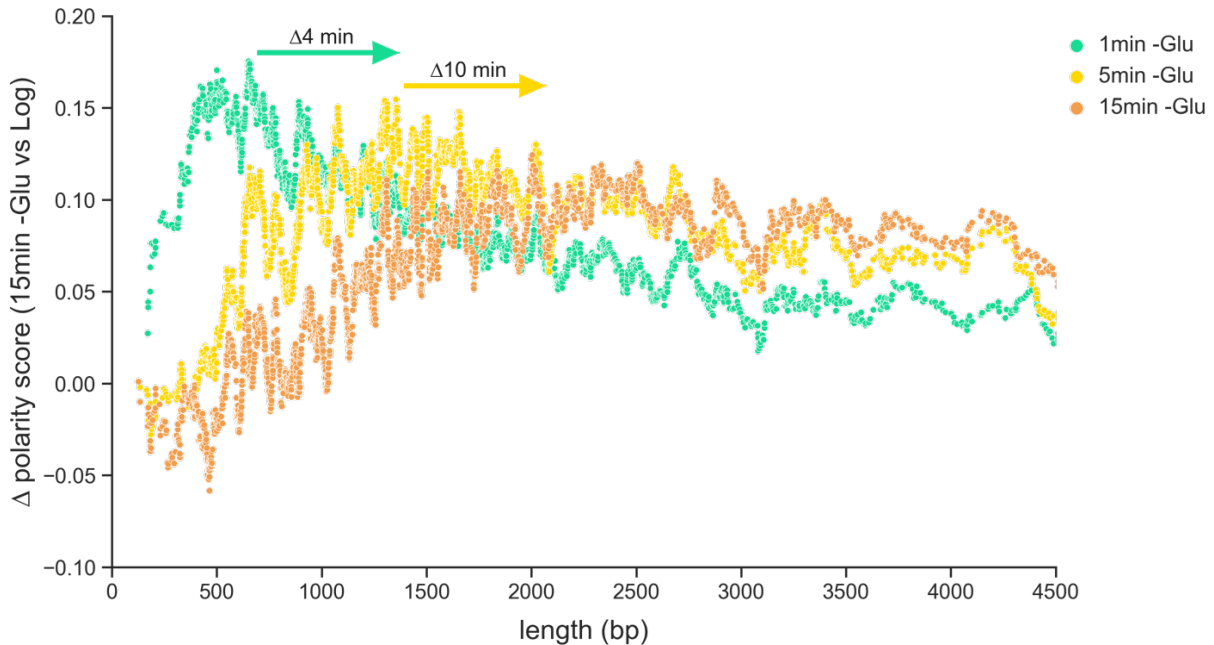
Figure 3.6: Polarity score changes plotted against gene length after acute glucose starvation show a slowing of ribosome movement over time.
For the top 2,500 expressed genes as assessed by RPF read TPM in log phase, genes were sorted by length and their change in polarity score (Δ polarity score) was calculated for each indicated time course sample by subtracting the polarity score for the same gene in log phase (without CHX pretreatment). The rolling average with a 30bp window of the Δ polarity score was plotted against gene length. Arrows were drawn at the position on the y-axis where the change in polarity score is greatest for the indicated sample. As in Figure S2, arrows are intended to be visual aids to indicate how the greatest positive change in score is similar between the Log: No CHX PT to 1min -Glu sample even though less time elapsed between collection (4 minutes versus 10 minutes).

3.3.3 *In vivo* measurements show elongation slows and the relationship between ribosome engagement and protein production changes after glucose starvation

We sought to test the hypothesis that, in response to glucose-limited conditions, ribosomes slow down and build up on the downstream ends of CDSs because of decreased elongation by directly measuring elongation rate. To accomplish this in living cells, we developed an inducible reporter assay that enabled us to calculate the time needed for elongation through a region upstream of a yeast-optimized Nanoluciferase (Nluc) reporter gene (Masser et al., 2016). The assay is designed so that the time it takes to produce luciferase signal from a Nluc-only reporter is compared to a second reporter, LacZ-Nluc, that is identical except it has an exogenous, long open reading frame (LacZ; 3,072bp) fused in front of the luciferase CDS (Figure 3.7A). An analysis technique known as Schleif plotting, which factors both reporter induction and the amount of time that elapses between expression of the Nluc and LacZ-Nluc reporters, was used to calculate the average elongation rate necessary to translate through LacZ (Schleif et al., 1973; Zhu et al., 2016). Utilizing this assay, we calculated elongation rate to be significantly decreased in cells subjected to acute glucose deprivation and postdiauxic shift conditions, respectively, relative to log phase (Figure 3.7B). Additionally, the elongation rates we found in log phase were consistent with previously reported rates (Karpinets et al., 2006; Riba et al., 2019).

We also directly examined the relationship between ribosome occupancy and protein production before and after glucose starvation. In general, it is often assumed that RO calculations from profiling data correlate with protein production in such a way that genes with high RPF read counts and ROs have high levels of protein synthesis. We were curious if the ribosomes that occupy an abundant pre-stress gene such as *PGK1* produce less protein than those occupying an upregulated, stress-responsive gene such as *HSP30*. To test this, we added

TAP tags to both and performed immunoprecipitations from log phase and glucose starvation cultures supplemented with S^{35} methionine (Figure 3.7C). Quantification of protein production revealed that, during log phase when *HSP30* has very few ribosome counts, we were unable to detect protein production above background while ribosomes bound to *PGK1* showed robust protein production (Figures 3.7D-E). Therefore, a consistent relationship exists between RPF reads and protein production in the absence of stress. However, during glucose starvation, despite *PGK1* having about 25-fold higher RPF counts along its transcripts, there was not a significant difference in S^{35} incorporation into Pgk1 and Hsp30 proteins. Together, this indicates that differential elongation during glucose starvation results in divergent levels of protein production in a gene-dependent manner. Importantly, this highlights that careful consideration must be made prior to assuming high levels of ribosome-mRNA interactions on a given transcript necessitate robust translation of that mRNA.
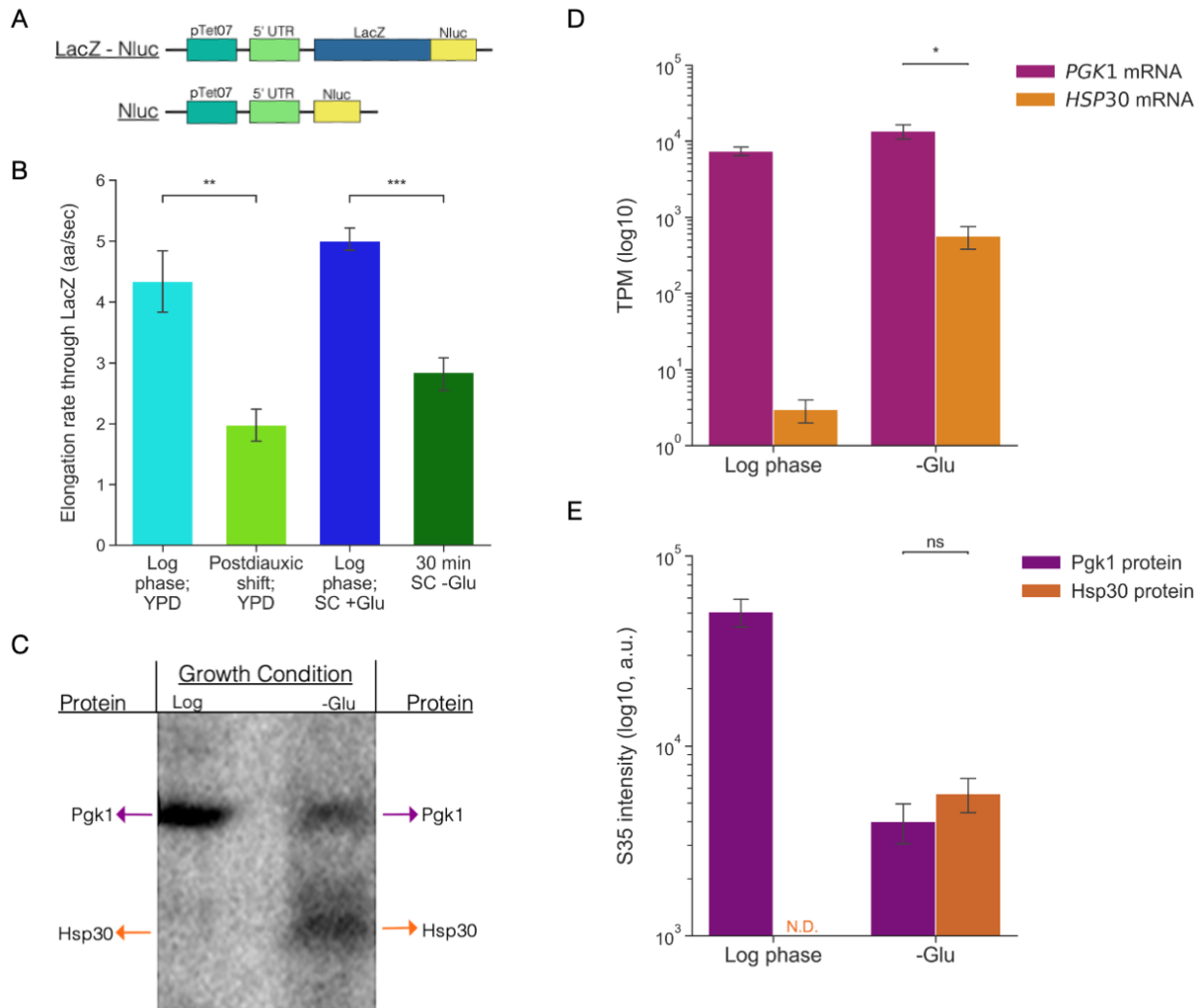
Figure 3.7: Glucose starvation impacts protein production in living cells by slowing elongation and altering the relationship between ribosome engagement and translation.
(A) Schematic of reporters used to determine elongation rates in B. (B) The elongation rate in amino acids per second (aa/sec) through LacZ calculated following reporter induction in the indicated growth and media conditions. (C) Representative image of autoradiography exposure used to calculate radiolabeled S35 methionine incorporation in E. For each lane, immunoprecipitation was performed on the indicated TAP-tagged proteins from cell lysates grown to log phase and, for the right lane, glucose starved for 30 minutes. The volume of lysate loaded for the log phase sample (left lane) was 1/10th the volume loaded of the starved lysate. (D) The TPM of RPF reads from replicate log phase and glucose starvation ribosome profiling libraries plotted as mean ± sem. TPM = transcripts per million, RPF = ribosome protected fragments. (E) S35 intensity from four biological replicates performed as described in C. a.u. = arbitrary units. For B, C, and E values are plotted as mean ± sem from a minimum of four biological replicates. Statistical significance was assessed by unpaired Student's t-test (***p<0.001; **p<0.01, * p<0.05, ns = not significant).

3.3.4 Glucose readdition causes translation to increase and elongation to proceed from ribosomes that built up on long mRNAs in response to glucose starvation

Finally, we sought to establish whether the ribosomes that slow or stall along CDSs during glucose starvation are competent to resume translation upon reintroduction of glucose to the environment. To do this, we again utilized both ribosome profiling and *in vivo* reporter assays. After acute glucose starvation, glucose was reintroduced and samples were collected for ribosome profiling, RNA-seq, and polysome profiling after one minute and five minutes (Figure 3.8). We were particularly interested in long genes which we expected to be poorly translated during glucose starvation but were earlier shown to remain associated with the polysome as assessed by qPCR (Figure 3.1E). Indeed, the changes in RO for all but two genes greater than 4,000bp are above 1 during glucose starvation compared to log phase (Figure 3.9). In general, longer genes have higher relative occupancy during starvation compared to shorter genes. This observation is consistent with our finding that ribosome elongation slows progressively in response to glucose starvation which means shorter genes are more likely to undergo greater runoff and have a decrease in occupancy.

Upon glucose readdition a 'wave' of increased RPF read density, suggestive of new initiation events, was detected near the start codon within the first minute (Figure 3.10A). By five minutes, this wave of newly initiated ribosomes was observed spanning the first approximately 2,200bp of mRNAs. To assess ribosome movement in response to glucose readdition in a gene-specific manner, we looked at the distribution of reads on two yeast genes that are particularly long, each over 6,000bp in log phase, starvation, and readdition conditions (Figure 3.10B). We wondered whether it would be possible to parse the engagements and movement of ribosomes that slowed on these mRNAs during starvation from those that were newly initiated. Intriguingly, the profile of ribosomes engaged during glucose starvation

82

appears to move down the transcript at the same time as new initiation events occur, resulting in a bimodal distribution of RPF reads at the 5' and 3' ends of these genes after 5 minutes of readdition. We hypothesized that there could be two populations of ribosomes on the CDSs: one population of ribosomes that underwent initiation during log phase, built up downstream during glucose starvation, and then resumed elongation and a second population that were newly initiated upon glucose readdition. This led us to wonder if we could directly test whether the former were actively elongating ribosomes and, furthermore, whether these ribosomes could finish translation and produce functional protein.

To test the potential for these ribosomes to resume translation upon relief of acute glucose starvation, we tagged endogenous *FAS1* and *URA2* with an E2A self-cleaving peptide followed by NLuc and monitored reporter expression in log phase, during glucose starvation, and following glucose readdition (Souza-Moreira et al., 2018) (Figure 3.10C). We used a Nluc reporter fused to a PEST domain. This allowed a short-lived luciferase reporter, with a reported half-life of approximately five minutes, to monitor recent protein production without perturbing the function of the endogenous, upstream Ura2 or Fas1 proteins following their cleavage from Nluc via E2A (Masser et al., 2016). We estimated these mRNAs were long enough that any new translation events would take longer than five minutes to complete as the 'wave' of ribosome density we saw in Figure 3.10A would correspond to translation of proteins less than 3,000bp and 1,000 amino acids. Additionally, once initiated, a ribosome would need to elongate at 7-8 amino acids per second to translate through these reporters within five minutes. This rate is faster than the elongation rates we observe even in log phase conditions (Figure 3.7B) and faster than the rate we would predict from our ribosome profiling data. Even still, to separate translation events that arise due to new initiation after glucose readdition from

translation events due to ribosomes that completed initiation prior to readdition, we developed an experimental approach that directly decoupled these two possibilities.

Specifically, we glucose starved cells expressing these reporters for 30 minutes, added glucose back, and then measured luciferase production in the presence (treated) and absence (untreated) of two different drugs: either CHX, a translation elongation inhibitor, or lactimidomycin (LTM), a translation inhibitor that preferentially inhibits initiation at the concentration used (Eisenberg et al., 2020; Hollerer et al., 2021) (Figure 3.10D). Since CHX addition prevents ribosomes from completing elongation and producing any functional luciferase, the difference in luciferase signal between the CHX-treated versus untreated samples represents all luciferase produced during signal measurement. In all conditions tested, there was a significant difference in luciferase signal with CHX treatment compared to untreated cultures, indicating expression was taking place in all conditions. As expected, expression was greatly reduced in glucose starvation conditions compared to log phase for both reporters. Intriguingly, after five minutes of glucose readdition, there was no difference in protein expression due to LTM treatment compared to the untreated samples. This suggests the Nluc expression that took place did not depend on new initiation events. If it had, using an initiation inhibitor would have reduced luciferase production compared to the untreated sample. On the other hand, we found that upon 15 minutes of glucose readdition, significantly less protein was produced from both CHX and LTM treatments. This suggests new initiation events were contributing to expression after 15 minutes, unlike after five minutes. Taken together, we interpret these results to demonstrate that there is indeed a population of ribosomes bound to the CDSs of our reporters that underwent initiation prior to glucose readdition, resumed elongation upon readdition, and produced functional protein.
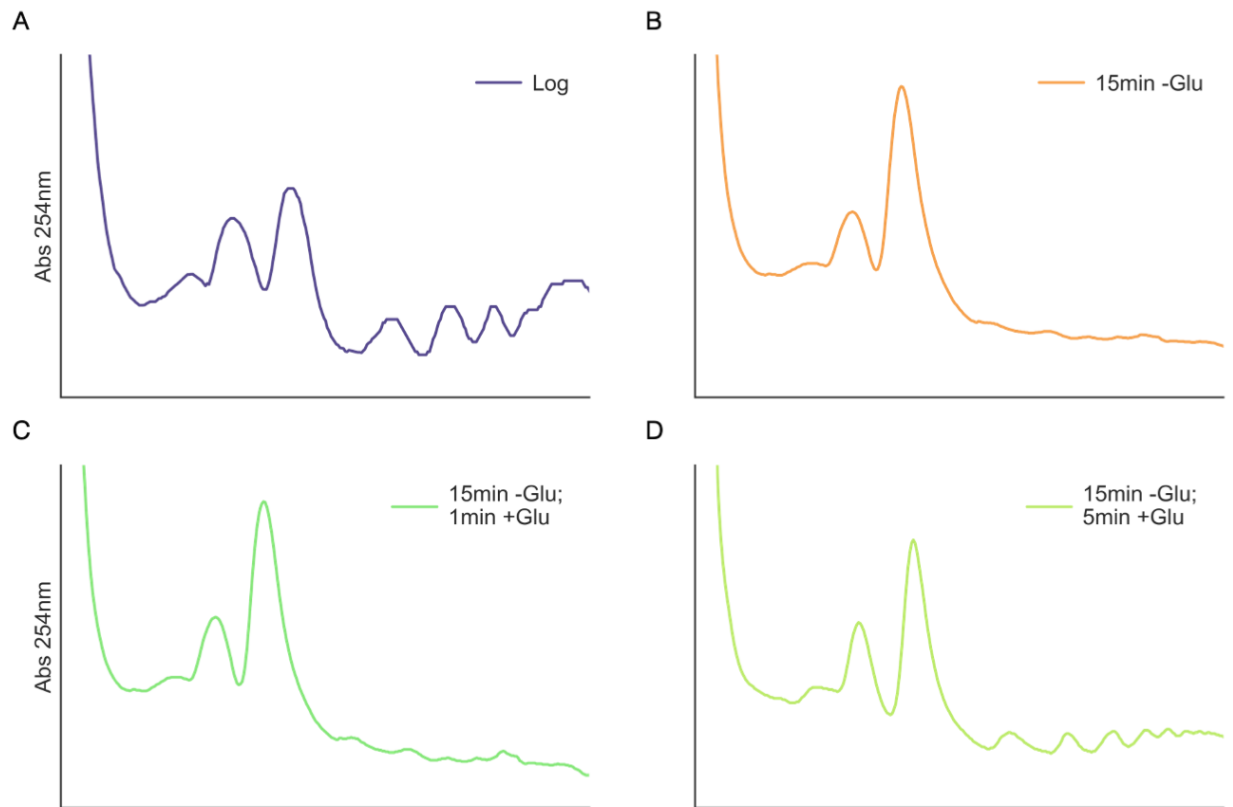
Figure 3.8: Polysome traces from log phase, glucose starved, and glucose readdition samples.
(A) Sedimentation profile of cells grown to log phase. (B) Sedimentation profile of log phase cells that underwent 15 minutes of glucose starvation. (C) Sedimentation profile of log phase cells that underwent 15 minutes of glucose starvation and then were supplemented with glucose for 1 minute. (D) Sedimentation profile of log phase cells that underwent 15 minutes of glucose starvation and then were supplemented with glucose for 5 minutes.

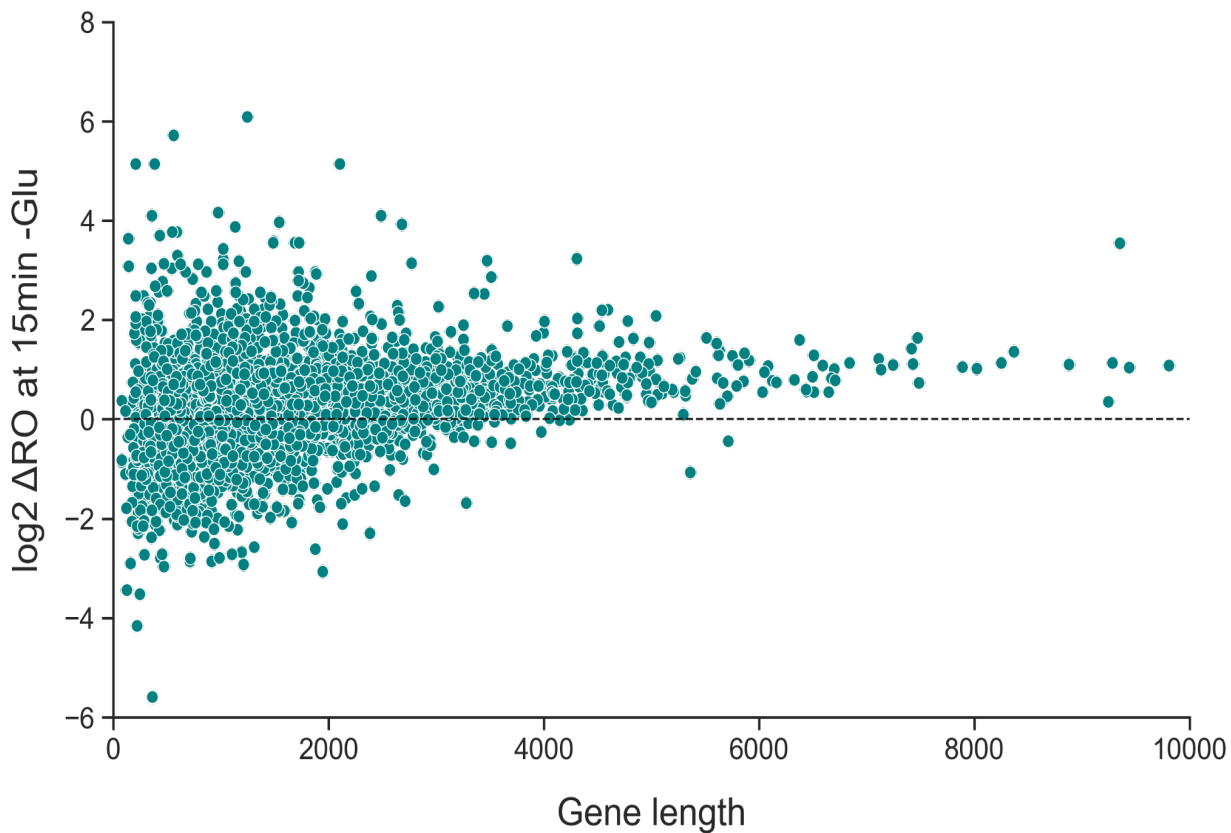**Figure 3.9: Ribosome occupancy change after 15 minutes glucose starvation against gene length shows longer genes have higher relative occupancy during stress.**
RO was calculated per gene as RPF reads divided by mRNA reads for the same gene. Log2 values of the difference in RO score per gene between fifteen minutes of glucose starvation and log phase (y-axis) were plotted against gene length in base pairs (x-axis).

Figure 3.10: Glucose readdition results in new initiation and continued elongation.
(A) Normalized read density plots for glucose starved cultures after one minute (green; left) and five minutes (yellow; right) of glucose readdition. To generate read density plots the aggregate number of reads per nucleotide position across all genes >3000bp with > 25 reads per gene were included and normalized to enable inter-library comparison. (B) RPF reads per million by position for the indicated genes in log phase (purple), glucose starvation (orange), after one minute readdition (green), and five minutes readdition (yellow). (C) Schematic of reporters used to determine luciferase production in D. (D) Each bar represents the mean difference ± sem in luciferase signal detected during measurement between aliquots of untreated culture and the same culture treated with the indicated translation inhibitor from a minimum of six biological replicates. For log phase and 30 min -Glu conditions the signal was recorded after 5 minutes of treatment and the difference was calculated and plotted on the y-axis. For readdition, the signal difference was taken at the indicated time points following glucose addition and plotted. Statistical significance was assessed by paired t-tests for differences in luciferase production between cultures that underwent either LTM or CHX treatment, respectively, paired against luciferase production from the same culture without treatment (***$p<0.001$; **$p<0.01$, * $p<0.05$, ns = not significant).
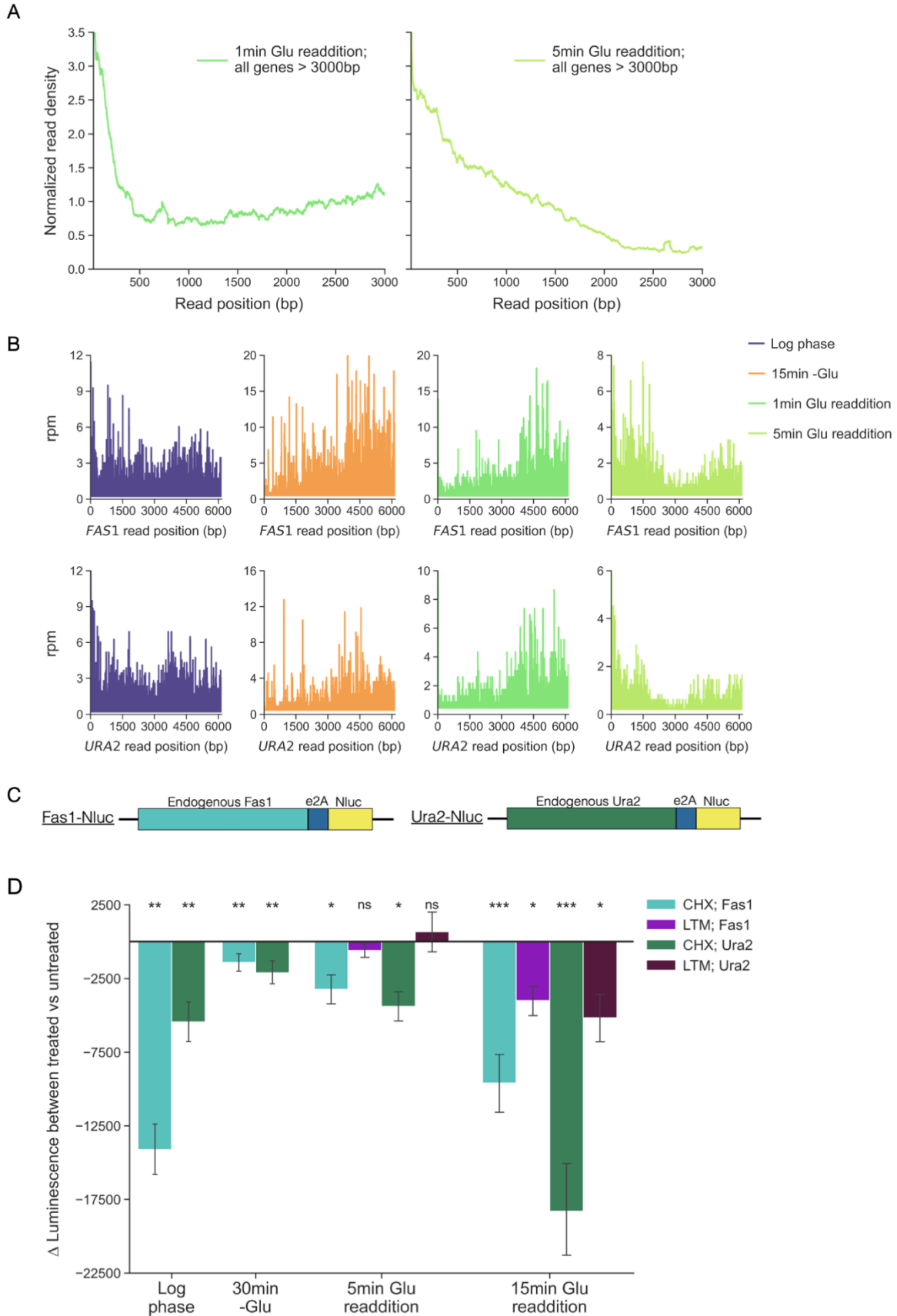
3.4 Discussion

Here, we explored the distribution of ribosomes across yeast mRNAs during acute glucose starvation to better understand how yeast regulate protein synthesis during stress. Notably, we found that many pro-growth mRNAs retain relatively robust ribosome occupancy, but the distribution of these ribosomes skew towards the 3' end and they have positive ribosome polarity scores in contrast to well-translated stress-induced genes such as *HSP30*. We hypothesize this altered ribosome distribution is driven by cessation of initiation followed by an elongation slowdown. Examining this observation concordantly with reports of polysome collapse during glucose starvation leads us to posit a nuanced interpretation of ribosome runoff in response to glucose starvation. Specifically, in the initial seconds following glucose removal, elongation continues at a rate comparable to pre-stress, log phase elongation. This rapid ribosome transit causes ribosomes to finish translating shorter genes, which we show are more likely to display a decrease in occupancy, as their short CDSs inherently require less time for runoff to take place. Then, as the duration of acute stress continues and seconds turn to minutes, ribosome transit slows more and more. This leads to an accumulation of downstream ribosome engagement on mRNAs of sufficient length such as *PGK1*. Meanwhile, shorter genes are more devoid of ribosomes. As the shortest yeast mRNAs tend to code for ribosomal proteins and ribosomal biogenesis genes, we conclude one way yeast responds to acute glucose starvation and downregulates bulk protein synthesis quickly is by reducing expression from these short transcripts. Conversely, comparatively longer, glycolytic genes like *PGK1* remain in the polysome to a larger degree, perhaps to retain their ability to quickly produce protein in the event that glucose is reintroduced to the environment for subsequent, rapid metabolism.

Moreover, polarity score analyses of ribosome profiling libraries proved to be an effective approach to compare ribosome engagement across various stresses. A polarity analysis of a postdiauxic shift sample displayed positive ribosome polarity like that observed during glucose starvation. Notably, a positive shift in polarity was unique to glucose-limited conditions and no polarity shift was observed in response to amino acid starvation or oxidative stress. The other stress that presented an altered polarity was heat shock. It has previously been reported that widespread elongation pausing takes place towards the 5' end of most mRNAs during high heat shock in mammalian cells (Shalgi et al., 2013). While elongation rates were not measured during heat shock, this may be the cause of the more negative polarity we noticed in yeast and indicate that elongation is regulated more quickly in response to heat shock compared to glucose starvation. Similarly, it could instead or concurrently represent a less severe reduction in initiation. Altogether, ribosome polarity score distributions are a useful proxy to explore ribosome movement before and after stress and provide additional insight not provided by ribosomal occupancy measurements alone.

We also note the impact of foregoing CHX-pretreatment during ribosome profiling library preparation on RPF read density near the AUG in our log phase samples, which is markedly decreased compared to our samples that received pretreatment. We speculate this absence of read density in samples that weren't exposed to CHX until lysis is an artifactual result from a brief stress response that resulted during the time required for vacuum filtration and cell scraping to take place after the yeast were removed from the incubator and poured into a filtration apparatus. This highlights that many technical nuances in each step of a protocol can impact the results of profiling experiments. Things as seemingly minute as the distance one must carry a flask from incubation to filtration and the strength of a vacuum line can influence

the amount of time it takes to harvest and then freeze cells, thereby potentially introducing artificial stress prior to library preparation from the harvesting process itself. Notably, other groups have reported on the complexities of interpreting CHX-induced alterations in read density (Duncan & Mata, 2017). In fact, the original article that describes ribosome profiling and established pretreatment also includes a comparison between pretreatment, no pretreatment, and the effects of flash freezing on read density (Ingolia et al., 2009). Typically, CHX-pretreatment in yeast experiments is done by adding CHX to a culture followed by continued shaking and incubation for two minutes prior to harvest. We posit that there might be a middle ground approach between this and foregoing pretreatment entirely, as has become commonplace. To attempt to minimize artifacts from pretreatment while simultaneously not unintentionally inducing stress and runoff during harvest, we would recommend researchers consider adding CHX to their culture as they begin vacuum filtration but skip the additional two minutes of pretreatment incubation. Future experiments using this approach in concert with traditional pretreatment and no pretreatment in matched cultures could provide insight into its impact on read density near the start codon and would test whether a brief CHX exposure during filtration is sufficient to prevent the slight runoff we observed. Such an approach might be particularly useful for researchers hoping to compare stress conditions to non-stressed controls.

In addition to ribosome profiling, we explored how glucose starvation impacts protein production in living cells. *In vivo* measurements of elongation rate using Nluc reporters showed elongation is slower during acute glucose starvation compared to log phase. Similar effects took place during the postdiauxic shift, a less acute manner of glucose starvation. While there has been a growing appreciation in recent years for the importance of translation regulation at

the step of elongation, much of this work has focused predominantly on codon-specific effects as it has been well-established that certain motifs cause ribosome elongation to stall and activate ribosome quality control pathways (Park & Subramaniam, 2019; Presnyak et al., 2015; Weinberg et al., 2016). Our findings are indicative of a more general phenomenon as elongation rates differ on the same reporter in a condition-dependent manner (Figure 3.7B). Ribosome elongation slows significantly during glucose starvation when compared to log phase growth. Our results also indicate that slowed and paused ribosomes are primed to resume elongation and finish translation if environmental conditions continue to fluctuate, but in a favorable way. Specifically, we show that long mRNAs can undergo translation from ribosomes bound before glucose readdition. Greater protein production was measured upon glucose readdition than would otherwise be expected from new initiation alone as samples treated with the initiation inhibitor LTM show no significant difference in protein expression during the first five minutes of glucose readdition. This indicates the expression detected comes from pre-existing ribosomes. We speculate that such pausing may allow for a population of mRNAs to remain bound to ribosomes for rapid continuation of growth once stress has been relieved, provided the duration of the stress is not too long. Additionally, the shift in ribosome distribution towards positive polarity which takes place upon the postdiauxic shift and acute glucose withdrawal suggests the general slowdown in elongation we identify during glucose starvation may play an important role in fine tuning translation during metabolic transitions to alternative carbon sources and metabolic pathways more generally, though this remains to be tested.

It is important to note that, though we compared elongation rates along identical mRNA sequences, we did not simultaneously test how fast elongation takes place on populations of

mRNAs transcribed prior to glucose starvation compared to mRNAs transcribed during glucose starvation. This is due to experimental limitations imposed by inducible reporters, an approach necessary to ensure that elongation rate calculations were not muddled by detecting protein expression from pre-stress reporter transcription events while only intending to measure protein production that takes place during stress. Given the necessity of inducing reporter expression after stress to measure elongation rates during stress, we conjecture that our calculated elongation rate, though slower than it is during log phase, still overestimates the elongation rate that would be observed for ribosomes moving along mRNAs that were transcribed before stress during log phase. This is based on our observation that ribosome engagement with pre-existing mRNAs remains abundant, even during glucose starvation, though protein synthesis from them is greatly reduced (Figures 3.7D-E). As such, we think the elongation rate of approximately two amino acids per second we calculated for LacZ in glucose starvation is more comparable to the elongation rate along a stress-responsive gene such as *HSP30* which is both transcribed and translated in response to stress and is not preexisting. The elongation rate on *PGK1*, a preexisting transcript poorly translated during stress but with high ribosome occupancy, would be even slower. Future experimental approaches to parse the difference in elongation rate during stress on mRNAs transcribed pre-stress compared to mRNAs transcribed during stress would provide more insight into this nuance.

Finally, while our previous results indicate there is a strong dependence on the promoter sequence with respect to localization and competency for translation during stress (Zid & O'Shea, 2014), we cannot rule out that the timing of transcription itself is another key determinant in cytoplasmic RNA fate more generally. For example, it is possible that a copy of *PGK1* mRNA transcribed before stress would be somehow differentially marked or associated

with proteins compared to a copy transcribed during stress and those mRNAs, though coding the same gene, would be regulated in contrasting ways. Future work in this vein would further elucidate the importance of transcription timing with regards to acute stress and parse how important timing is for localization to either P-bodies or stress granules independent of mRNA sequence motifs. Additionally, further investigation is necessary to determine the mechanism or mechanisms that mediate the general slowdown in elongation we characterized in response to acute glucose starvation in yeast. Such a mechanism would have to allow discrimination between preexisting and stress-induced genes. Indeed, mechanisms that facilitate the expression of stress-induced genes like heat shock proteins during severe stress have been a topic of extensive and detailed study for decades and understanding how they work in concert with repressive mechanisms will be crucial to fully understanding how organisms adapt gene expression in response to acute stress. Overall, this work demonstrates how ribosome profiling and reporter assays can complement one another and it highlights the importance of examining read distribution instead of just using ribosome counts as a proxy for translational efficiency, especially during fluctuating environmental conditions.

3.5 Materials and Methods

3.5.1 Yeast strain information

Yeast strains used are listed in Supplementary Table 1. All ribosome profiling libraries including those from log phase, glucose starvation, glucose readdition, postdiauxic shift, and stationary phase samples prepared for this study were made with strain BY4741 (MATa his3Δ1 leu2Δ0 met15Δ0 ura3Δ0). Strains with either TAP-tagged Hsp30 or Pgk1 were from the Yeast-TAP Tagged ORF library collection (Ghaemmaghami et al., 2003). For luciferase measurements during glucose readdition, the E2A-NlucPEST sequence was inserted into a pKT vector containing a hygromycin selection marker (Sheff & Thorn, 2004). Endogenous genes were tagged with E2A-NlucPEST through the integration of PCR products including 40 bp overhangs homologous to the sequence immediately upstream and downstream of the 3'-end of the target gene. P_{TetO7}-LacZ-NlucPEST and P_{TetO7}-NlucPEST were assembled into a pRS305 integration vector with homology for the LEU2 locus. Polysome profiling was performed with strain ZY185. Plasmid pST1760 (Tanaka et al., 2015) was integrated in strain EY0690. Endogenous Dhh1 was C-terminally tagged by PCR amplification of a 3xmini auxin inducible degron from plasmid pST1932 (Tanaka et al., 2015) with homology for the 3'-end of Dhh1. Yeast transformations were performed using lithium acetate and PEG as previously described (Ito et al., 1983).

3.5.2 Yeast growth and glucose starvation for RNA-seq and ribosome profiling

Ribosome profiling experiments were performed with strain BY4741 grown in batch culture at 30°C with shaking at 250rpm to OD_{600} between 0.4-0.6 for all log phase samples. Synthetic complete (SC) media with 2% (w/v) glucose was used to grow cells for all acute

starvation experiments. Glucose starvation was performed in SC media prepared without glucose (SC -G). For each starvation sample, half the volume of a culture was filtered for transfer to SC -G media while the other half remained incubating in glucose replete media in log phase, non-stressed conditions. Cells were collected with a vacuum filtration apparatus onto cellulose filter membranes. For glucose starvation, the cells were collected, quickly rinsed in 50-100mL of pre-warmed SC -G media, re-filtered, and resuspended in prewarmed SC -G with continued rotation at 30°C for either 1 minutes, 5 minutes, 10 minutes, 15 minutes, 20 minutes, or 30 minutes, as indicated. Log phase cells still in SC media were harvested while starvation samples were incubating in SC -G. For glucose readdition experiments, cultures that underwent starvation were supplemented with a 2% (w/v) final concentration of glucose added back to the media with continued shaking at 30°C for the indicated times prior to harvest. For the multi-day growth experiments, yeast was grown in liquid YPD (2% peptone, 1% yeast extract, 2% dextrose). Samples were collected at log phase (0 day), postdiauxic shift (1 day), and stationary phase (5 day) conditions as in (Noree et al., 2019). Following vacuum filtration, all cells were flash frozen in liquid nitrogen and stored at -80°C until library preparation.

3.5.3 RNA-seq and ribosome profiling library preparation

For CHX-pretreatment log phase, glucose readdition, and glucose starvation samples, libraries were prepared in Zid & O'Shea, 2014. Briefly, prior to harvesting, CHX was added to a final concentration of 100µg/mL for 1 min with continued shaking at 30°C. Cells were pulverized under cryogenic conditions, extracts were digested with RNase I, and RPFs were isolated from monosome fractions via sucrose gradient sedimentation. Then, 28mer RPFs were selected, polyadenylated, and reverse transcribed. RNA-seq libraries from these samples were

prepared following or poly(A)+-selected RNA using Oligo(dT) Dynabeads (Invitrogen), also as described in Zid & O'Shea, 2014.

Libraries that did not undergo CHX-pretreatment, including log phase, acute glucose starvation, postdiauxic shift, and stationary phase samples, were prepared according to previously published methods (McGlincy & Ingolia, 2017) with minor modifications. Briefly, after cells were flash frozen, they were ground with yeast footprint lysis buffer (20 mM Tris-Cl (pH8.0), 140 mM KCl, 1.5 mM $MgCl_2$, 1% Triton X-100) via cryogenic ball milling with boiling in liquid nitrogen between cycles. Lysates were thawed, digested with RNase I (Epicentre), and monosomes were isolated with size exclusion chromatography (Vaidyanathan et al., 2013). RPFs were separated and size-selected via TBE-Urea PAGE. Next, footprints underwent dephosphorylation with T4 PNK and linker ligation with T4 enzyme Rnl2(tr) K227Q (NEB). Ligation reactions were excised following separation and size-selection on a TBE-Urea gel and pooled. Next, pools underwent reverse transcription with Protoscript II (NEB), circularization with CircLigase II (Lucigen), quantification with qPCR, and PCR amplification. Libraries were sequenced at the Institute for Genomic Medicine sequencing core at UC San Diego on an Illumina HiSeq 4000.

3.5.4 Ribosome profiling bioinformatic analysis

For libraries prepared with CHX-pretreatment, read trimming and alignment took place as described in Zid & O'Shea, 2014. For libraries prepared without CHX-pretreatment, read trimming and alignment took place as follows. First, unprocessed fastq files were trimmed with Cutadapt (Martin, 2011) to remove the adapter sequence AGATCGGAAGAGCAC. Reads less than 17bp or without adapters were discarded. For files that required manual demultiplexing, Cutadapt was used again to demultiplex with a custom fasta containing the barcode sequence

97

corresponding to a given biological sample. Next, Cutadapt output files had their unique

molecular identifiers (UMIs) removed from the read line of the fastq and appended to the

header line with a custom python script for subsequent deduplication of PCR artifacts. Next,

reads were aligned to S. cerevisiae ncRNA using bowtie (Langmead et al., 2009) with the

following flags: -k 1 --best -t -S -q. Reads that did not align to ncRNA were filtered to remove

low quality reads based on Phred score with fastqx_toolkit

(http://hannonlab.cshl.edu/fastx_toolkit/). Those that passed this quality control step were

aligned against the S. cerevisiae genome. Index files generated via bowtie were from genome

assembly R64-1-1 (SGD). Next, files were deduplicated with custom python scripts. Read

features were counted using htseq-count (Anders et al., 2015), feature files were also obtained

from SGD using genome assembly R-64-1-1. To calculate polarity scores per gene custom

python scripts were run based on Schuller et al., 2017. All scripts are available at

https://github.com/ZidLab and sequencing data has been deposited at the NCBI GEO database.

3.5.5 Polysome profiling

800 mL cultures of strain ZY185 were inoculated in SC media and grown overnight to

early log phase (0.4-0.6 OD_{600}). 400 mL were rapidly filtered, washed, and resuspended in SC -

G media to begin glucose starvation. The remaining half of the glucose replete culture was

rapidly filtered, and the cell paste was scraped into liquid nitrogen for flash freezing. 1.2 mL of

polysome gradient lysis buffer (20 mM Tris-Cl (pH7.5), 140 mM KCl, 2 mM $MgCl_2$, 100

µg/mL CHX, 20 U/mL SUPERase•In™ (Invitrogen), 1% Triton X-100) was flash frozen

dropwise with the cell paste. After 15 minutes of glucose starvation, SC -G cultures were

filtered down and the cell paste was flash frozen with 1.2 mL of lysis buffer. Cell pastes were

stored at -80°C. Cell lysis was performed by cryogenic ball milling for 4x3 minute cycles and

cooled with liquid nitrogen between each cycle. The resulting lysates were gently thawed to room temperature in a water bath and treated with DNase I (12.5 U/mL). Lysates were centrifuged at 4°C for 5 min at 3000xg and the supernatant was centrifuged once more for 10 min at 20,000xg. Approximate concentrations were estimated by A_{260} measurements.

A 7-47% sucrose gradient in polysome gradient buffer without Triton X-100 was prepared with a gradient maker. Clarified supernatants were added and centrifuged at 4°C for 3 hours at 35,000RPM in a Beckman SW41Ti rotor. The gradient was fractionated into 1 mL aliquots using a gradient fractionator and UA-6 detector (Isco/Brandel). Polysome traces were monitored through absorbance measurements at 254nm. 2 ng of *in vitro* transcribed renilla luciferase (rLuc) RNA was added to each aliquot as a spike-in control. Transcription reactions were performed with a mMessage mMachine T7 Transcription Kit according to manufacturer's instructions and RNA was purified with acid phenol:cholorform extraction (Invitrogen). After adding the rLuc spike-in, 600µL of Guanidine HCl and 600µL isopropanol were added to 400uL of each fraction and incubated overnight at -20°C. Fractions were centrifuged at 10,000g for 25 minutes to isolate RNA pellets. Samples were washed with 70% EtOH and resuspended in 400µL of TE buffer. Cleanup was performed by precipitation with 40 µL of NaOAC and 2.5 volumes of 100% EtOH. Samples were centrifuged for 25 min at 10,000xg, pellets were washed with 70% EtOH, dried, and resuspended. Fractions corresponding to free RNA, 80S, disome/trisome, and dense polysomes were pooled and the RNA was then treated with RQ1-DNase (Promega) and reverse transcribed with Protoscript II Reverse Transcriptase (NEB), both according to manufacturer's instructions. qPCR measurements with SYBR green were performed with the cDNA libraries and primers designed for each respective gene. The 18S rRNA primer set was adopted from (Cankorur-Cetinkaya et al., 2012). CT values for the rLuc

spike-in were used to normalize variance in cDNA concentration arising due to sample cleanup and RT efficiency.

3.5.6 S^{35} methionine and autoradiography

15mLs of tap-tagged strains were grown in SC media lacking histidine (SC -His) to an OD$_{600}$ of 0.4. Two cultures of *HSP30-TAP* and *PGK1-TAP* of equal OD were then mixed to make 30mLs. Cultures were pelleted, resuspended, and grown in SC -His and 0.01x methionine for 30 minutes. To 15mLs of this combined culture, 0.2 mCi of [^{35}S] methionine-cysteine (EXPRESS[^{35}S] protein labeling mix; Perkin-Elmer) was added and incubated at 30°C for 30 minutes. To the remaining 15mLs, cells were pelleted and resuspended in SC -G, -His, 0.01x Met + 0.2 mCi [^{35}S] and incubated at 30°C for 30 min. Labeled cells were pelleted and lysed in 400uL RIPA buffer (50mM Tris pH8, 1% NP-40, 0.1% SDS, 0.5% Sodium Deoxycholate, 150 mM NaCl) with glass beads. Supernatants were isolated before being applied to immunoprecipitation with IgG-coupled beads. Dynabeads M270 Epoxy were coupled with IgG as described previously (https://commonfund.nih.gov/sites/default/files/Conjugation-of-Dynabeads.pdf).

Supernatants were incubated with Dynabeads for 30 minutes at RT, then washed 3 times with RIPA buffer. The Dynabeads were then resuspended in 25µl of 1× loading buffer (50 mM Tris, pH 7.0, 2.5% sodium dodecyl sulfate [SDS], 0.02% bromophenol blue, 10% glycerol), and TAP-tagged proteins were eluted from the beads with moderate heat treatment at 65°C for 10 min. Loading buffer was transferred to a new tube, and 2-β-mercaptoethanol was added to a final concentration of 200mM. Samples were boiled for 5 min, and 20µl was loaded and resolved on 4-20% polyacrylamide gradient gels followed by autoradiography and quantitation

with a PhosphorImager (Molecular Dynamics). Signal intensity was quantified using background subtraction and the 'rectangles' option in Quantity One software (Bio-Rad).

3.5.7 Nanoluciferase reporter assays

Nluc assays were adapted from methods previously described (Masser et al., 2016). Briefly, cells were grown in SC media and added to a 96-well plate. Promega Nano-Glo substrate was diluted 1:100 with PBS and added 1:10 to each well immediately prior to measurement. Luminescence was measured every 30 seconds with a Tecan Infinite 200 PRO plate reader. For glucose starvation, cells were sedimented by centrifugation, washed 2x with SC -G media, and resuspended in SC G- media for 30 minutes of incubation at 30°C with rotating. 2% glucose was added with the substrate to monitor expression upon glucose readdition. For CHX-treated samples, 10 mg/mL CHX in deionized H_2O was added to achieve a final concentration of 100 µg/mL. For LTM-treated samples, 3.5mM LTM in DMSO was added to achieve a final concentration of 3.5 µM. To measure elongation rates during the diauxic shift, log-phase cultures were inoculated in YPD media at 0.1 OD_{600} and incubated overnight for 24 hours. Assays were performed on the cultures at the indicated timepoints afterwards using the same methods described above.

3.5.8 Elongation measurements

Doxycycline was added to a final concentration of 10 mg/ml to induce transcription of the LacZ-Nluc and nLuc reporters in liquid culture. Luciferase expression was monitored as described in the preceding section. Data was linearized using Schleif plots to estimate the minimum reaction time required for complete translation (1973 Schleif). The reaction time of the Nluc reporter was subtracted from the reaction time of LacZ-Nluc to calculate the time

required for translation of the LacZ sequence alone. An RNA transcription speed of 2000nt/min was used to calculate the estimated time required to transcribe the LacZ sequence (Mason & Struhl, 2005) (Table 3.2). Subtracting the transcription time from the LacZ reaction time provides the elongation rate for LacZ.

3.5.9 Yeast gene length calculations

Median yeast gene length was calculated from information retrieved from the Saccharomyces genome database (SGD) on June 21st, 2021 (https://yeastmine.yeastgenome.org/yeastmine/bagDetails.do?scope=all&bagName=Verified_O RFs). The median length was calculated from the list of 5,195 genes are each categorized as verified ORFs

Table 3.1: List of yeast strains used in this study

Strain	Genetic Background	Reference source
BY4741	MATa his3Δ1 leu2Δ0 met15Δ0 ura3Δ0	Euroscarf
EY0690	MATa trp1-1 leu2-3 ura3-1 his3-11 can1-100	W303
P_{TetO7}-Nluc only reporter	BY4741, P_{ERV14}-rtTA::URA3, P_{TetO7}-NlucPEST-MS2(v4)::HIS3	This study
P_{TetO7}-LacZ-Nluc reporter	BY4741, P_{ERV14}-rtTA::URA3, P_{TetO7}-LacZ-NlucPEST-MS2(v4)::HIS3	This study
Pgk1 TAP tag	S288C: (ATCC 201388: MATa his3Δ1 leu2Δ0 met15Δ0 ura3Δ0)	Yeast-TAP Tagged ORF library collection (Horizon Discovery)
Hsp30 TAP tag	S288C: (ATCC 201388: MATa his3Δ1 leu2Δ0 met15Δ0 ura3Δ0)	Yeast-TAP Tagged ORF library collection (Horizon Discovery)
ZY185	EY0690, HIS3 OsTIR1, tTA, TetR'-SSN6, Dhh1-3xmini-AID-5xFlag-KanMX	This study
Fas1-E2A-NlucPEST	EY0690, Fas1::E2A-NlucPEST::HIS3	This study
Ura2-E2A-NlucPEST	EY0690, Ura2::E2A-NlucPEST::HIS3	This study

Table 3.2: List of qPCR primers used in this study

qPCR Gene and Primer Set	Forward Primer	Reverse Primer
18S rRNA (ZO995/996)	AATCATCAAAGAGTCCGAAGACATTG	CCTTTACTACATGGTATAACTGTGG
Acc1 (ZO 1014/1015)	TTTCTGCCATTTTCTCTACTCC	TGTTCAGTTCTTTCCTTGACC
Act (ZO83/84)	CTGCCGGTATTGACCAAACT	CGGTGATTTCCTTTTGCATT
Fas1 (ZO787/788)	CGCTGCATCATTCTCTCAAG	TTGACGATTTCAACCAACCA
Hsp30 (OS262/263)	TTGGACTGGTGTTCAAGCTG	CAGGACAAGAACCAGGCAAT
Hsp104 (OS803/804)	CGACGCTGCTAACATCTTGA	CACTTGGTTCAGCGACTTCA
Pab1 (ZO95/96)	TCTCTGTGTTTGGTGACATCTT	TTGGCAGCACCTTCTTCTT
Pgk1 (OS773/774)	GGACAAGCGTGTCTTCATCA	CGTTCTTTCACCGTTTGGT
RPS8A (ZO952/953)	TCAACCAGCCAACACCAAG	CAGAAGCCCAAGAAAAGTTACC
Ura2 (ZO1018/1019)	ATTCCCCGCTTACACGAAC	AACACCAGAACCCAAGACC

Acknowledgements

References

Advani, V. M., & Ivanov, P. (2019). Translational Control under Stress: Reshaping the Translatome. *BioEssays: News and Reviews in Molecular, Cellular and Developmental Biology*, *41*(5), e1900009. https://doi.org/10.1002/bies.201900009

Anders, S., Pyl, P. T., & Huber, W. (2015). HTSeq—A Python framework to work with high-throughput sequencing data. *Bioinformatics*, *31*(2), 166–169. https://doi.org/10.1093/bioinformatics/btu638

Arribere, J. A., Doudna, J. A., & Gilbert, W. V. (2011). Reconsidering movement of eukaryotic mRNAs between polysomes and P bodies. *Molecular Cell*, *44*(5), 745–758. https://doi.org/10.1016/j.molcel.2011.09.019

Ashe, M. P., De Long, S. K., & Sachs, A. B. (2000). Glucose depletion rapidly inhibits translation initiation in yeast. *Molecular Biology of the Cell*, *11*(3), 833–848. https://doi.org/10.1091/mbc.11.3.833

Brengues, M., Teixeira, D., & Parker, R. (2005). Movement of eukaryotic mRNAs between polysomes and cytoplasmic processing bodies. *Science*, *310*(5747), 486–489. https://doi.org/10.1126/science.1115791

Cankorur-Cetinkaya, A., Dereli, E., Eraslan, S., Karabekmez, E., Dikicioglu, D., & Kirdar, B. (2012). A novel strategy for selection and validation of reference genes in dynamic multidimensional experimental design in yeast. *PloS One*, *7*(6), e38351. https://doi.org/10.1371/journal.pone.0038351

Costello, J. L., Kershaw, C. J., Castelli, L. M., Talavera, D., Rowe, W., Sims, P. F. G., Ashe, M. P., Grant, C. M., Hubbard, S. J., & Pavitt, G. D. (2017). Dynamic changes in eIF4F-mRNA interactions revealed by global analyses of environmental stress responses. *Genome Biology*, *18*(1), 201. https://doi.org/10.1186/s13059-017-1338-4

Diaz-Ruiz, R., Rigoulet, M., & Devin, A. (2011). The Warburg and Crabtree effects: On the origin of cancer cell energy metabolism and of yeast glucose repression. *Biochimica et Biophysica Acta (BBA) - Bioenergetics*, *1807*(6), 568–576. https://doi.org/10.1016/j.bbabio.2010.08.010

Duncan, C. D. S., & Mata, J. (2017). Effects of cycloheximide on the interpretation of ribosome profiling experiments in Schizosaccharomyces pombe. *Scientific Reports*, *7*(1), 10331. https://doi.org/10.1038/s41598-017-10650-1

Eisenberg, A. R., Higdon, A. L., Hollerer, I., Fields, A. P., Jungreis, I., Diamond, P. D., Kellis, M., Jovanovic, M., & Brar, G. A. (2020). Translation Initiation Site Profiling Reveals

Widespread Synthesis of Non-AUG-Initiated Protein Isoforms in Yeast. *Cell Systems*, *11*(2), 145-160.e5. https://doi.org/10.1016/j.cels.2020.06.011

Gerashchenko, M. V., & Gladyshev, V. N. (2014). Translation inhibitors cause abnormalities in ribosome profiling experiments. *Nucleic Acids Research*, *42*(17), e134. https://doi.org/10.1093/nar/gku671

Gerashchenko, M. V., Lobanov, A. V., & Gladyshev, V. N. (2012). Genome-wide ribosome profiling reveals complex translational regulation in response to oxidative stress. *Proceedings of the National Academy of Sciences of the United States of America*, *109*(43), 17394–17399. https://doi.org/10.1073/pnas.1120799109

Ghaemmaghami, S., Huh, W.-K., Bower, K., Howson, R. W., Belle, A., Dephoure, N., O'Shea, E. K., & Weissman, J. S. (2003). Global analysis of protein expression in yeast. *Nature*, *425*(6959), 737–741. https://doi.org/10.1038/nature02046

Gismondi, A., Caldarola, S., Lisi, G., Juli, G., Chellini, L., Iadevaia, V., Proud, C. G., & Loreni, F. (2014). Ribosomal stress activates eEF2K-eEF2 pathway causing translation elongation inhibition and recruitment of terminal oligopyrimidine (TOP) mRNAs on polysomes. *Nucleic Acids Research*, *42*(20), 12668–12680. https://doi.org/10.1093/nar/gku996

Gonçalves, P., & Planta, R. J. (1998). Starting up yeast glycolysis. *Trends in Microbiology*, *6*(8), 314–319. https://doi.org/10.1016/s0966-842x(98)01305-5

Hollerer, I., Powers, E. N., & Brar, G. A. (2021). Global mapping of translation initiation sites by TIS profiling in budding yeast. *STAR Protocols*, *2*(1), 100250. https://doi.org/10.1016/j.xpro.2020.100250

Holmes, L. E. A., Campbell, S. G., De Long, S. K., Sachs, A. B., & Ashe, M. P. (2004). Loss of translational control in yeast compromised for the major mRNA decay pathway. *Molecular and Cellular Biology*, *24*(7), 2998–3010. https://doi.org/10.1128/MCB.24.7.2998-3010.2004

Ingolia, N. T., Ghaemmaghami, S., Newman, J. R. S., & Weissman, J. S. (2009). Genome-wide analysis in vivo of translation with nucleotide resolution using ribosome profiling. *Science*, *324*(5924), 218–223. https://doi.org/10.1126/science.1168978

Ito, H., Fukuda, Y., Murata, K., & Kimura, A. (1983). Transformation of intact yeast cells treated with alkali cations. *Journal of Bacteriology*, *153*(1), 163–168. https://doi.org/10.1128/jb.153.1.163-168.1983

Janapala, Y., Preiss, T., & Shirokikh, N. E. (2019). Control of Translation at the Initiation Phase During Glucose Starvation in Yeast. *International Journal of Molecular Sciences*, *20*(16), E4043. https://doi.org/10.3390/ijms20164043

Jochem, M., Ende, L., Isasa, M., Ang, J., Schnell, H., Guerra-Moreno, A., Micoogullari, Y., Bhanu, M., Gygi, S. P., & Hanna, J. (2019). Targeted Degradation of Glucose Transporters Protects against Arsenic Toxicity. *Molecular and Cellular Biology*, *39*(10), e00559-18. https://doi.org/10.1128/MCB.00559-18

Kafri, M., Metzl-Raz, E., Jona, G., & Barkai, N. (2016). The Cost of Protein Production. *Cell Reports*, *14*(1), 22–31. https://doi.org/10.1016/j.celrep.2015.12.015

Kang, K. R., & Lee, S. Y. (2001). Effect of serum and hydrogen peroxide on the Ca2+/calmodulin-dependent phosphorylation of eukaryotic elongation factor 2(eEF-2) in Chinese hamster ovary cells. *Experimental & Molecular Medicine*, *33*(4), 198–204. https://doi.org/10.1038/emm.2001.33

Karpinets, T. V., Greenwood, D. J., Sams, C. E., & Ammons, J. T. (2006). RNA:protein ratio of the unicellular organism as a characteristic of phosphorous and nitrogen stoichiometry and of the cellular requirement of ribosomes for protein synthesis. *BMC Biology*, *4*, 30. https://doi.org/10.1186/1741-7007-4-30

Kasari, V., Margus, T., Atkinson, G. C., Johansson, M. J. O., & Hauryliuk, V. (2019). Ribosome profiling analysis of eEF3-depleted Saccharomyces cerevisiae. *Scientific Reports*, *9*(1), 3037. https://doi.org/10.1038/s41598-019-39403-y

Kenney, J. W., Moore, C. E., Wang, X., & Proud, C. G. (2014). Eukaryotic elongation factor 2 kinase, an unusual enzyme with multiple roles. *Advances in Biological Regulation*, *55*, 15–27. https://doi.org/10.1016/j.jbior.2014.04.003

Khong, A., & Parker, R. (2018). MRNP architecture in translating and stress conditions reveals an ordered pathway of mRNP compaction. *Journal of Cell Biology*, *217*(12), 4124–4140. https://doi.org/10.1083/jcb.201806183

Kim, J.-H., Roy, A., Jouandot, D., & Cho, K. H. (2013). The glucose signaling network in yeast. *Biochimica Et Biophysica Acta*, *1830*(11), 5204–5210. https://doi.org/10.1016/j.bbagen.2013.07.025

Langmead, B., Trapnell, C., Pop, M., & Salzberg, S. L. (2009). Ultrafast and memory-efficient alignment of short DNA sequences to the human genome. *Genome Biology*, *10*(3), R25. https://doi.org/10.1186/gb-2009-10-3-r25

Lee, C.-Y., & Seydoux, G. (2019). Dynamics of mRNA entry into stress granules. *Nature Cell Biology*, *21*(2), 116–117. https://doi.org/10.1038/s41556-019-0278-5

Leprivier, G., Remke, M., Rotblat, B., Dubuc, A., Mateo, A.-R. F., Kool, M., Agnihotri, S., El-Naggar, A., Yu, B., Somasekharan, S. P., Faubert, B., Bridon, G., Tognon, C. E., Mathers, J., Thomas, R., Li, A., Barokas, A., Kwok, B., Bowden, M., … Sorensen, P. H. (2013). The eEF2 kinase confers resistance to nutrient deprivation by blocking translation elongation. *Cell*, *153*(5), 1064–1079. https://doi.org/10.1016/j.cell.2013.04.055

Li, W., Wang, W., Uren, P. J., Penalva, L. O. F., & Smith, A. D. (2017). Riborex: Fast and flexible identification of differential translation from Ribo-seq data. *Bioinformatics*, *33*(11), 1735–1737. https://doi.org/10.1093/bioinformatics/btx047

Liu, B., & Qian, S.-B. (2014). Translational reprogramming in cellular stress response. *Wiley Interdisciplinary Reviews. RNA*, *5*(3), 301–315. https://doi.org/10.1002/wrna.1212

Martin, M. (2011). Cutadapt removes adapter sequences from high-throughput sequencing reads. *EMBnet.Journal*, *17*(1), 10–12. https://doi.org/10.14806/ej.17.1.200

Mason, P. B., & Struhl, K. (2005). Distinction and relationship between elongation rate and processivity of RNA polymerase II in vivo. *Molecular Cell*, *17*(6), 831–840. https://doi.org/10.1016/j.molcel.2005.02.017

Masser, A. E., Kandasamy, G., Kaimal, J. M., & Andréasson, C. (2016). Luciferase NanoLuc as a reporter for gene expression and protein levels in Saccharomyces cerevisiae. *Yeast*, *33*(5), 191–200. https://doi.org/10.1002/yea.3155

McGlincy, N. J., & Ingolia, N. T. (2017). Transcriptome-wide measurement of translation by ribosome profiling. *Methods*, *126*, 112–129. https://doi.org/10.1016/j.ymeth.2017.05.028

Moon, S. L., Morisaki, T., Khong, A., Lyon, K., Parker, R., & Stasevich, T. J. (2019). Multicolour single-molecule tracking of mRNA interactions with RNP granules. *Nature Cell Biology*, *21*(2), 162–168. https://doi.org/10.1038/s41556-018-0263-4

Morales-Polanco, F., Bates, C., Lui, J., Casson, J., Solari, C. A., Pizzinga, M., Forte, G., Griffin, C., Garner, K. E. L., Burt, H. E., Dixon, H. L., Hubbard, S., Portela, P., & Ashe, M. P. (2021). Core Fermentation (CoFe) granules focus coordinated glycolytic mRNA localization and translation to fuel glucose fermentation. *IScience*, *24*(2), 102069. https://doi.org/10.1016/j.isci.2021.102069

Mühlhofer, M., Berchtold, E., Stratil, C. G., Csaba, G., Kunold, E., Bach, N. C., Sieber, S. A., Haslbeck, M., Zimmer, R., & Buchner, J. (2019). The Heat Shock Response in Yeast Maintains Protein Homeostasis by Chaperoning and Replenishing Proteins. *Cell Reports*, *29*(13), 4593-4607.e8. https://doi.org/10.1016/j.celrep.2019.11.109

Noree, C., Begovich, K., Samilo, D., Broyer, R., Monfort, E., & Wilhelm, J. E. (2019). A quantitative screen for metabolic enzyme structures reveals patterns of assembly across the yeast metabolic network. *Molecular Biology of the Cell*, *30*(21), 2721–2736. https://doi.org/10.1091/mbc.E19-04-0224

Park, H., & Subramaniam, A. R. (2019). Inverted translational control of eukaryotic gene expression by ribosome collisions. *PLoS Biology*, *17*(9), e3000396. https://doi.org/10.1371/journal.pbio.3000396

Pineau, L., & Ferreira, T. (2010). Lipid-induced ER stress in yeast and β cells: Parallel trails to a common fate. *FEMS Yeast Research*, *10*(8), 1035–1045. https://doi.org/10.1111/j.1567-1364.2010.00674.x

Pop, C., Rouskin, S., Ingolia, N. T., Han, L., Phizicky, E. M., Weissman, J. S., & Koller, D. (2014). Causal signals between codon bias, mRNA structure, and the efficiency of translation and elongation. *Molecular Systems Biology*, *10*, 770. https://doi.org/10.15252/msb.20145524

Presnyak, V., Alhusaini, N., Chen, Y.-H., Martin, S., Morris, N., Kline, N., Olson, S., Weinberg, D., Baker, K. E., Graveley, B. R., & Coller, J. (2015). Codon optimality is a major determinant of mRNA stability. *Cell*, *160*(6), 1111–1124. https://doi.org/10.1016/j.cell.2015.02.029

Riba, A., Di Nanni, N., Mittal, N., Arhné, E., Schmidt, A., & Zavolan, M. (2019). Protein synthesis rates and ribosome occupancies reveal determinants of translation elongation rates. *Proceedings of the National Academy of Sciences of the United States of America*, *116*(30), 15023–15032. https://doi.org/10.1073/pnas.1817299116

Sanchez, M., Lin, Y., Yang, C.-C., McQuary, P., Rosa Campos, A., Aza Blanc, P., & Wolf, D. A. (2019). Cross Talk between eIF2α and eEF2 Phosphorylation Pathways Optimizes Translational Arrest in Response to Oxidative Stress. *IScience*, *20*, 466–480. https://doi.org/10.1016/j.isci.2019.09.031

Santos, D. A., Shi, L., Tu, B. P., & Weissman, J. S. (2019). Cycloheximide can distort measurements of mRNA levels and translation efficiency. *Nucleic Acids Research*, *47*(10), 4974–4985. https://doi.org/10.1093/nar/gkz205

Schaaff, I., Heinisch, J., & Zimmermann, F. K. (1989). Overproduction of glycolytic enzymes in yeast. *Yeast*, *5*(4), 285–290. https://doi.org/10.1002/yea.320050408

Schleif, R., Hess, W., Finkelstein, S., & Ellis, D. (1973). Induction kinetics of the L-arabinose operon of Escherichia coli. *Journal of Bacteriology*, *115*(1), 9–14. https://doi.org/10.1128/jb.115.1.9-14.1973

Schuller, A. P., Wu, C. C.-C., Dever, T. E., Buskirk, A. R., & Green, R. (2017). EIF5A Functions Globally in Translation Elongation and Termination. *Molecular Cell*, *66*(2), 194-205.e5. https://doi.org/10.1016/j.molcel.2017.03.003

Sen, N. D., Zhou, F., Ingolia, N. T., & Hinnebusch, A. G. (2015). Genome-wide analysis of translational efficiency reveals distinct but overlapping functions of yeast DEAD-box RNA helicases Ded1 and eIF4A. *Genome Research*, *25*(8), 1196–1205. https://doi.org/10.1101/gr.191601.115

Shah, P., Ding, Y., Niemczyk, M., Kudla, G., & Plotkin, J. B. (2013). Rate-limiting steps in yeast protein translation. *Cell*, *153*(7), 1589–1601. https://doi.org/10.1016/j.cell.2013.05.049

Shalgi, R., Hurt, J. A., Krykbaeva, I., Taipale, M., Lindquist, S., & Burge, C. B. (2013). Widespread regulation of translation by elongation pausing in heat shock. *Molecular Cell*, *49*(3), 439–452. https://doi.org/10.1016/j.molcel.2012.11.028

Sharma, A. K., Sormanni, P., Ahmed, N., Ciryam, P., Friedrich, U. A., Kramer, G., & O'Brien, E. P. (2019). A chemical kinetic basis for measuring translation initiation and elongation rates from ribosome profiling data. *PLoS Computational Biology*, *15*(5), e1007070. https://doi.org/10.1371/journal.pcbi.1007070

Sheff, M. A., & Thorn, K. S. (2004). Optimized cassettes for fluorescent protein tagging in Saccharomyces cerevisiae. *Yeast*, *21*(8), 661–670. https://doi.org/10.1002/yea.1130

Sheikh, M. S., & Fornace, A. J. (1999). Regulation of translation initiation following stress. *Oncogene*, *18*(45), 6121–6128. https://doi.org/10.1038/sj.onc.1203131

Souza-Moreira, T. M., Navarrete, C., Chen, X., Zanelli, C. F., Valentini, S. R., Furlan, M., Nielsen, J., & Krivoruchko, A. (2018). Screening of 2A peptides for polycistronic gene expression in yeast. *FEMS Yeast Research*, *18*(5). https://doi.org/10.1093/femsyr/foy036

Tanaka, S., Miyazawa-Onami, M., Iida, T., & Araki, H. (2015). iAID: An improved auxin-inducible degron system for the construction of a "tight" conditional mutant in the budding yeast Saccharomyces cerevisiae. *Yeast*, *32*(8), 567–581. https://doi.org/10.1002/yea.3080

Tavares, C. D. J., Ferguson, S. B., Giles, D. H., Wang, Q., Wellmann, R. M., O'Brien, J. P., Warthaka, M., Brodbelt, J. S., Ren, P., & Dalby, K. N. (2014). The molecular mechanism of eukaryotic elongation factor 2 kinase activation. *Journal of Biological Chemistry*, *289*(34), 23901–23916. https://doi.org/10.1074/jbc.M114.577148

Teige, M., Scheikl, E., Reiser, V., Ruis, H., & Ammerer, G. (2001). Rck2, a member of the calmodulin-protein kinase family, links protein synthesis to high osmolarity MAP kinase signaling in budding yeast. *Proceedings of the National Academy of Sciences of the United States of America*, *98*(10), 5625–5630. https://doi.org/10.1073/pnas.091610798

Vaidyanathan, R., Kuersten, S., Radek, A., Swami, S., & Syed, F. (2013). Assessing mRNA Translation: Deep Sequencing of Ribosome Footprints. *Journal of Biomolecular Techniques*, *24*(Suppl), S60.

Wang, Z., Sun, X., Wee, J., Guo, X., & Gu, Z. (2019). Novel insights into global translational regulation through Pumilio family RNA-binding protein Puf3p revealed by ribosomal profiling. *Current Genetics*, *65*(1), 201–212. https://doi.org/10.1007/s00294-018-0862-4

Weinberg, D. E., Shah, P., Eichhorn, S. W., Hussmann, J. A., Plotkin, J. B., & Bartel, D. P. (2016). Improved Ribosome-Footprint and mRNA Measurements Provide Insights into Dynamics and Regulation of Yeast Translation. *Cell Reports*, *14*(7), 1787–1799. https://doi.org/10.1016/j.celrep.2016.01.043

Wu, C. C.-C., Zinshteyn, B., Wehner, K. A., & Green, R. (2019). High-Resolution Ribosome Profiling Defines Discrete Ribosome Elongation States and Translational Regulation during Cellular Stress. *Molecular Cell*, *73*(5), 959-970.e5. https://doi.org/10.1016/j.molcel.2018.12.009

Zhu, M., Dai, X., & Wang, Y.-P. (2016). Real time determination of bacterial in vivo ribosome translation elongation speed based on LacZα complementation system. *Nucleic Acids Research*, *44*(20), e155. https://doi.org/10.1093/nar/gkw698

Zid, B. M., & O'Shea, E. K. (2014). Promoter sequences direct cytoplasmic localization and translation of mRNAs during starvation in yeast. *Nature*, *514*(7520), 117–121. https://doi.org/10.1038/nature13578

Chapter 4:

Acute glucose starvation in a yeast *in vitro* translation system recapitulates reduced translation observed *in vivo*

4.1 Abstract

Repression of translation is a hallmark of how living cells respond to severe environmental stress. Stress-induced regulation and alteration of protein synthesis is well-conserved and well-studied. Additionally, many molecular changes that occur during stress responses in cells have been isolated and characterized with *in vitro* systems. Currently lacking, however, is knowledge about the general impact that undergoing a stress response prior to cell collection has on *in vitro* systems prepared with those cells. Here, we used extracts from log phase and glucose-starved yeast to study how stress response impacts expression in an *in vitro* translation assay. We found that starved extracts reproducibly produce less protein than their non-stressed counterpart extracts. This finding is remarkably consistent when various alterations are made to the reporter transcripts used. Our results demonstrate that, to a certain extent, the reduced propensity for protein synthesis that yeast mount in response to glucose starvation is maintained in their extracts.

4.2 Introduction

At the onset of my thesis research, our laboratory was newly established and in need of assay development, optimization, and implementation. We reasoned that, as a lab interested in translation, it could be useful to employ *in vitro* translation (IVT), commonly called cell-free protein synthesis (CFPS). In general, *in vitro* approaches are powerful systems as they allow researchers to reconstitute steps in biological pathways and examine roles of individual factors. Additionally, these systems can be manipulated in a highly modular and controlled way through varying the inclusion or concentration of an individual component of interest. *In vitro* approaches have proven invaluable in advancing our understanding of phase separation and membraneless granule formation and dynamics (Alberti et al., 2018; Begovich & Wilhelm, 2020; Brangwynne et al., 2011; Li et al., 2012; Molliex et al., 2015). Notably, the stress-induced granules discussed in Chapter 2 are widely thought to form via phase separation and are highly relevant to comprehensively understanding how cells respond to stress. Given this, we reasoned we might be able to utilize an *in vitro* approach as a complement to our genomics and *in vivo* reporter experiments discussed in Chapter 3 to further study how cells react to stress at the level of translation.

Historically, IVT systems have been essential for biochemically elucidating the protein-protein and protein-mRNA interactions that facilitate discrete steps of protein synthesis and for investigating non-canonical translation initiation through mechanisms such as internal ribosome entry sites (Chong, 2014; Kozak, 1999; Merrick, 1992; Nirenberg & Matthaei, 1961). More recently, they have allowed for site-specific incorporation of non-canonical amino acids and have been used to study minimal requirements for developing artificial cells in synthetic biology (Gao et al., 2019; Kopniczky et al., 2020; Laohakunakorn et al., 2020; Perez et al.,

2016; Stech et al., 2021, 2021; Venkat et al., 2019). Furthermore, the production of many bio-pharmaceutical drugs is accomplished with CFPS systems (Richardson et al., 2018). To accomplish these outcomes, researchers often purchase commercially available *in vitro* translation systems. Most are derived from *E. coli*, wheat germ, insect, HeLa, or rabbit reticulocyte extracts prepared under non-stressful growth conditions. These systems were chosen because they tend to translate exogenous RNAs efficiently with low background and relatively low rates of RNA degradation from endogenous nucleases (Gregorio et al., 2019). These advantages result in robust protein production and so, if one desires to synthesize large amounts of protein, they are excellent options. However, being that our lab uses yeast as a model system, we wondered if we could develop a translation assay from yeast extracts made in-house. Furthermore, we reasoned that IVT systems could be useful for examining translation itself rather than simply being a way to obtain high yields of protein for subsequent downstream applications.

The decision to adopt an *in vitro* approach to study translation was further motivated by the overarching question motivating this dissertation-how does acute stress impact protein synthesis? We were motivated, in part, by wondering not just whether we could see translation from our own yeast lysates but whether the reduced translational capacity that has been characterized in intact cells subjected to acute glucose starvation would be mirrored in their extracts. As discussed in Chapter 3, it is widely reported that there is substantial polysome collapse in response to acute glucose starvation. Additionally, bulk levels of S^{35} incorporation are greatly reduced in acutely starved cells compared to log phase, non-stressed cells (Ashe et al., 2000). These results suggest that stressed extracts might be compromised in their ability to translate but, to our knowledge, published literature does not currently exist that establishes

whether IVT systems derived from log phase and glucose-starved yeast extracts differ in their ability to synthesize protein.

Although the direct impact of glucose starvation on a CFPS yeast system has not been reported, decades of research have established a precedent for studying links between stress and translation with CFPS techniques. It is common for researchers to isolate stress-induced factors like proteins or RNAs from cells and see how they impact IVT, though this is typically done in extracts prepared from non-stressed cells. For instance, one report used yeast to examine how heat shock-induced Ded1 protein (Ded1p) condensates impact expression *in vitro*. They found that, in the presence of Ded1p condensates, translation of reporters with structured 5' untranslated regions (UTRs) typical of housekeeping genes was more inhibited than translation of reporters regulated by unstructured 5' UTRs from heat shock genes (Iserman et al., 2020). Another study tested the effects of RNA fragments derived from snoRNAs upregulated in stressed yeast and found they inhibit translation in extracts from log phase cells (Mleczko et al., 2019). Similar findings were reported in a study that showed stress-induced tRNA fragments, also commonly produced in yeast subjected to a variety of environmental stresses, bind to yeast monosomes and reduce *in vitro* expression (Bąkowska-Żywicka et al., 2016). Intriguingly, the parasite *T. brucei* also upregulated the production of tRNA-derived fragments in response to stress and, contrastingly, these fragments had a positive impact on IVT in *T. brucei* extracts (Fricker et al., 2019). Together, these studies highlight that CFPS approaches can provide insight into how stress-induced cytoplasmic changes can be isolated to explore their impact on translation and therefore complement *in vivo* studies.

Aside from investigating how stress-induced cellular components can change translation *in vitro*, other reports have looked directly at synthesis in extracts isolated from

stressed cells, though this is not as common of a method. This more general approach

determines how a stress response prior to extract preparation impacts *in vitro* assays as opposed

to determining how specific, individual components might alter expression during the

translation reaction. Historically, this approach has been used to explore the translation of heat

shock proteins. A set of classical, contemporaneous reports took extracts from heat shocked

and non-stressed *Drosophila* extracts and tested their ability to discriminate between heat shock

versus pre-stress transcripts (Krüger & Benecke, 1981; Scott & Pardue, 1981; Storti et al.,

1980). They found that stressed extracts preferentially translated heat shock mRNAs while

control extracts did not, thereby recapitulating an *in vivo* paradigm (McKenzie et al., 1975).

This indicates that stressed translation machinery maintains a competency to discern stress-

induced transcripts from the general mRNA pool independent of an intact cellular environment.

More recently, another group showed that extracts made from nutrient stressed, stationary

phase *E. coli* are competent to translate high protein yield. This result was surprising given the

translation machinery came from cells that were largely not translating at the time of harvest

(Failmezger et al., 2017). Studies like these demonstrate that the performance of IVT extracts

cannot necessarily be predicted from the *in vivo* behavior of a given model system in a

straightforward manner. Ultimately, questions about the ways in which diverse stress responses

in different organisms influence *in vitro* protein expression remain open.

In this study, we examined the competence of minimally-processed yeast extracts to

perform IVT of various luciferase reporter mRNAs. Our motivation was to determine whether

we could test if the reduced translational capacity during acute glucose starvation observed *in*

vivo is sustained *in vitro*. Consequently, we did not aim to isolate individual components like

single transcripts, P-bodies, or stress granules from stressed cells nor to heavily process their

extracts after lysis to optimize yield. With this approach, we demonstrated that extracts from log phase and glucose starved cells both can translate luciferase reporter mRNAs and, furthermore, that log phase extracts reproducibly translated more protein than starved ones when used in otherwise equivalent reactions. We then characterized the impacts of performing a micrococcal nuclease (MN) digestion on extracts or of modifying reporter mRNAs in our CFPS through changes to ribonucleotide identity, 5' cap structure, and polyadenylated (polyA) tail length. We found that increasing polyA tail length increased expression while addition of noncanonical caps or bases decreased expression. Surprisingly, we also found that MN treatment reduced expression in our hands. Finally, we corroborated that the difference in expression between log phase versus stress extracts is maintained upon the use of additional reporter mRNAs and we examined mRNA stability in IVT reactions, finding that increased mRNA decay in stressed extracts did not occur and therefore does not seem to explain their decreased expression.

4.3 Results

4.3.1 Lysis technique, stress, and micrococcal nuclease treatment impact expression in yeast IVT systems

To determine whether glucose starvation impacts CFPS we first established a protocol to create functional extracts from yeast. Although yeast is not a common model in commercially available CFPS kits, it is commonplace for academic labs that use yeast to perform *in vitro* translation with their extracts. Given that, we turned to protocols published by other academic labs to develop our own workflow (Hodgman & Jewett, 2013; Wu et al., 2007; Wu & Sachs, 2014). Notably, our first attempts at protein expression were not successful as assessed by measuring expression of an *in vitro* transcribed *renilla* luciferase (*rLuc*) reporter in log phase extracts. Our initial protocol relied upon bead beating, a common and relatively simple method of lysis, that uses mechanical disruption to break apart cell walls and membranes. In my hands, use of a standard beat beating procedure with 400µm silica beads and intermittent cooling on ice generated lysates that did not translate luciferase above background. Robust expression was observed after translating the same *rLuc* reporter in a commercial HeLa CFPS kit (data not shown) which led us to conclude the lack of expression was linked to the extracts, not to the reporter.

After this initial failure we opted to switch lysis techniques to cryogenic lysis with a planetary ball mill to grind our cells under liquid nitrogen conditions. This lysis technique is more technically complicated than beat beating but offers the advantage of maintaining colder and more constant temperatures during the disruption process. Pilot experiments produced luciferase signal above background (data not shown). Next, we standardized a protocol to create extracts and quantify translation from a culture that was divided into two: a control from

log phase yeast grown in glucose replete conditions (+G or +Glu) and an experimental extract from cells that underwent 15 minutes of glucose starvation (-G or -Glu). After lysis and clarification these extracts were incubated with reporter mRNAs in a translation buffer and protein expression was recorded (Figure 4.1).
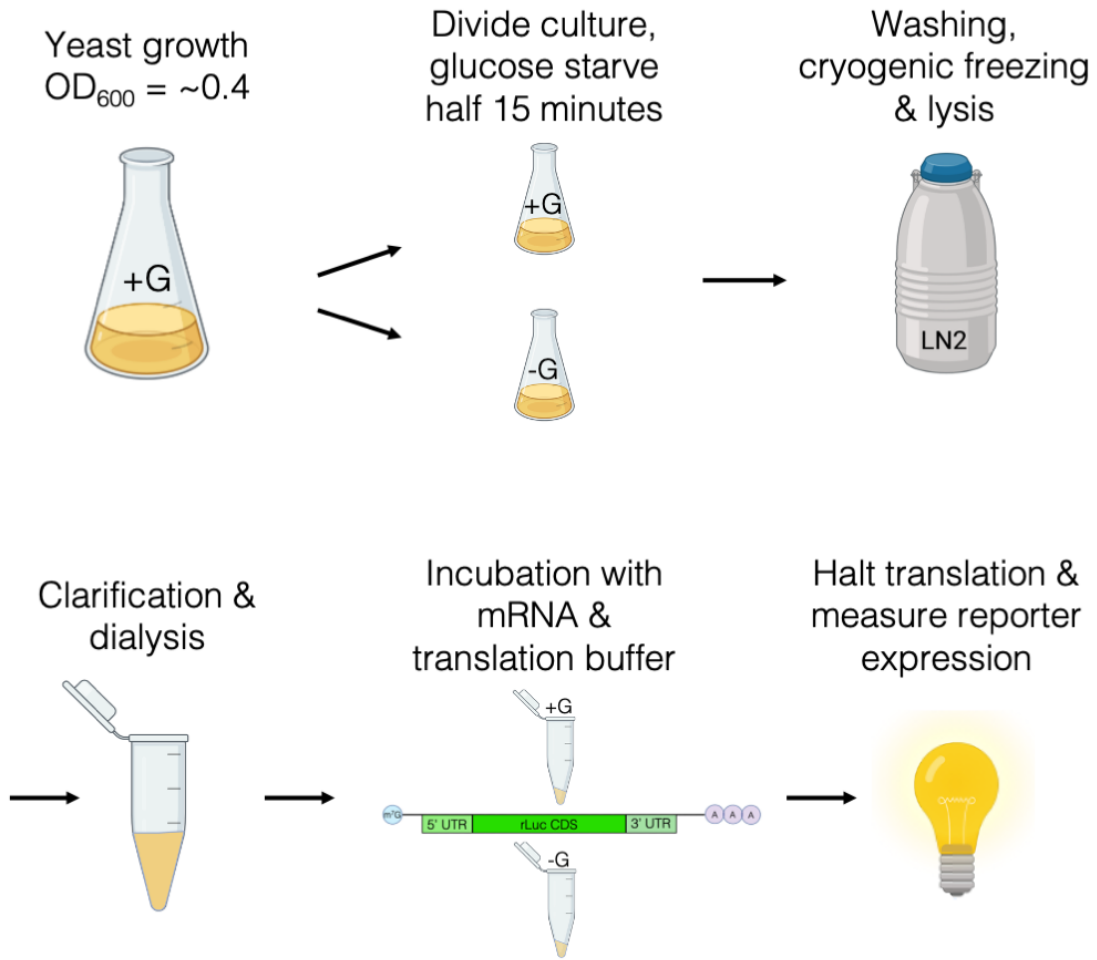
Figure 4.1. *In vitro* **translation protocol.**
IVT takes place over a series of steps. First, a yeast culture is grown to mid-log phase and split into two halves. One half remains in glucose replete medium (+G) while the other is glucose starved for 15 minutes (-G). Then cells are washed, harvested via vacuum filtration, and cryogenically lysed. Lysates are taken through clarification and dialysis. Translation reactions are set up with *in vitro* transcribed luciferase reporters, incubated, and expression is monitored. Images in Figure 4.1 were obtained from BioRender.com.

Once our translation protocol was up and running, we tested whether there was a difference in expression between +Glu and -Glu extracts. Strikingly, we observed that +Glu and -Glu extracts from the same starting culture translated different amounts of reporter protein. Additional aspects of the assay including concentration of the extracts, amount of reporter mRNA added, volumes used, incubation times, temperatures, and translation buffer used were kept consistent between +Glu and -Glu extracts to best isolate the impact of stress alone on the system. Moreover, we made different batches of extracts from different starter cultures and, though the absolute amount of protein translated varied somewhat day-to-day and extract-to-extract, the differential expression between +Glu and -Glu extracts was consistent between experimental trials (Figure 4.2A). To simplify the interpretation of this data, we normalized expression to the +Glu control reactions (Figure 4.2B). This simplification gives a ratio whereby approximately 0.4 RLU (relative light units) was produced in -Glu extracts for every 1 RLU from +Glu extracts (Figure 4.3). We interpret this result to suggest that, for every functional rLuc protein produced in a -Glu extract, approximately 2.5 more may be produced in a +Glu extract. We next wondered if and how a micrococcal nuclease (MN) digestion of our lysates would impact these results. It is common for researchers and companies preparing CFPS systems to include a MN digest to decrease the concentration of endogenous nucleic acids that might compete for translation machinery. To our surprise, we found that MN digestion decreased protein production in both extracts (Figure 4.4). Additionally, the relative decrease in expression observed from the -Glu extracts was significantly more pronounced in the digested samples.

A
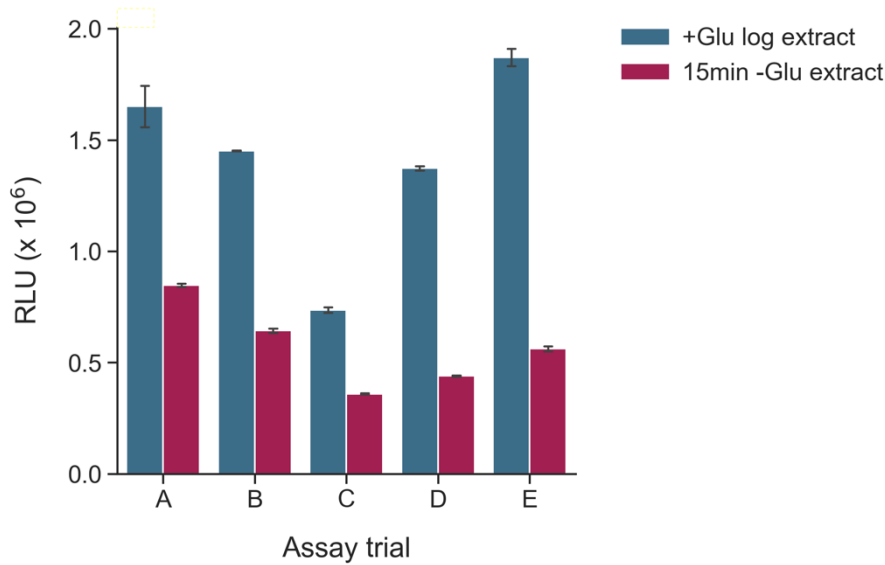
B
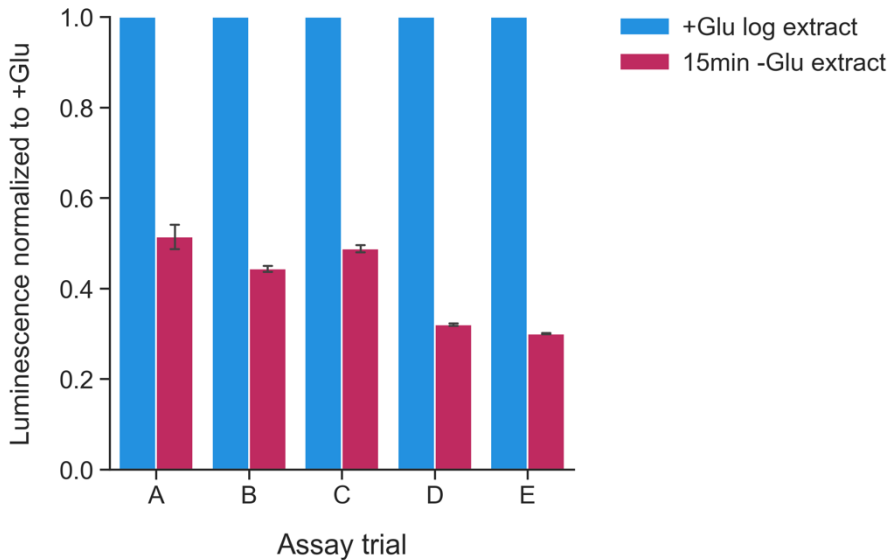
Figure 4.2. Stressed yeast extracts produce less protein than non-stressed extracts.
(A) The difference in luciferase expression between extracts of log phase (+Glu) cells versus extracts of cells that underwent 15 minutes of acute glucose starvation (-Glu). Expression was quantified by background subtraction of RLU values across five independent trials. In each experiment, reactions were set up and monitored in triplicate. RLU = relative light unit. (B) Signal normalization of expression from 4.2A showing the difference in luciferase production between extracts for each experiment normalized to expression in +Glu conditions for each trial. For A and B, values are plotted as mean ± standard deviation (sd).
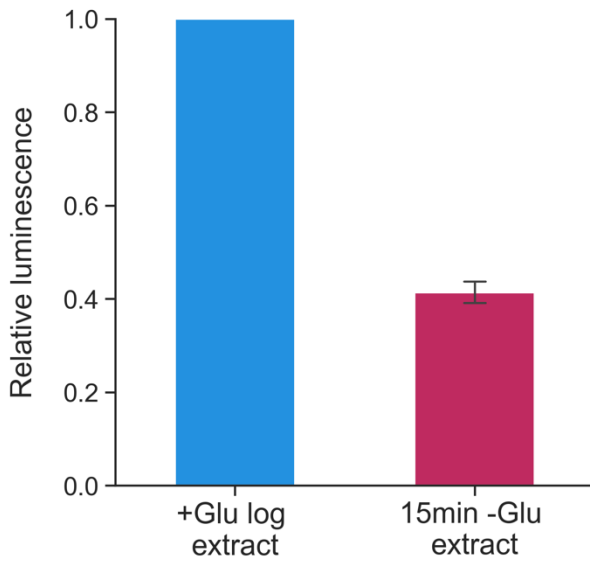
Figure 4.3. The magnitude of expression changes between -Glu and +Glu extracts.
For the glucose starvation (-Glu) extracts, the mean ± standard error of the mean (sem) of the normalized luminescence values from Figure 4.2B was calculated and plotted relative to control extracts. For each trial, the luminesce from the +Glu extracts was set to 1. Data was taken from trials A-E, as individually shown in in Figure 4.2A-B.
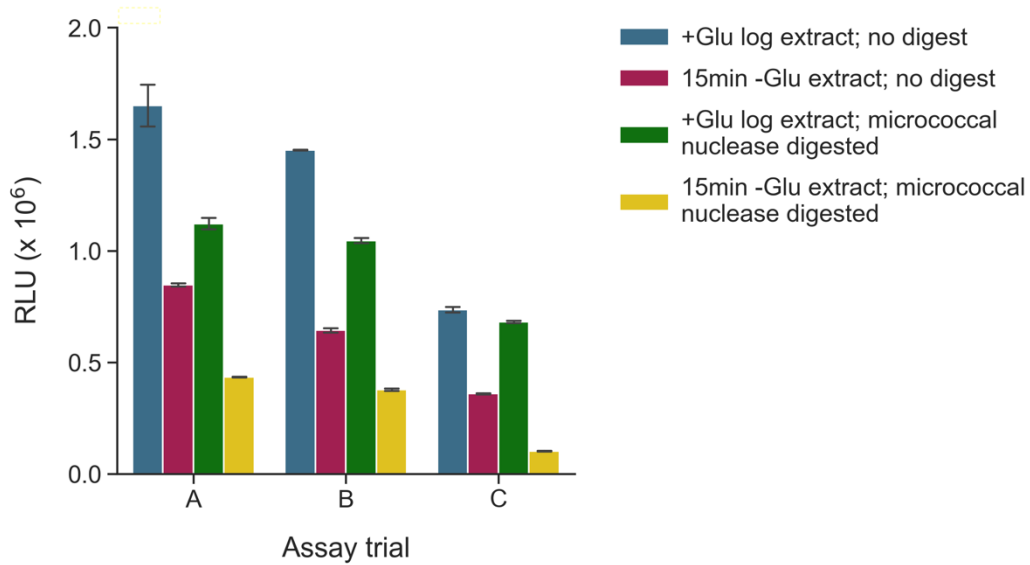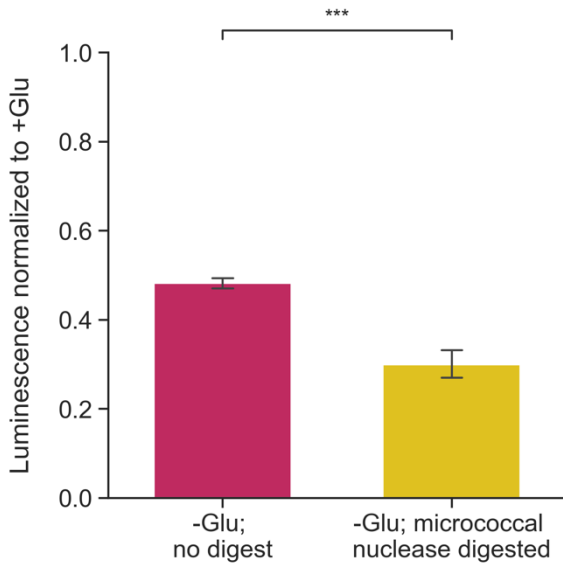
A

B

Figure 4.4. Micrococcal nuclease digestion decreases *in vitro* translation performance.
(A) The difference in luciferase expression between extracts that did or did not undergo digestion with micrococcal nuclease, as indicated. Expression was quantified by background subtraction of RLU values across three independent trials. In each experiment, reactions were set up and monitored in triplicate. Values are plotted as mean ± sd. (B) The mean of normalized luminescence ratio values from A. Data was prepared as in Figure 4.3 where luminescence for the +Glu extract was set to 1.0 and proportionate expression from the -Glu extracts was calculated. Values are plotted as mean ± sem and statistical significance was assessed by unpaired Student's t-test (***p<0.001)

4.3.2 Epitranscriptomic mRNA modifications decrease expression in stressed and control IVT extracts but do not alter their comparative performance

We next wondered whether various alterations to the reporter mRNAs used in our IVT assays would have the ability to alter expression, either generally with respect to overall luciferase signal or specifically to the luminescence ratio observed between +Glu and -Glu extracts. First, we tested whether incorporation of chemically modified nucleotide bases into *rLuc* mRNA would alter their translatability. To accomplish this, we separately doped transcription reactions with either N^6-methyladenosine (m^6A) or pseudouridine (Ψ). These modifications were of interest as both are epitranscriptomic marks incorporated into yeast mRNAs in a regulated manner. In particular, yeast and mammalian cells orchestrate their discrete removal and addition on the bases of mRNAs in response to stress. Reactions with unmodified and modified *rLuc* reporters were set up and measured simultaneously. We found that the modifications had a profound, negative impact on rLuc signal and therefore generally decreased translation. The presence of m^6A decreased luciferase signal by one order of magnitude in log phase extracts while Ψ decreased it by two orders of magnitude. In stress extracts, both modifications decreased expression by one order of magnitude (Figure 4.5A). Notably, though overall translation was down, the ratio between +Glu and -Glu extract performance did not vary (Figure 4.5B).
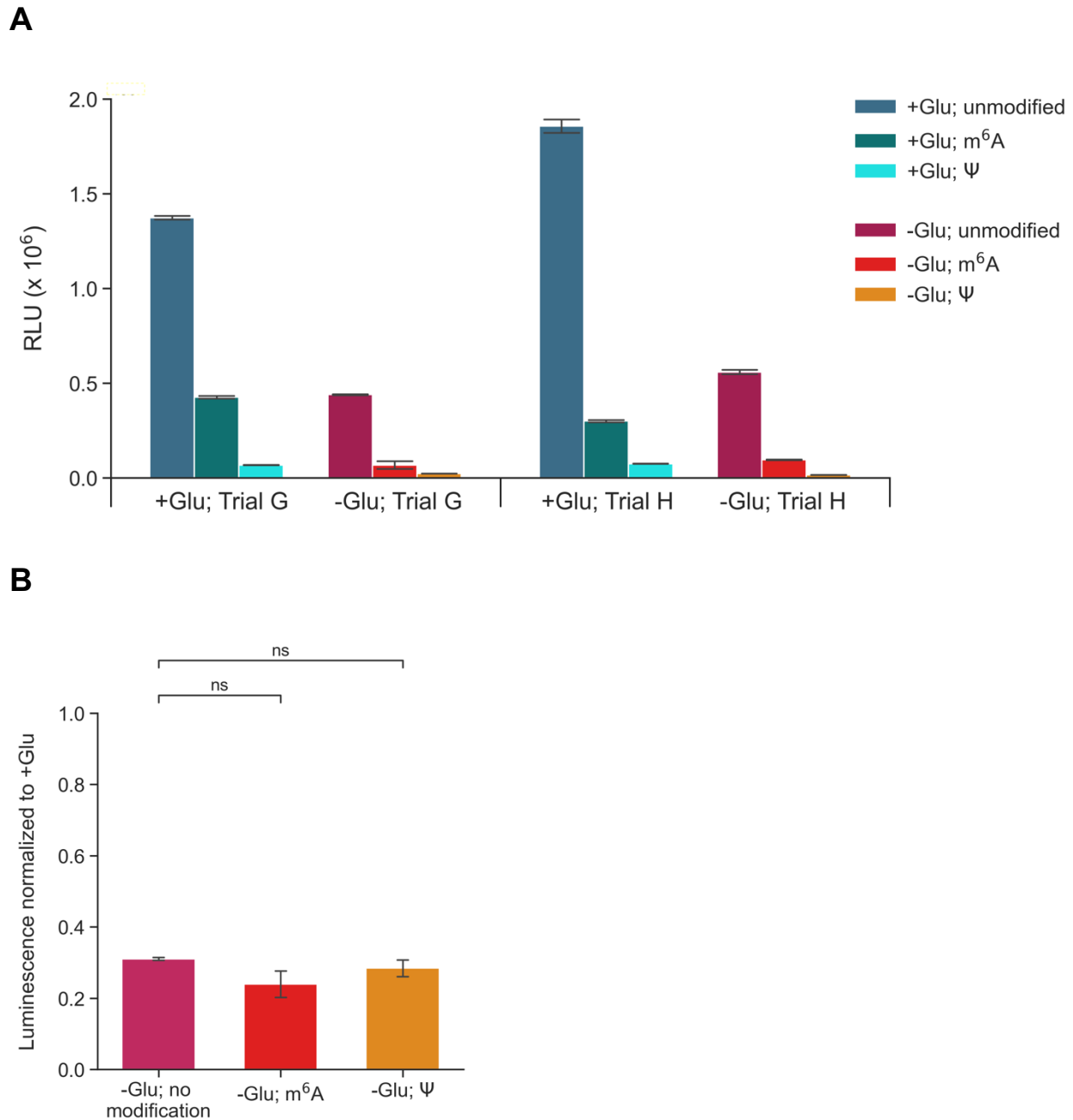
A

B

Figure 4.5. Incorporation of N⁶-methyladenosine or pseudouridine into reporter mRNAs decreases *in vitro* translation performance.
(A) The difference in luciferase expression from reporters transcribed with N⁶-methyladenosine (m⁶A) or pseudouridine (Ψ) compared to reporters transcribed with only canonical ribonucleoside triphosphates. Expression was quantified by background subtraction of RLU values across two independent trials. In each experiment, reactions were set up and monitored in triplicate. RLU = relative light unit. Values are plotted as mean ± sd. (B) The mean of normalized luminescence ratio values from A. Data was prepared as in Figure 4.3 where the luminescence for the +Glu extract is set to 1.0 and proportionate expression from the -Glu extracts was calculated. Values are plotted as mean ± sem and statistical significance was assessed by unpaired Student's t-test (ns = not significant)

4.3.3 Changes to polyA tailing and 5' cap identity differentially alter expression in stressed and control IVT extracts

Aside from epitranscriptomic marks, other features frequently occur on mRNAs that can influence their translation and are tightly regulated in living cells. Two canonical, intensively studied, and well-conserved examples include the methylated guanosine cap structure at the 5' end of an mRNA and the polyA tail at the 3' end. Here, we analyzed how substitution of the canonical m^7G cap for a non-methylated analog impacts expression in our CFPS system. We also took our *rLuc* mRNA through an extended polyA tailing reaction to produce longer tails than those normally added to the reporters with a standard tailing reaction. As with the m^6A- or Ψ-modified reporters, we set up reactions in parallel with unmodified reporters to test how the cap analog and the longer tail each alter translation.

We found that the cap analog drastically reduced expression in both extracts, doing so over 20-fold in +Glu conditions and 14-fold in -Glu conditions (Figure 4.6A). Consequently, the ratio of relative performance between extracts increased significantly (Figure 4.7). Intriguingly, we found the opposite for long tailing. When longer polyA tails were present on the reporters, expression increased in both extracts. This was particularly true in the +Glu extracts where luciferase signal was 3.5-fold greater (Figure 4.6B). The increase in -Glu extracts was more modest as it only increased by approximately 20%. In turn, the ratio of relative performance between the extracts was significantly decreased when the reporters had a longer polyA tail (Figure 4.7).
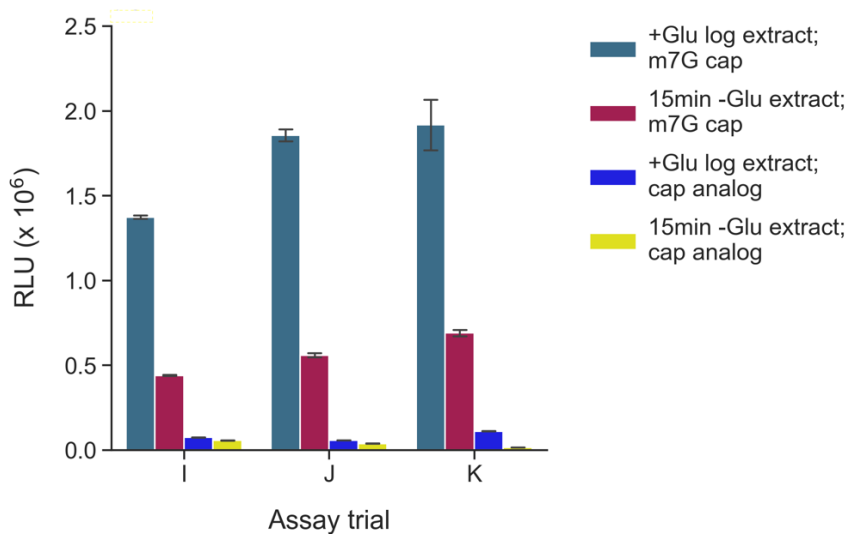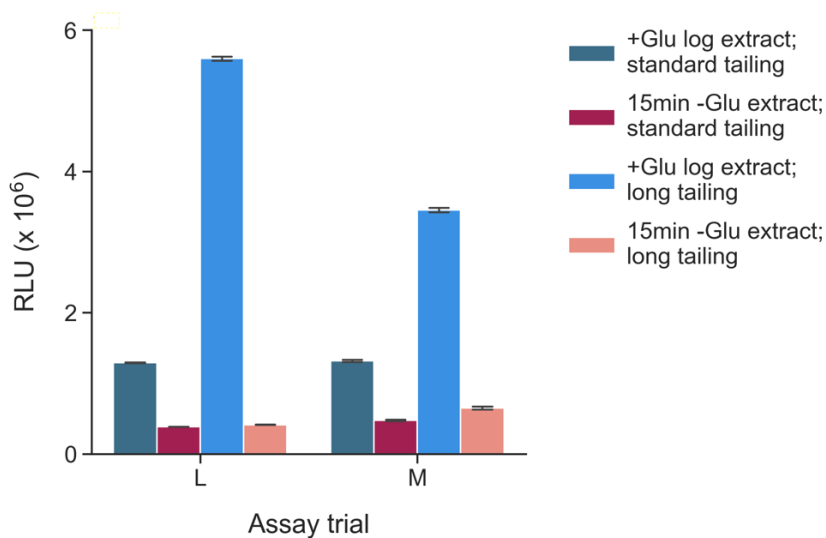
Figure 4.6. Reporter mRNAs with noncanonical caps severely decrease *in vitro* translation in stressed and non-stressed extracts while increased polyA tail length improves performance.
(A) The difference in luciferase expression from reporters transcribed with a canonical m^{7}G cap compared to those transcribed with a noncanonical, unmethylated cap analog. Expression was quantified by background subtraction of RLU values across three independent trials. In each experiment, reactions were set up and monitored in triplicate. RLU = relative light unit. Values are plotted as mean ± sd. (B) The difference in luciferase expression from reporters transcribed with polyA tailing according to manufacturer's specifications to reporters transcribed with increased tail length. Expression was quantified by background subtraction of RLU values across two independent trials. In each experiment, reactions were set up and monitored in triplicate.
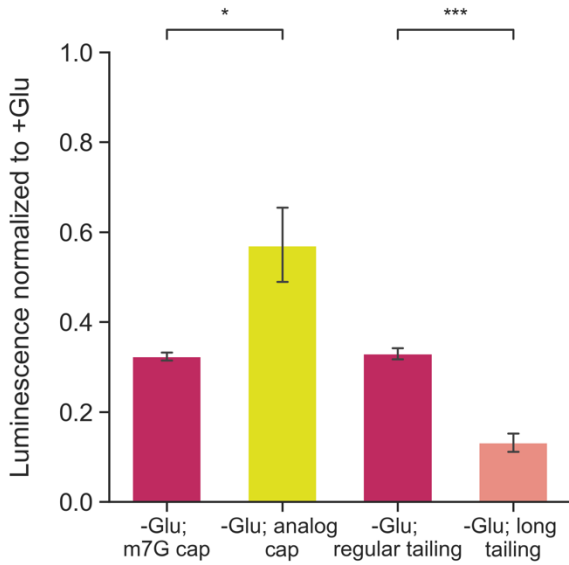
Figure 4.7. Reporter mRNAs with noncanonical caps cause a relatively higher rate of protein production from stressed extracts when compared to non-stressed extracts while increased polyA tail length leads to a relative decrease in protein production in stressed extracts.
The mean of normalized luminescence ratio values from Figure 4.6. Data was prepared as in Figure 4.3 where the luminescence for the +Glu extract is set to 1.0 and proportionate expression from the -Glu extracts was calculated. Values are plotted as mean ± sem and statistical significance was assessed by unpaired Student's t-test (***p<0.001, * p<0.05)

4.3.4 Differential protein expression between stressed and non-stressed extracts is robust against extract mixing and changing reporter gene identity

We were struck by the consistency with which the extracts performed relative to one another across the various assays described so far. Although we observed that digestion as well as base, cap, or tail modifications can alter the performance of -Glu extracts when compared to +Glu, it is also very apparent that a general rule holds firm: across the board, stressed extracts do not translate as well as non-stressed ones (Figures 4.2-7). To further explore this result, we next asked what would happen if +Glu and -Glu extracts were combined. To do so, we set up IVT reactions using +Glu and -Glu extracts alone and then introduced a third sample in which equal proportions of the two were mixed (Figure 4.8). Remarkably, the expression observed from the mixed extract reactions was halfway between the other two.

We also wanted to test whether the differential translation between extracts was dependent on the reporter protein being expressed or on mRNA stability. To do so, we transcribed two different luciferase reporters that lack sequence homology to *rLuc*. The first was a Nanoluciferase reporter, *nLuc*, and the second was *nLuc* fused to an additional, upstream ORF encoding *LacZ* and separated by a linker. In addition to being dissimilar from *rLuc* in terms of sequence, these reporters were also chosen because *nLuc* (639bp) is shorter than *rLuc* (936bp) while *LacZ-nLuc* is much longer (3,735bp). CFPS reactions were set up with these two alternate reporter mRNAs at equimolar concentration and expression was monitored (Figure 4.9A). Although the same copy number of reporters was introduced to the reactions, the overall expression detected from the longer *LacZ-nLuc* was decreased compared to *nLuc* only. Nonetheless, the relative expression difference held whereby +Glu extracts translate roughly 4-fold or greater when compared to -Glu extracts (Figure 4.9B).

Finally, we performed RNA extraction, cDNA synthesis, and qPCR on IVT reactions that were performed with unmodified *rLuc* reporters in +Glu and -Glu extracts. The threshold cycle (C_t) values obtained between extracts from qPCR reactions performed with rLuc primers did not vary significantly. In fact, we found the C_t was slightly decreased in -Glu extracts compared to +Glu extracts by a mean value of 0.83 cycles. We interpret these results to suggest that there is not a substantial difference in mRNA degradation between our +Glu and -Glu extracts and therefore do not think mRNA stability changes are a major determinant of the differential expression observed between them. Crucially, this procedure was only performed on unmodified reporters and so these experiments would need to be repeated on translation reactions performed with modified reporters to conclusively determine that this result is consistent in all conditions we tested.
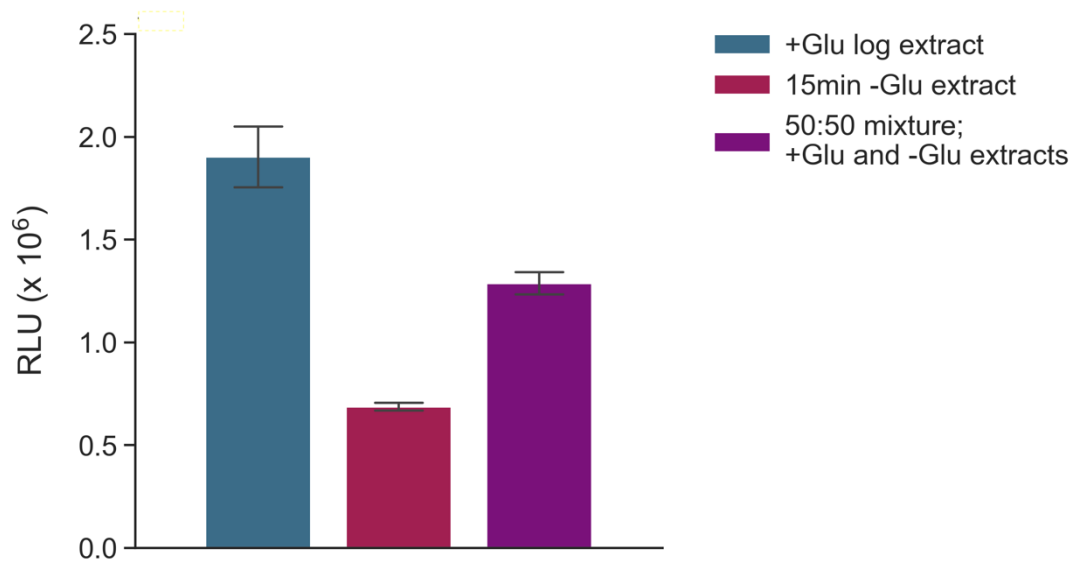
Figure 4.8. Combining stressed and non-stressed extracts in a single *in vitro* translation reaction results in expression between that of individual extracts.
Expression measurements from three conditions: extracts from log phase cells, extracts of cells that underwent 15 minutes of acute glucose starvation, or a 1:1 ratio of log and starvation extracts combined (50:50 mixture). Expression was quantified by background subtraction of RLU values from two replicates. Values are plotted as mean ± sd.
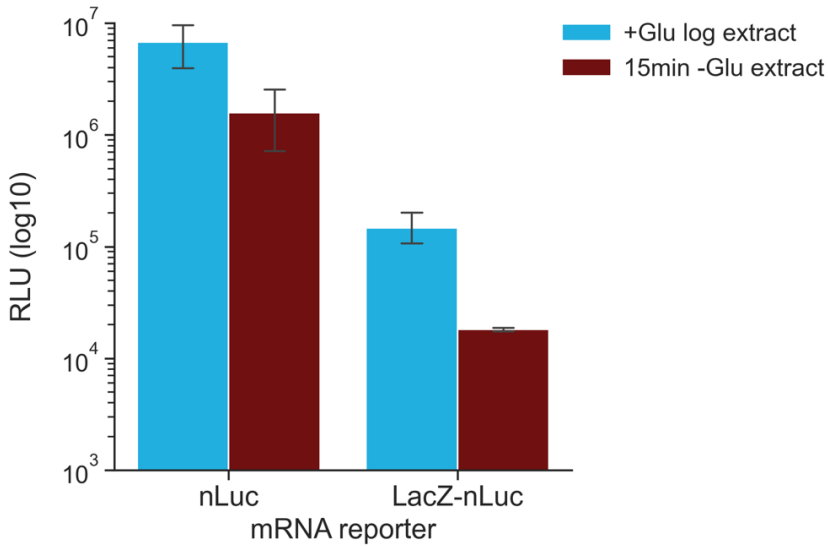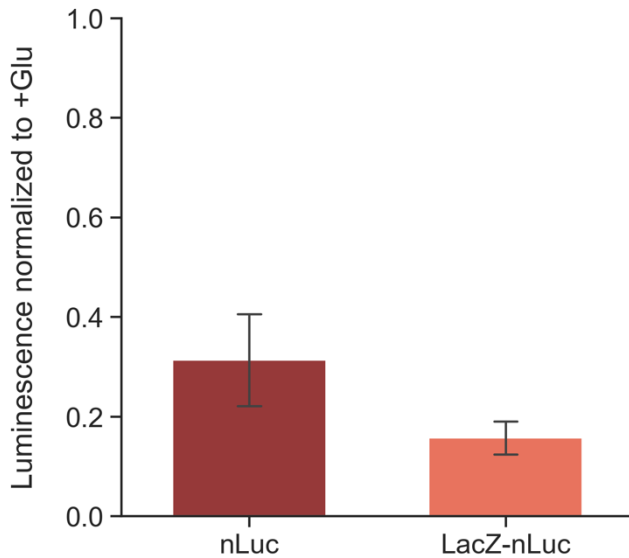
A

B

Figure 4.9. Expression results are similar when *in vitro* translation is performed with different reporter mRNAs of varying lengths.
(A) The difference in luciferase expression from two reporters: nanoLuciferase (*nLuc*) and *LacZ-nLuc* in +Glu and -Glu extracts. Expression was quantified by background subtraction of RLU values across two independent trials. In each experiment, reactions were set up and monitored in duplicate. RLU = relative light unit. Values are plotted as mean of all replicates combined ± sd. (B) The mean of normalized luminescence ratio values from A. Data was prepared as in Figure 4.3 where the luminescence for the +Glu extract is set to 1.0 and proportionate expression from the -Glu extracts was calculated.

4.4 Discussion

Here, we explored the ability of yeast extracts to perform CFPS. Most notably, we found that extracts prepared from cells after 15 minutes of acute glucose starvation do not translate as much reporter protein as extracts from unstressed, log phase cells under a variety of conditions (Figure 4.10, Table 4.1). This result recapitulates previous research done in intact yeast that demonstrated protein synthesis is generally downregulated in response to short periods of this acute starvation stress (Ashe et al., 2000; Brengues et al., 2005; Zid & O'Shea, 2014). Therefore, some influence from the biophysical and/or molecular regulatory responses that limit translation are retained upon lysis.

We also demonstrated that biologically relevant alterations to reporter mRNAs influence IVT. For instance, addition of the epitranscriptomic marks m^{6}A and Ψ lead to decreased reporter expression. Importantly, these modified bases were doped into to a transcription reaction and incorporated into transcripts at random and so were not included or excluded from specific sequence motifs. Nonetheless, they were able to influence translatability. An interesting future direction would be to test the influence these base modifications have in reporters that are modified only at particular motifs through site-specific incorporation techniques like splint ligation or addition of modification writer enzymes during transcription. Previous work has shown that m^{6}A and Ψ are deposited on specific messages during stress and that those changes alter transability. For example, genes responsible for sporulation in yeast have been shown to undergo increased m^{6}A methylation under nitrogen starvation (Schwartz et al., 2013). During heat shock, preferential m^{6}A methylation events occur on the 5' untranslated regions of specific transcripts in mammalian cells and led to increased expression (Zhou et al., 2015). A third study showed that, in yeast, pseudouridylation

of mRNAs increased during nutrient starvation (Carlile et al., 2014). Studies such as these would be useful starting points in determining what motifs would be most relevant for either methylation or pseudouridylation to occur. Strategically designed reporters could then be assayed to test whether non-random incorporation influences translation differently than random incorporation.

In addition to studying chemical nucleotide modifications, we explored the influence of changing the 5' or 3' identity of reporters. First, we tested how an unmethylated cap analog impacts expression relative to a canonical, m^7G cap. This substitution results in a striking decease in expression. This result was not particularly surprising as the m^7G cap is known to be critical for canonical, cap-dependent translation (Ramanathan et al., 2016). This, in turn, suggests that a large extent of expression in our system occurs by, or at the least is facilitated by, cap-dependent initiation. Interestingly, the cap analog was the only modification that significantly increased luciferase expression in -Glu extracts relative to +Glu extracts. This suggests that the -Glu extract, though poorer at translating overall, is more resistant to removal of m^7G caps and therefore might have an increased propensity to translate messages in a cap-independent manner. In the future, it would be interesting to incorporate internal ribosome entry site (IRES) motifs into the 5' UTRs of reporters and assess how they perform in stressed and control extracts.

In opposition to the cap analog, addition of longer polyA tails improved expression in both extracts, particularly in +Glu conditions. Synthesis of a polyA tail generally is known to be very important for mRNA stability and translatability. However, due to technical challenges posed by sequencing repetitive mononucleotide stretches, parsing how tail length impacts translatability genome-wide is still a subject of active investigation, debate, and reconsideration

(Jalkanen et al., 2014; Nicholson & Pasquinelli, 2019). Historically, it has been assumed that longer tails tend to lend more stability to transcripts but, importantly, this does not necessitate that they are better translated. Indeed, much nuance surrounds the relationships that exist between deadenylases, translation machinery, and the RNA-binding proteins that interact with the polyA tail. One recent study using direct RNA sequencing in yeast showed that high expression genes tend to have shorter polyA tails (Tudek et al., 2021). Furthermore, this report demonstrated that tail lengths tend to decrease globally in cells grown in nutrient-limited media compared to those grown in rich media. This, when considered alongside our result that longer tail length improves translation *in vitro*, suggests that there might be different impacts between tail length and translatability *in vitro* versus *in vivo*. These findings suggest additional work could shed light on the relationship between IVT and polyA tail in a more systematic way. In particular, it could be useful to synthesize a range of tail lengths, quantify them, and test them with CFPS. Here, we validated that our longer tailing reactions produced longer reporter mRNAs (section 4.5), but we did not quantify length. In the future, one could use a variety of tailing reaction conditions to produce a larger range of tail lengths and then quantify them with highly sensitive electrophoresis techniques. Systematically testing the performance of known tail lengths in +Glu and -Glu extracts would then provide a higher resolution look into how tail length impacts expression in a stressed *in vitro* system.

Lastly, additional investigations could shed light on what glucose starvation-induced cellular changes are relevant to the differential translation observed in our IVT systems. As discussed in Chapter 3, the mechanisms that rapidly limit protein synthesis in response to acute glucose starvation are incompletely understood but it seems regulation of elongation is important. It would be interesting to test extracts from mutant yeast cells lacking factors that

have important roles in translation elongation to determine what factors may influence the differential translation observed in log and starved extracts. Additionally, researchers have characterized other biophysical alternations that take in yeast in the initial seconds and minutes following acute starvation. For instance, within a minute intracellular ATP levels, intracellular pH, and cytoplasmic diffusion all decrease (Ashe et al., 2000; Joyner et al., 2016; Orij et al., 2009). Notably, our translation buffer included creatine kinase and phosphate to facilitate ATP regeneration. It is quite possible, however, that ATP levels still varied between -Glu and +Glu extracts. Future approaches that alter the concentration of this ATP regeneration system, measure ATP levels in extracts and reactions directly, change the pH, or vary diffusion by altering molecular crowding would each provide insight into what factors influence the differential translation observed between extracts.
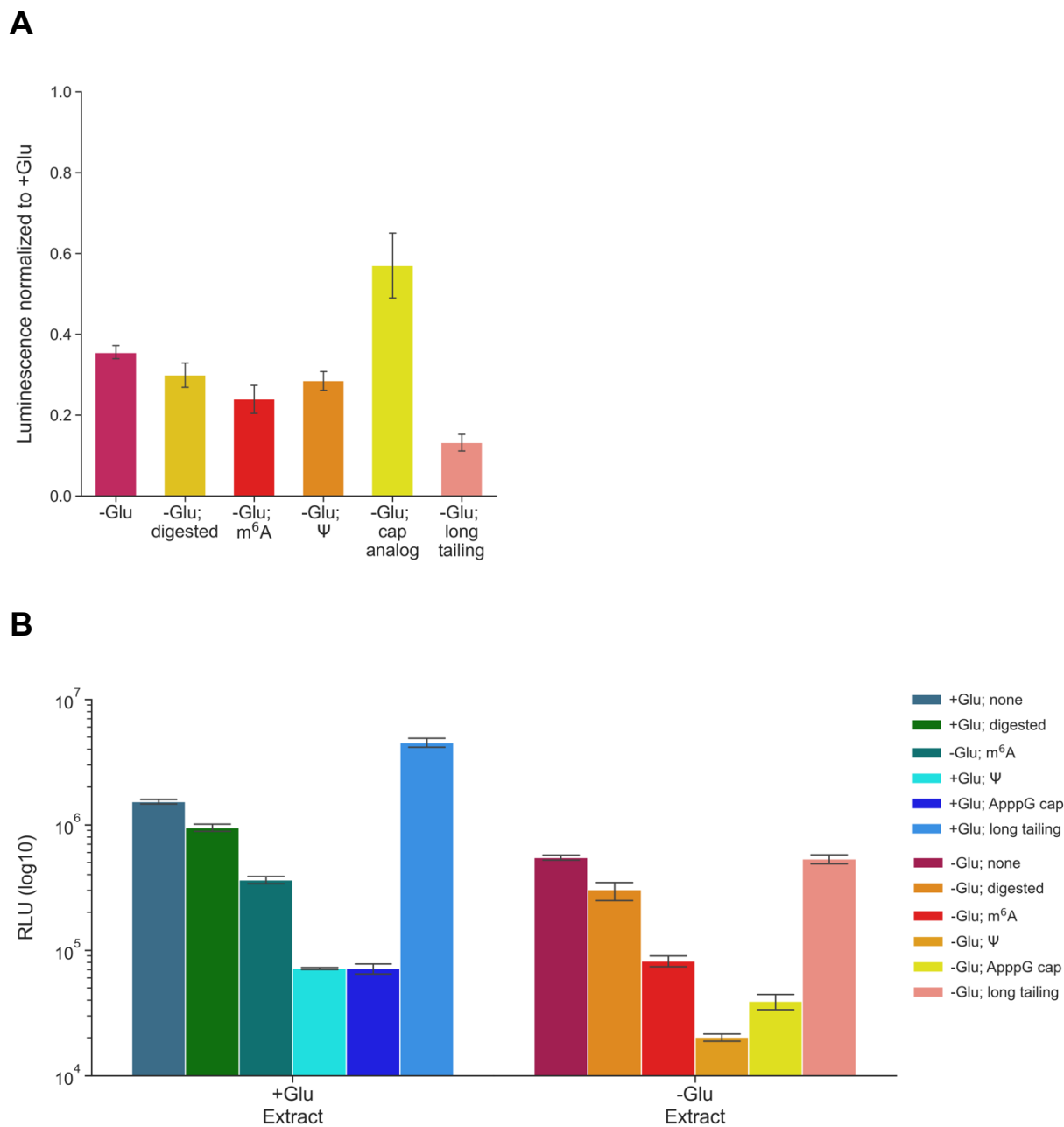
Figure 4.10. Summary of how tested modifications to reporter mRNAs impact translation *in vitro*. (A) The mean ± sem of normalized luminescence ratios from all experimental trials. Data was prepared as in Figure 4.3 where the luminescence for the +Glu extract is set to 1.0 and proportionate expression from the -Glu extracts was calculated. For the -Glu alone sample, the normalized luminescence was calculated from every replicate performed in trials A – M. (B) Summary of expression measurements from the indicated conditions performed in trials A - M. Expression was quantified by background subtraction of RLU. The y-axis is shown on a log10 scale to facilitate visualization of expression from assays performed with either pseudouridine or cap analog modifications, respectively.

Table 4.1. Summary of expression data from IVT reactions performed with modified reporter mRNAs.

mRNA modification		Mean expression in +Glu extract	Mean expression in -Glu extract
None		1,533,350	549,412
m6A		363,374	82,109
Ψ		71,710	20,210
Cap analog		71,377	39,176
Long polyA tailing		4,524,816	533,515

4.5 Materials and Methods

4.5.1 Yeast strain and growth information

All extracts were made from yeast strain BY4741 (MATa his3Δ1 leu2Δ0 met15Δ0 ura3Δ0; Euroscarf). Cells were grown and glucose starved according to the same procedures described in Chapter 3. Briefly, cells were grown in SC media grown in batch culture with shaking at 30°C to mid-log phase. Glucose starvation was performed in SC media prepared without glucose (SC -G). For each extract preparation, half the volume of a culture was filtered for transfer to SC -G media while the other half remained incubating in glucose replete media in log phase, non-stressed conditions. Cells were collected via vacuum filtration, washed 2x in ice cold mannitol buffer (30mM HEPES, pH 7.4, 100mM KOAc, 2mM MgOAc, 2mM DTT, 8.5% mannitol), scraped, and flash frozen in liquid nitrogen in 50mL conical tubes. All -Glu extracts were prepared from cells that underwent 15 minutes of glucose starvation.

4.5.2 Extract preparation

Lysis buffer was added to frozen cell paste dropwise under liquid nitrogen at a ratio of 3mL lysis buffer (30mM HEPES, pH 7.4, 100mM KOAc, 2mM MgOAc, 2mM DTT, 8.5% mannitol, 0.5mM PMSF, 1x EDTA-free Protease Inhibitor Cocktail (Roche)) to every 1L of culture harvested. For example, if a 250mL culture was harvested, then 750μL of lysis buffer was added. Cells were lysed in a planetary ball mill with standard settings (3 minutes cycles at 400rpm with a direction switch every 1 minute) and cooling for 2 minutes in liquid nitrogen between cycles. The resulting powder was returned to 50mL conicals and the lysate was warmed gently in a RT water bath with stirring and intermittent transfer to ice. Once the mixture was barely thawed tubes were spun at 4,000xg for 5 minutes at 4°C. The supernatant

was transferred to microcentrifuge tubes and centrifuged at 20,000xg for 10 minutes at 4°C. Next, dialysis was performed to remove mannitol. Supernatants were loaded into 2K MWCO dialysis cassettes (Thermo CA# 66203) and dialyzed in 1L of dialysis buffer (30mM HEPES, pH 7.4, 100mM KOAc, 2mM MgOAc, 2mM DTT, 0.5mM PMSF, 1x EDTA-free Protease Inhibitor Cocktail (Roche)) for 2 hours with 2 buffer exchanges at 4°C. Lysates were removed from cassettes and centrifuged for 10min at 12,000xg, 4°C. Finally, extract concentration was assessed by measuring the A_{260} and A_{280} values with a Nanodrop 2000c (Thermofisher). Typically, the values were consistent between extracts. If slight absorbance values were different between +Glu and -Glu extracts, then the more concentrated sample had a proportionate volume of dialysis buffer added for normalization.

4.5.3 Transcription of reporter mRNAs

All templates for transcription were PCR amplified to generated constructs containing a T7 promoter and cleaned with a DNA clean and concentrator kit (Zymo). The rLuc reporter was a gift from the Simpson lab (UCSD) of Promega's pRL Renilla Luciferase Control Reporter Vector (CA # E2231). The nLuc and LacZ-nLuc were amplified from existing, in-house plasmid stocks. The unmodified rLuc, nLuc, and LacZ-nLuc reporters as well as the long tail reporters were transcribed and extracted with a mMessage mMachine™ T7 Transcription Kit (Invitrogen) according to manufacturer instructions. Briefly, following transcription, reactions underwent DNase treatment with kit-provided reagents. RNA was extracted with acetate precipitation and acid phenol: chloroform extraction. Following extraction, RNA was left precipitating overnight at -20°C and centrifuged at 20,000xg, 4°C the following day for 30 minutes. RNA pellets were then washed in 80% EtOH and air-dried for 10-15min followed by

resuspension in diH$_2$0. RNA was quantified on a Nanodrop, diluted, aliquoted, and stored at -80°C.

The base modified and alternatively capped rLuc reporters were transcribed and extracted with a MEGAscript™ T7 Transcription Kit (Invitrogen) according to manufacturer instructions. For the cap analog, the amount of provided GTP solution was reduced, and cap analog (NEB) was substituted at a 4:1 analog:GTP ratio. Reactions were also incubated an additional 2 hours to account for the decreased yield that occurs when limiting GTP. For the base modifications, m^{6}A or Ψ were added to the transcription reaction and the amount of either ATP or UTP solution, respectively, were decreased proportionately such that the ratio of unmodified:modified bases was 3:1 ratio. RNA extraction, precipitation, and resuspension were carried out as described above for the unmodified mRNAs.

PolyA tailing of all reporters was performed with polyA polymerase (NEB) according to manufacturer's instructions with 2µL of 10mM ATP added per 10µg RNA. For the long tailing reaction, 2µL of 10mM ATP was added per 2µg RNA and the reaction time was extended from 30 minutes to 2 hours. The presence of a longer tail was confirmed by resolving the long tailing product next to a standard tailing reaction on a denaturing gel. In addition to the long tailing mRNAs, all reporters were run on a denaturing 2% agarose gel (0.4M MOPS, pH 7.0, 0.1 M sodium acetate, 0.01 M EDTA, 37% formaldehyde) in 1X MOPS running buffer (0.4M MOPS, pH 7.0, 0.1 M sodium acetate, 0.01 M EDTA) to confirm they were the expected size and to check for degradation. The presence of either m^{6}A or Ψ in the reporter constructs was confirmed with dot blotting. Briefly, RNAs were serially diluted onto positively charged nylon membranes, incubated overnight at 4°C in either m^{6}A- or Ψ-specific antibodies in 2% milk in TBST, washed 3x5 minutes in TBST, incubated in HRP-conjugated 2° antibodies

against the relevant species, developed in chemiluminescent substrate according to manufacturer's instructions, and imaged on a Chemi-Doc MP Imaging System (Bio-Rad).

4.5.4 *In vitro* translation assays

For translation reactions, extracts were thawed and held on ice while the translation buffer was assembled at RT from reagents held on ice. Stock reagents were combined to create fresh translation buffer each day an assay was performed. The translation buffer was assembled at a 2X concentration, 100ng of reporter mRNA was added per reaction replicate, and the buffer + mRNA was mixed 1:1 with extract to create 1X translation buffer in a translation reaction (22mM HEPES, 120mM KOAc,2mM MgOAc,1mM ATP,0.1mM GTP, 0.04mM amino acid mixture (Promega), 5U RNasin RNase inhibitor (Promega), 25mM creatine phosphate, 1.7mM DTT, 0.3mg/mL creatine kinase) with extracts and mRNA mixed simultaneously.

Typically, 2X translation buffer was made in excess and subsequently divided into the necessary number of aliquots required for the number of extracts/reporter combinations being tested on a given day. After reactions were assembled, they were incubated at RT for 30minutes and moved to ice to halt further translation. Meanwhile, Nano-Glo or Renilla-Glo substrates were prepared according to manufacturer's instructions (Promega). Briefly, luciferase substrate was diluted and aliquoted into wells of a 96 well plate. Then, translation reactions were added to the wells with a multichannel pipette and luminesce was monitored with a 2500ms integration time on a Spark plate reader (Tecan). To ensure signal detection was linear in the range of RLU detection by the instrument used in this study, pilot experiments were performed with dilutions of rLuc at different concentrations and signal intensity was shown to change proportionately (data not shown).

Acknowledgements

References

Alberti, S., Saha, S., Woodruff, J. B., Franzmann, T. M., Wang, J., & Hyman, A. A. (2018). A User's Guide for Phase Separation Assays with Purified Proteins. *Journal of Molecular Biology*, *430*(23), 4806–4820. https://doi.org/10.1016/j.jmb.2018.06.038

Ashe, M. P., De Long, S. K., & Sachs, A. B. (2000). Glucose depletion rapidly inhibits translation initiation in yeast. *Molecular Biology of the Cell*, *11*(3), 833–848. https://doi.org/10.1091/mbc.11.3.833

Bąkowska-Żywicka, K., Kasprzyk, M., & Twardowski, T. (2016). TRNA-derived short RNAs bind to Saccharomyces cerevisiae ribosomes in a stress-dependent manner and inhibit protein synthesis in vitro. *FEMS Yeast Research*, *16*(6), fow077. https://doi.org/10.1093/femsyr/fow077

Begovich, K., & Wilhelm, J. E. (2020). An In Vitro Assembly System Identifies Roles for RNA Nucleation and ATP in Yeast Stress Granule Formation. *Molecular Cell*, *79*(6), 991-1007.e4. https://doi.org/10.1016/j.molcel.2020.07.017

Brangwynne, C. P., Mitchison, T. J., & Hyman, A. A. (2011). Active liquid-like behavior of nucleoli determines their size and shape in Xenopus laevis oocytes. *Proceedings of the National Academy of Sciences of the United States of America*, *108*(11), 4334–4339. https://doi.org/10.1073/pnas.1017150108

Brengues, M., Teixeira, D., & Parker, R. (2005). Movement of eukaryotic mRNAs between polysomes and cytoplasmic processing bodies. *Science*, *310*(5747), 486–489. https://doi.org/10.1126/science.1115791

Carlile, T. M., Rojas-Duran, M. F., Zinshteyn, B., Shin, H., Bartoli, K. M., & Gilbert, W. V. (2014). Pseudouridine profiling reveals regulated mRNA pseudouridylation in yeast and human cells. *Nature*, *515*(7525), 143–146. https://doi.org/10.1038/nature13802

Chong, S. (2014). Overview of cell-free protein synthesis: Historic landmarks, commercial systems, and expanding applications. *Current Protocols in Molecular Biology*, *108*, 16.30.1-11. https://doi.org/10.1002/0471142727.mb1630s108

Failmezger, J., Rauter, M., Nitschel, R., Kraml, M., & Siemann-Herzberg, M. (2017). Cell-free protein synthesis from non-growing, stressed Escherichia coli. *Scientific Reports*, *7*(1), 16524. https://doi.org/10.1038/s41598-017-16767-7

Fricker, R., Brogli, R., Luidalepp, H., Wyss, L., Fasnacht, M., Joss, O., Zywicki, M., Helm, M., Schneider, A., Cristodero, M., & Polacek, N. (2019). A tRNA half modulates translation as stress response in Trypanosoma brucei. *Nature Communications*, *10*(1), 118. https://doi.org/10.1038/s41467-018-07949-6

Gao, W., Bu, N., & Lu, Y. (2019). Efficient Incorporation of Unnatural Amino Acids into Proteins with a Robust Cell-Free System. *Methods and Protocols*, *2*(1), E16. https://doi.org/10.3390/mps2010016

Gregorio, N. E., Levine, M. Z., & Oza, J. P. (2019). A User's Guide to Cell-Free Protein Synthesis. *Methods and Protocols*, *2*(1), E24. https://doi.org/10.3390/mps2010024

Hodgman, C. E., & Jewett, M. C. (2013). Optimized extract preparation methods and reaction conditions for improved yeast cell-free protein synthesis. *Biotechnology and Bioengineering*, *110*(10), 2643–2654. https://doi.org/10.1002/bit.24942

Iserman, C., Desroches Altamirano, C., Jegers, C., Friedrich, U., Zarin, T., Fritsch, A. W., Mittasch, M., Domingues, A., Hersemann, L., Jahnel, M., Richter, D., Guenther, U.-P., Hentze, M. W., Moses, A. M., Hyman, A. A., Kramer, G., Kreysing, M., Franzmann, T. M., & Alberti, S. (2020). Condensation of Ded1p Promotes a Translational Switch from Housekeeping to Stress Protein Production. *Cell*, *181*(4), 818-831.e19. https://doi.org/10.1016/j.cell.2020.04.009

Jalkanen, A. L., Coleman, S. J., & Wilusz, J. (2014). Determinants and Implications of mRNA Poly(A) Tail Size—Does this Protein Make My Tail Look Big? *Seminars in Cell & Developmental Biology*, *0*, 24–32. https://doi.org/10.1016/j.semcdb.2014.05.018

Joyner, R. P., Tang, J. H., Helenius, J., Dultz, E., Brune, C., Holt, L. J., Huet, S., Müller, D. J., & Weis, K. (2016). A glucose-starvation response regulates the diffusion of macromolecules. *ELife*, *5*, e09376. https://doi.org/10.7554/eLife.09376

Kopniczky, M. B., Canavan, C., McClymont, D. W., Crone, M. A., Suckling, L., Goetzmann, B., Siciliano, V., MacDonald, J. T., Jensen, K., & Freemont, P. S. (2020). Cell-Free Protein Synthesis as a Prototyping Platform for Mammalian Synthetic Biology. *ACS Synthetic Biology*, *9*(1), 144–156. https://doi.org/10.1021/acssynbio.9b00437

Kozak, M. (1999). Initiation of translation in prokaryotes and eukaryotes. *Gene*, *234*(2), 187–208. https://doi.org/10.1016/S0378-1119(99)00210-3

Krüger, C., & Benecke, B. J. (1981). In vitro translation of Drosophila heat-shock and non—Heat-shock mRNAs in heterologous and homologous cell-free systems. *Cell*, *23*(2), 595–603. https://doi.org/10.1016/0092-8674(81)90155-0

Laohakunakorn, N., Grasemann, L., Lavickova, B., Michielin, G., Shahein, A., Swank, Z., & Maerkl, S. J. (2020). Bottom-Up Construction of Complex Biomolecular Systems With Cell-Free Synthetic Biology. *Frontiers in Bioengineering and Biotechnology*, *8*, 213. https://doi.org/10.3389/fbioe.2020.00213

Li, P., Banjade, S., Cheng, H.-C., Kim, S., Chen, B., Guo, L., Llaguno, M., Hollingsworth, J. V., King, D. S., Banani, S. F., Russo, P. S., Jiang, Q.-X., Nixon, B. T., & Rosen, M. K.

(2012). Phase transitions in the assembly of multivalent signalling proteins. *Nature*, *483*(7389), 336–340. https://doi.org/10.1038/nature10879

McKenzie, S. L., Henikoff, S., & Meselson, M. (1975). Localization of RNA from heat-induced polysomes at puff sites in Drosophila melanogaster. *Proceedings of the National Academy of Sciences of the United States of America*, *72*(3), 1117–1121. https://doi.org/10.1073/pnas.72.3.1117

Merrick, W. C. (1992). Mechanism and regulation of eukaryotic protein synthesis. *Microbiological Reviews*, *56*(2), 291–315. https://doi.org/10.1128/mr.56.2.291-315.1992

Mleczko, A. M., Machtel, P., Walkowiak, M., Wasilewska, A., Pietras, P. J., & Bąkowska-Żywicka, K. (2019). Levels of sdRNAs in cytoplasm and their association with ribosomes are dependent upon stress conditions but independent from snoRNA expression. *Scientific Reports*, *9*(1), 18397. https://doi.org/10.1038/s41598-019-54924-2

Molliex, A., Temirov, J., Lee, J., Coughlin, M., Kanagaraj, A. P., Kim, H. J., Mittag, T., & Taylor, J. P. (2015). Phase separation by low complexity domains promotes stress granule assembly and drives pathological fibrillization. *Cell*, *163*(1), 123–133. https://doi.org/10.1016/j.cell.2015.09.015

Nicholson, A. L., & Pasquinelli, A. E. (2019). Tales of Detailed Poly(A) Tails. *Trends in Cell Biology*, *29*(3), 191–200. https://doi.org/10.1016/j.tcb.2018.11.002

Nirenberg, M. W., & Matthaei, J. H. (1961). The dependence of cell-free protein synthesis in E. coli upon naturally occurring or synthetic polyribonucleotides. *Proceedings of the National Academy of Sciences of the United States of America*, *47*, 1588–1602. https://doi.org/10.1073/pnas.47.10.1588

Orij, R., Postmus, J., Ter Beek, A., Brul, S., & Smits, G. J. (2009). In vivo measurement of cytosolic and mitochondrial pH using a pH-sensitive GFP derivative in Saccharomyces cerevisiae reveals a relation between intracellular pH and growth. *Microbiology*, *155*(Pt 1), 268–278. https://doi.org/10.1099/mic.0.022038-0

Perez, J. G., Stark, J. C., & Jewett, M. C. (2016). Cell-Free Synthetic Biology: Engineering Beyond the Cell. *Cold Spring Harbor Perspectives in Biology*, *8*(12), a023853. https://doi.org/10.1101/cshperspect.a023853

Ramanathan, A., Robb, G. B., & Chan, S.-H. (2016). mRNA capping: Biological functions and applications. *Nucleic Acids Research*, *44*(16), 7511–7526. https://doi.org/10.1093/nar/gkw551

Richardson, D., Itkonen, J., Nievas, J., Urtti, A., & Casteleijn, M. G. (2018). Accelerated pharmaceutical protein development with integrated cell free expression, purification,

and bioconjugation. *Scientific Reports*, *8*(1), 11967. https://doi.org/10.1038/s41598-018-30435-4

Schwartz, S., Agarwala, S. D., Mumbach, M. R., Jovanovic, M., Mertins, P., Shishkin, A., Tabach, Y., Mikkelsen, T. S., Satija, R., Ruvkun, G., Carr, S. A., Lander, E. S., Fink, G. R., & Regev, A. (2013). High-resolution mapping reveals a conserved, widespread, dynamic mRNA methylation program in yeast meiosis. *Cell*, *155*(6), 1409–1421. https://doi.org/10.1016/j.cell.2013.10.047

Scott, M. P., & Pardue, M. L. (1981). Translational control in lysates of Drosophila melanogaster cells. *Proceedings of the National Academy of Sciences of the United States of America*, *78*(6), 3353–3357. https://doi.org/10.1073/pnas.78.6.3353

Stech, M., Rakotoarinoro, N., Teichmann, T., Zemella, A., Thoring, L., & Kubick, S. (2021). Synthesis of Fluorescently Labeled Antibodies Using Non-Canonical Amino Acids in Eukaryotic Cell-Free Systems. *Methods in Molecular Biology*, *2305*, 175–190. https://doi.org/10.1007/978-1-0716-1406-8_9

Storti, R. V., Scott, M. P., Rich, A., & Pardue, M. L. (1980). Translational control of protein synthesis in response to heat shock in D. melanogaster cells. *Cell*, *22*(3), 825–834. https://doi.org/10.1016/0092-8674(80)90559-0

Tudek, A., Krawczyk, P. S., Mroczek, S., Tomecki, R., Turtola, M., Matylla-Kulińska, K., Jensen, T. H., & Dziembowski, A. (2021). Global view on the metabolism of RNA poly(A) tails in yeast Saccharomyces cerevisiae. *Nature Communications*, *12*(1), 4951. https://doi.org/10.1038/s41467-021-25251-w

Venkat, S., Chen, H., Gan, Q., & Fan, C. (2019). The Application of Cell-Free Protein Synthesis in Genetic Code Expansion for Post-translational Modifications. *Frontiers in Pharmacology*, *10*, 248. https://doi.org/10.3389/fphar.2019.00248

Wu, C., Amrani, N., Jacobson, A., & Sachs, M. S. (2007). The use of fungal in vitro systems for studying translational regulation. *Methods in Enzymology*, *429*, 203–225. https://doi.org/10.1016/S0076-6879(07)29010-X

Wu, C., & Sachs, M. S. (2014). Preparation of a Saccharomyces cerevisiae cell-free extract for in vitro translation. *Methods in Enzymology*, *539*, 17–28. https://doi.org/10.1016/B978-0-12-420120-0.00002-5

Zhou, J., Wan, J., Gao, X., Zhang, X., Jaffrey, S. R., & Qian, S.-B. (2015). Dynamic m(6)A mRNA methylation directs translational control of heat shock response. *Nature*, *526*(7574), 591–594. https://doi.org/10.1038/nature15377

Zid, B. M., & O'Shea, E. K. (2014). Promoter sequences direct cytoplasmic localization and translation of mRNAs during starvation in yeast. *Nature*, *514*(7520), 117–121. https://doi.org/10.1038/nature13578

Chapter 5:

Conclusion

5.1 Future Directions

This dissertation sets the stage for a range of experimental approaches that have the potential to build upon our understanding of how cells respond to stress. First, much work remains to elucidate the roles of stress granules and P-bodies and the regulatory mechanisms that control phase separated granules *in vivo* more generally. Though we have a solid understanding of their resident proteins, much remains unknown about the RNA content in stress-induced granules and their function in controlling gene expression. In fact, the soundness of assuming there is a function for phase separated granules based on largely descriptive studies has been called into question recently and remains a topic of open debate (A & Weber, 2019; McSwiggen et al., 2019). Additionally, it is worthwhile to remember that studies that perturb granule formation tend to do so by mutating, overexpressing, or removing factors that nucleate or aid in their assembly and it can be hard to disentangle if phenotypic consequences arise strictly from aberrant granules or simply from the genetic consequences of lacking or gaining function.

One important direction would be to take a more quantitative look at the concentration of resident proteins in granules and compare that to the larger cytoplasm and then, importantly, to test whether there are functional consequences to those concentration changes. Previous studies have set a precedent for the first part of such an approach. For example, researchers have looked at the concentration of G3BP1 inside and outside of mammalian stress granules as well as the concentration of Dcp2 in yeast P-bodies (Jain et al., 2016; Xing et al., 2020). Additionally, more work is needed to parse how much overlap exists between stress granules and P-bodies. This can mean literally as in physical overlap within the cytoplasm and more esoterically in terms of what constituents make something a bona fide P-body or stress granule.

Advancements in microscopy will be essential to get a higher resolution and more complete portrait of the range of granule sizes that occur during different severities of stress and the extent of their coexistence and overlap. Intriguingly, one recent study showed the importance of both stoichiometry and competitive protein-protein and protein-RNA interaction networks in organizing stress-induced granules and demonstrated that specific cellular contexts can give rise to granules that are neither entirely stress granule nor p-body (Sanders et al., 2020).

In addition to understanding how cellular components are organized within the cytoplasm during stress, more work remains to reveal how these components regulate gene expression. One of the most interesting findings to come from the works discussed here is the progressive, general slowing of elongation we observed in response to acute glucose starvation. An obvious question arises from this, "what is the mechanism?" Previous studies have highlighted the importance of codon-specific effects in slowing elongation on genes (Park & Subramaniam, 2019; Weinberg et al., 2016). However, our elongation rate reporter results suggest that the mechanism or mechanisms slowing elongation in this context are codon independent. There are known regulatory processes that slow elongation globally in response to stress such at the phosphorylation of eEF2 (Gismondi et al., 2014; Wu et al., 2019). However, in my hands, pilot experiments to test if eEF2 phosphorylation increases in response to acute glucose starvation yielded negative results. Therefore, experiments that take an unbiased approach to interrogate ribosomal regulation are warranted. Recently, evidence has emerged that ribosome heterogeneity as well as a complicated network of post-translational modifications can impact ribosome function and gene expression (Emmott et al., 2019; Genuth & Barna, 2018). Additionally, it is well established that non-ribosomal proteins interact with ribosomes to modulate translation in a variety of contexts (Pause et al., 1994; Simsek et al.,

2017; Sweet et al., 2012). Future directions that use a cross-linking immunoprecipitation (CLIP) based approach to purify ribosomes from log phase cells and during a time course of glucose starvation would be a logical starting point to identify what factors differentially associate with ribosomes over the duration of the stress response. Moreover, an RNA-centric version of an affinity-capture approach like RNA antisense purification and mass spectrometry (RAP-MS) that uses RNA as the pull-down bait would be a way to further parse potential regulatory mechanisms that influence translation in response to glucose starvation (McHugh et al., 2014). Such an approach would complement a more general, CLIP-based interrogation of ribosome interactions by providing information on what factors differentially interact with preexisting versus stress-induced transcripts. For example, one could design antisense probes against *PGK1* and *HSP30* mRNAs. This approach would not only provide information about how ribosome-associated factors change in response to stress but would also provide information about possible factors that distinctly interact with the ribosomes bound to stress-induced or preexisting genes. Upon completion of these experiments, resources such as the *Saccharomyces* genome deletion library and the power of yeast genetics could be used to manipulate the expression of candidate proteins and validate their role in translation elongation during stress. In addition, examining the function of conserved candidates in more complicated organisms like mammalian models would be useful.

Finally, results from our *in vitro* translation system open the door for future work in a CFPS setting. One avenue to take would be to test extracts from cells undergoing different stress responses such as heat shock, osmotic stress, and amino acid starvation. These could be used to determine if any additional stresses cause reduced expression in stress extracts like glucose starvation was shown to. It would also be informative to transcribe messages with

regulatory elements from stress-induced genes such as the 5' UTR of a heat shock protein and determine if they are preferentially translated in stress extracts. Previous work in *Drosophila* has shown that heat-shocked extracts preferentially translate heat shock messages transcribed *in vivo* (Krüger & Benecke, 1981; Scott & Pardue, 1981; Storti et al., 1980) which suggests that there is potential for *in vitro* transcribed messages to show similar behavior. In addition, it would be worthwhile to harness the power of *in vitro* systems to modulate the physical characteristics of the environment where translation is happening. For example, alterations could be made to molecular crowding, pH, and ATP levels and their impact on expression could be monitored. In addition, a strong precedent exists for studying phase separation, RNA-protein interactions, and stress granule assembly in an *in vitro* setting (Begovich & Wilhelm, 2020; Budkina et al., 2021; Van Treeck et al., 2018). Inspiration could be drawn from these studies to monitor phase separation and CFPS simultaneously to parse how gene expression is impacted by the addition of specific proteins or RNAs previously shown to modulate granule dynamics.

5.2 Concluding Remarks

Using a combination of NGS, *in vitro*, and reporter assay approaches, we have investigated the relationship between translation and stress response. To accomplish this, we used yeast as a model organism and acute glucose starvation as a model stress. We highlighted the importance of understanding the spatial confinement and organization of membraneless regions of cytoplasm before and after stress. We also demonstrated the utility of interrogating the interactions that take place between mRNAs and ribosomes at nucleotide resolution with sequencing-based approaches. This, in combination with *in vivo* reporter assays, revealed that elongation is slowed over time in response to glucose starvation. We also showed translation can resume from previously initiated ribosomes upon stress relief. Additionally, we showed that *in vitro* translation systems can be powerful complements to studying stress response *in vivo* as the reduced propensity for protein synthesis in living cells was maintained in extracts. Taken together, these approaches provide a blueprint for studying stress response in a comprehensive way.

References

A, P., & Weber, S. C. (2019). Evidence for and against Liquid-Liquid Phase Separation in the Nucleus. *Non-Coding RNA*, *5*(4), E50. https://doi.org/10.3390/ncrna5040050

Begovich, K., & Wilhelm, J. E. (2020). An In Vitro Assembly System Identifies Roles for RNA Nucleation and ATP in Yeast Stress Granule Formation. *Molecular Cell*, *79*(6), 991-1007.e4. https://doi.org/10.1016/j.molcel.2020.07.017

Budkina, K., El Hage, K., Clément, M.-J., Desforges, B., Bouhss, A., Joshi, V., Maucuer, A., Hamon, L., Ovchinnikov, L. P., Lyabin, D. N., & Pastré, D. (2021). YB-1 unwinds mRNA secondary structures in vitro and negatively regulates stress granule assembly in HeLa cells. *Nucleic Acids Research*, *49*(17), 10061–10081. https://doi.org/10.1093/nar/gkab748

Emmott, E., Jovanovic, M., & Slavov, N. (2019). Ribosome stoichiometry: From form to function. *Trends in Biochemical Sciences*, *44*(2), 95–109. https://doi.org/10.1016/j.tibs.2018.10.009

Genuth, N. R., & Barna, M. (2018). The Discovery of Ribosome Heterogeneity and Its Implications for Gene Regulation and Organismal Life. *Molecular Cell*, *71*(3), 364–374. https://doi.org/10.1016/j.molcel.2018.07.018

Gismondi, A., Caldarola, S., Lisi, G., Juli, G., Chellini, L., Iadevaia, V., Proud, C. G., & Loreni, F. (2014). Ribosomal stress activates eEF2K-eEF2 pathway causing translation elongation inhibition and recruitment of terminal oligopyrimidine (TOP) mRNAs on polysomes. *Nucleic Acids Research*, *42*(20), 12668–12680. https://doi.org/10.1093/nar/gku996

Jain, S., Wheeler, J. R., Walters, R. W., Agrawal, A., Barsic, A., & Parker, R. (2016). ATPase-Modulated Stress Granules Contain a Diverse Proteome and Substructure. *Cell*, *164*(3), 487–498. https://doi.org/10.1016/j.cell.2015.12.038

Krüger, C., & Benecke, B. J. (1981). In vitro translation of Drosophila heat-shock and non—Heat-shock mRNAs in heterologous and homologous cell-free systems. *Cell*, *23*(2), 595–603. https://doi.org/10.1016/0092-8674(81)90155-0

McHugh, C. A., Russell, P., & Guttman, M. (2014). Methods for comprehensive experimental identification of RNA-protein interactions. *Genome Biology*, *15*(1), 203. https://doi.org/10.1186/gb4152

McSwiggen, D. T., Mir, M., Darzacq, X., & Tjian, R. (2019). Evaluating phase separation in live cells: Diagnosis, caveats, and functional consequences. *Genes & Development*, *33*(23–24), 1619–1634. https://doi.org/10.1101/gad.331520.119

Park, H., & Subramaniam, A. R. (2019). Inverted translational control of eukaryotic gene expression by ribosome collisions. *PLoS Biology*, *17*(9), e3000396. https://doi.org/10.1371/journal.pbio.3000396

Pause, A., Belsham, G. J., Gingras, A. C., Donzé, O., Lin, T. A., Lawrence, J. C., & Sonenberg, N. (1994). Insulin-dependent stimulation of protein synthesis by phosphorylation of a regulator of 5'-cap function. *Nature*, *371*(6500), 762–767. https://doi.org/10.1038/371762a0

Sanders, D. W., Kedersha, N., Lee, D. S. W., Strom, A. R., Drake, V., Riback, J. A., Bracha, D., Eeftens, J. M., Iwanicki, A., Wang, A., Wei, M.-T., Whitney, G., Lyons, S. M., Anderson, P., Jacobs, W. M., Ivanov, P., & Brangwynne, C. P. (2020). Competing Protein-RNA Interaction Networks Control Multiphase Intracellular Organization. *Cell*, *181*(2), 306-324.e28. https://doi.org/10.1016/j.cell.2020.03.050

Scott, M. P., & Pardue, M. L. (1981). Translational control in lysates of Drosophila melanogaster cells. *Proceedings of the National Academy of Sciences of the United States of America*, *78*(6), 3353–3357. https://doi.org/10.1073/pnas.78.6.3353

Simsek, D., Tiu, G. C., Flynn, R. A., Byeon, G. W., Leppek, K., Xu, A. F., Chang, H. Y., & Barna, M. (2017). The Mammalian Ribo-interactome Reveals Ribosome Functional Diversity and Heterogeneity. *Cell*, *169*(6), 1051-1065.e18. https://doi.org/10.1016/j.cell.2017.05.022

Storti, R. V., Scott, M. P., Rich, A., & Pardue, M. L. (1980). Translational control of protein synthesis in response to heat shock in D. melanogaster cells. *Cell*, *22*(3), 825–834. https://doi.org/10.1016/0092-8674(80)90559-0

Sweet, T., Kovalak, C., & Coller, J. (2012). The DEAD-Box Protein Dhh1 Promotes Decapping by Slowing Ribosome Movement. *PLoS Biology*, *10*(6), e1001342. https://doi.org/10.1371/journal.pbio.1001342

Van Treeck, B., Protter, D. S. W., Matheny, T., Khong, A., Link, C. D., & Parker, R. (2018). RNA self-assembly contributes to stress granule formation and defining the stress granule transcriptome. *Proceedings of the National Academy of Sciences of the United States of America*, *115*(11), 2734–2739. https://doi.org/10.1073/pnas.1800038115

Weinberg, D. E., Shah, P., Eichhorn, S. W., Hussmann, J. A., Plotkin, J. B., & Bartel, D. P. (2016). Improved Ribosome-Footprint and mRNA Measurements Provide Insights into Dynamics and Regulation of Yeast Translation. *Cell Reports*, *14*(7), 1787–1799. https://doi.org/10.1016/j.celrep.2016.01.043

Wu, C. C.-C., Zinshteyn, B., Wehner, K. A., & Green, R. (2019). High-Resolution Ribosome Profiling Defines Discrete Ribosome Elongation States and Translational Regulation

during Cellular Stress. *Molecular Cell*, *73*(5), 959-970.e5. https://doi.org/10.1016/j.molcel.2018.12.009

Xing, W., Muhlrad, D., Parker, R., & Rosen, M. K. (2020). A quantitative inventory of yeast P body proteins reveals principles of composition and specificity. *ELife*, *9*, e56525. https://doi.org/10.7554/eLife.56525